ДОКЛАДЫ
АКАДЕМИИ НАУК СССР

SOVIET PHYSICS

"Doklady"

VOLUME 2 NUMBER 6

A Translation

of the

"Physics Section"

of the

Proceedings of the Academy of Sciences of the USSR

(RUSSIAN ORIGINAL VOL. 117, NOS. 1-6)

Published by the
AMERICAN INSTITUTE OF PHYSICS
INCORPORATED

SOVIET PHYSICS

"Doklady"

A translation of the "Physics Section" of the Proceedings of the Academy of Sciences of the USSR.

A publication of the

AMERICAN INSTITUTE OF PHYSICS

Governing Board

FREDERICK SEITZ, *Chairman*

Members

WALTER S. BAIRD
JESSE W. BEAMS
RAYMOND T. BIRGE
R. H. BOLT
J. W. BUCHTA
J. H. DILLON
VERNET E. EATON
HERBERT A. ERF
IRVINE C. GARDNER
S. A. GOUDSMIT
C. KITTEL
WINSTON E. KOCK
R. BRUCE LINDSAY
WALTER C. MICHELS
G. E. PAKE
R. RONALD PALMER
JOSEPH B. PLATT
RALPH A. SAWYER
H. D. SMYTH
JOHN STRONG
GEORGE E. UHLENBECK

Officers and Staff

ELMER HUTCHISSON
Director
HENRY A. BARTON
Associate Director
WALLACE WATERFALL
Secretary and Treasurer
THEODORE VORBURGER
Advertising Manager
RUTH F. BRYANS
Publication Manager
KATHRYN SETZE
Assistant Treasurer
ALICE MASTROPIETRO
Circulation Manager
EUGENE H. KONE
Director of Public Relations

American Institute of Physics Advisory Board on Russian Translations

ROBERT T. BEYER, *Chairman*

FREEMAN DYSON, DWIGHT GRAY, MORTON HAMERMESH,
DAVID HARKER, VLADIMIR ROJANSKY

Advisory Editor, Soviet Physics—"Doklady": VLADIMIR ROJANSKY,
Ramo-Wooldridge Corporation, Los Angeles, California

SOVIET PHYSICS—"Doklady" is a bi-monthly journal published by the American Institute of Physics for the purpose of making available in English reports of current Soviet research in physics as contained in the "Physics Section" of the Proceedings of the Academy of Sciences of the USSR. The Proceedings appears thirty-six times per year and the "Physics Sections" are accumulated and English translations of them are published in six issues per year.

Transliteration of the names of Russian authors follows the system employed by the Library of Congress.

This translating and publishing project was undertaken by the Institute in the conviction that dissemination of the results of research everywhere in the world is invaluable to the advancement of science. The National Science Foundation of the United States encouraged the project initially and is supporting it in large part by a grant. Translation and printing are being handled by Consultants Bureau, Inc.

The American Institute of Physics and its translators propose to translate faithfully all of the scientific material in the "Physics Section" of the Proceedings of the Academy of Sciences of the USSR appearing after January 1, 1956. The views expressed in the translated material, therefore, are intended to be those expressed by the original authors, and not those of the translators nor of the American Institute of Physics.

One volume is published annually. Volume 2 will consist of six issues and will contain all scientific material published in the "Physics Section" of the original Russian journal during the 1957 calendar year.

Subscription Prices:

Per year (6 issues)	
United States and Canada	$25.00
Elsewhere	27.50
Back Numbers	
Single copies	$ 5.00

Subscriptions should be addressed to the American Institute of Physics, 335 East 45th Street, New York 17, New York.

Copyright by American Institute of Physics 1958

SOVIET PHYSICS

"Doklady"

VOLUME 2, NUMBER 6 NOVEMBER-DECEMBER, 1957

THE CONVERSION SPECTRUM OF Ho^{160}

E. P. Grigor'ev, B. S. Dzhelepov, Corr. Member, Acad. Sci. USSR, A. V. Zolotavin, B. Kratsik, B. K. Preobrazhenskii and I. S. Ianchevskaia

We have investigated the conversion spectrum which appears in the radioactive transformation $Er^{160} \rightarrow Ho^{160} \rightarrow Dy^{160}$. A double-focusing spectrometer was used [1], which was adjusted mainly for work with an instrumental resolution amounting to 0.5%. A considerable portion of the measurements were obtained with a resolution of 0.3%, for which purpose, following a suggestion in [1], the source and receiving slit in the spectrometer were made narrower than usual.

The conversion spectrum, as has already been noted in [2], is the same in both fractions: Er^{160} does not yield conversion electrons, all of the electrons belonging to Ho^{160}. The results of an investigation of the conversion spectrum accompanying the decay of both fractions is given in Table 1.

TABLE 1

Internal Conversion Lines of Ho^{160}

No.	E_e, kev	Identification	$h\nu$, kev	I/I_0	No.	E_e, kev	Identification	$h\nu$, kev	I/I_0
1	51.2	L_I+L_{II}	60.1	1150	31	638.4	L	647.1	0.85
2	52.05	L_{III}	60.1	1050	32	647.0	M	648.3	0.26
3	57.9	M	60	480	33	675.9	K	729.7	6.9
4	59.2	N	59.6	110	34	720.5	L	729.3	1.1
5	33.0	K	86.8	814	35	729.4	$M+N$	730.7	0.32
6	76.3	L_I+L_{II}	86.2	790	36	700.9	K	754.7	0.6
7	78 4	L_{III}	86.2	610	37	713	K	766.7	0.8
8	84.5	M	86.3	400	38	819.4	K	873.2	0.92
9	86.1	N	86.5	100	39	863.8	L	872.9	0.1
10	53.9	K	107.7	10	40	826.0	K	879.8	2.6
11	99.3	L	107.2	28	41	871.0	L	880.0	0.4
12	142.2	K	196.2	100	42	879.6	M	880.3	0.15
13	189.7	L	197	37	43	909.6	K	963.4	2.1
14	195.6	M	197	8.4	44	912.9	K	966.6	1.8
15	161.0	K	214.8	0.3	45	960.1	L	968.0	0.72
16	243.4	K	297.2	} 3.0	46	994	K	1048	0.11
17	244.6	K	298.4		47	1040	L	1048	0.03
18	290.7	L	298.5	0.9	48	1015	K	1069	0.24
19	297.0	M	298.3	0.26	49	1061	L	1069	0.048
20	256	K	310	0.16	50	1079	K	1133	0.085
21	301	K	365	0.22	51	1126	K	1180	0.066
22	339	K	393	0.09	52	1147	K	1201	0.07
23	353	K	407	0.4	53	1210	K	1264	0.077
24	399	L	407	0.06	54	1219	K	1273	0.082
25	460.6	K	514.4	0.75	55	1231	K	1285	0.035
26	506.1	L	514.8	0.08	56	1323	K	1377	0.070
27	485	K	538.9	2.25	57	1381	K	1435	0.045
28	531.1	L	540.0	0.42	58	1427	L	1435	0.034
29	539.4	M	540.6	0.15	59	1665	K	1719	0.023
30	593.8	K	647.6	5.25					—

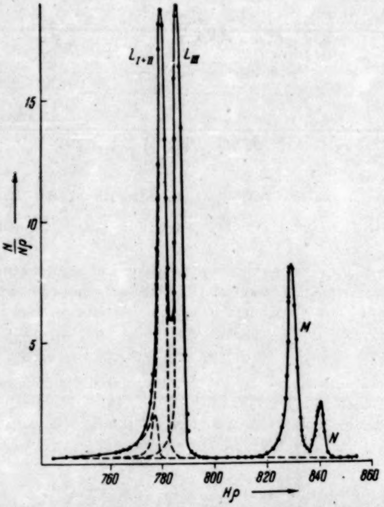

Fig. 1. Conversions in the L, M and N shells for the 60-kev transition. The dashed line shows the resolution of the L line. The conversion of the 86.4-kev transition is similar.

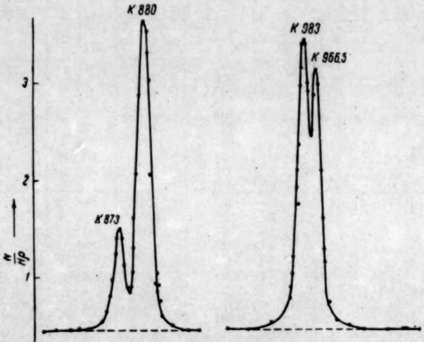

Fig. 2. K conversion lines: doublets 873-800 and 963-967 kev. Halfwidth of lines 0.3%.

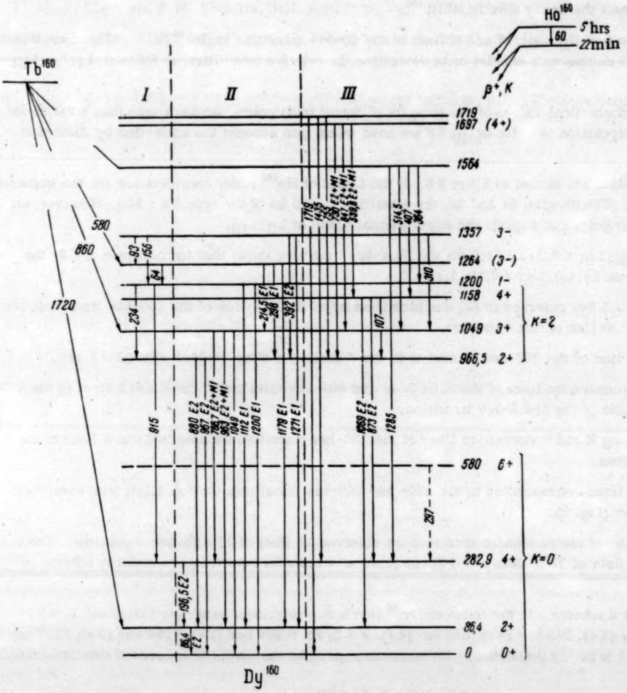
Ho^{160}
5 hrs
60
22 min
β^+, K
Tb^{160}
I
II
III
580
860
1720
1719
1697 (4+)
1564
1357 3-
1264 (3-)
1200 1-
1158 4+
1049 3+
966,5 2+
K=2
580 6+
282,9 4+
K=0
86,4 2+
0 0+
93
156
64
234
915
214,5 E1
298 E1
392 E2
880 E2
967 E2
766,7 E2+M1
963 E2+M1
1049
1112 E1
1200 E1
1179 E1
1271 E1
1719
1435
753
730 E2+M1
847 E2+M1
539,8 E2+M1
514,5
407
364
310
107
1069 E2
873 E2
1285
297
196,5 E2
86,4 E2
Dy^{160}

Fig. 3. Scheme of excited Dy^{160} levels. In region I only Tb^{160} lines were observed; in region II Tb^{160} and Ho^{160}; and in region III only Ho^{160}.

TABLE 2

Theoretical Values of the Ratios $L_I : L_{II} : L_{III}$

	$L_I : L_{II} : L_{III}$		$L_I : L_{II} : L_{III}$
E1	2.3 : 0.86 : 1	M1	107 : 7.1 : 1
E2	0.09 : 1.2 : 1	M2	3.0 : 0.30 : 1
E3	0.01 : 1.2 : 1	M3	0.58 : 0.08 : 1
E4	0.17 : 0.68 : 1	M4	0.8 : 0.12 : 1
E5	0.008 : 0.45 : 1	M5	0.04 : 0.007 : 1
Experimental value			1.0 : 1.0 : 1.0

The experimental data for the 215-, 310-, 364- and 394-kev transitions and the hard transitions beginning with 1048 kev were obtained in only two series of measurements with a single erbium source and with resolutions of 0.5% and 0.3%. The other lines were studied with several erbium and holmium sources. The intensities of all observed lines diminished with the half-lives of the respective fractions: 29 hours for the erbium fraction and 5 hours for the holmium fraction. The K-L energy difference for all measured transitions equals the difference between the binding energies in the corresponding Dy shells.

The errors in determination of the line energies varied from 0.1 to 0.3% depending on their intensity. The statistical error in determining the relative intensities is also determined by the counting rate for the lines and amounts to a few percent for the strongest lines.

The general shape of the conversion spectrum agrees in the main with that in [2], but a number of new facts enabled us to construct the decay scheme of Ho^{160}.

1. We observed the $L_I + L_{II}$, L_{III}, M and N lines of the 60-kev transition in Ho^{160} [2, 3]. These are shown in Fig. 1. Resolution into components enables us to determine the relative intensities, as follows: $L_I : L_{II} : L_{III} : M : N = 0.1 : 1.0 : 1.0 : 0.47 : 0.1$.

Table 2 gives the theoretical values of the ratio for different multipoles; we have used Rose's values for α_L with Dranitsyna's interpolation [4]; for $\alpha_{L_{III}}$, E 3 we have taken into account the correction by Andersson and Bergström [5].

The experimental data are closest to E 2 or E 3. If the levels of Ho^{160} under consideration are the isomeric levels predicted by Pekar [6] with spins 5+ and 2+, the transition should be of the type E 4 + M 3. However, no combination of these multipoles can explain the experimental value of $L_{II} : L_{III}$.

2. Our ratios $L_I : L_{II} : L_{III} = 0.2 : 1.1 : 1.0$ for the 86.4-kev transition shows that its multipole is E 2; the theoretical ratios for E 2 are $L_I : L_{II} : L_{III} = 0.19 : 1.1 : 1.0$.

3. The line E_e = 99.3 kev observed in [2] was identified by us as the L line of the 107-kev transition. We have found the K conversion line of this transition.

4. The conversion line of the 298-kev transition in the K shell is a close doublet with $\Delta E \approx 1$ kev.

5. We observed K-conversion lines of the 310- 364- and 394-kev transitions, the K and L lines of the 407-kev transition and the L line of the 514.5-kev transition.

6. Between the strong K and L conversion lines of the 730-kev transition we observed the K lines of the 755- and 767-kev transitions.

7. The conversion lines corresponding to the 880- and 967-kev transitions were doublets with energy differences ΔE of 7 and 3 kev (Fig. 2).

8. In the hard region of the conversion spectrum we observed 14 lines of 11 different transitions. The results of this work and the data of Tb^{160} decay [7-12] can serve as a basis for constructing the decay scheme of Tb^{160} and Ho^{160}.

Figure 3 shows such a scheme. In the series of Dy^{160} levels two rotational bands are indicates: K = 0, E^* = 0 kev (0+), 86.4 kev (2+), 283 kev (4+), 580 kev (6+), k = 2, E^* = 966 kev (2+), 1050 kev (3+), 1157 kev (4+). The 1697-kev level is highly populated, with transitions going to the levels of the second rotational band.*

LITERATURE CITED

[1] A. V. Zolotavin, Izv. Akad. Nauk SSSR, Ser. Fiz. 18, 1 (1954).

[2] B. S. Dzhelepov, B. A. Preobrazhenskii, I. M. Rogachev, and P. A. Tishkin, Izv. Akad. Nauk SSSR, Ser. Fiz. 21, 7 (1957).

[3] G. Seaborg and H. Nervik, Phys. Rev. 97, 1092 (1955).

[4] G. Dranitsyna, Coefficients of Internal Conversion in L_I, L_{II}, L_{III} Subshells [in Russian] (Izd. AN SSSR ,1957).

[5] G. Andersson and I. Bergström, Nucl. Phys. 3, 541 (1957).

[6] L. K. Peker, Izv. Akad. Nauk SSSR, Ser. Fiz. 21, 7 (1957).

[7] F. McGowan, Phys. Rev. 85, 142 (1952).

[8] S. Burson, W. Jordan, and J. Le Blanc, Phys. Rev. 94, 103 (1954).

[9] V. Keshishian, H. Kruse, R. Klotz, and C. Fowler, Phys. Rev. 96, 1050 (1954).

---

* This scheme was worked out with the assistance of L. K. Peker.

[10] G. Bertolini, M. Bettoni, and E. Lazzarini, Nuovo Cim. 3, 754, 1172 (1956).

[11] M. A. Clark and J. W. Knowles, Bull. Am. Phys. Soc. 2, 231 (1957).

[12] M. P. Avotina, E. P. Grigor'ev, A. V. Zolotavin and B. Kratsik, Doklady Akad. Nauk (in press).

Received September 13, 1957

Physical Institute, A. A. Zhdanov Leningrad State University

ON THE QUESTION OF A BARRIER-LAYER PHOTOELECTROMOTIVE FORCE IN PHOTOCELLS CONTAINING DYES

I. A. Karpovich and A. T. Vartanian

(Presented by Academician A. N. Terenin June 1, 1957)

Noddack and Meier [1-3] have investigated the photoelectromotive force which arises from "longitudinal" illumination of layers of dyes deposited on the surface of a massive metal electrode and clamped against a translucent electrode. The dye layers were deposited from alcohol solutions and were illuminated in air with visible light. The rectifying properties of the photocells led these investigators to the conclusion that the photoelectromotive force resulted from a barrier layer. Since upon exhaustion of the air to 5 mm the rectification and the photo emf almost completely disappeared, Noddack and Meier concluded that in the formation of the barrier layer adsorbed gas plays an essential role. They are of the opinion that a barrier layer is formed at a natural (unclamped) contact between the dye and the metallic electrode. The sign of the photo emf as determined from the sign of the photo potential on the back electrode, since the photo emf was considered to be of the "backwall" type, was negative for almost all of the dyes investigated.

Our experiments have shown* that when a layer of dye deposited from a solution on a quartz surface, to which platinum electrodes had been applied, is illuminated in air by a light probe at one of the electrodes, a photo emf is observed even for "transverse" illumination. But for the majority of our dyes the sign of the photo emf was positive. Since the dye made ohmic contacts with the electrodes the emf could not be attributed to a barrier-layer photoeffect. From the characteristics of the photo emf and the conditions under which it arose we concluded that we were dealing with a photoelectrochemical phenomenon which in its general features is analogous to the Becquerel photovoltaic effect in layers of dyes immersed in electrolytic solutions [4]. We then performed experiments to determine the role of the barrier layer in photocells with "longitudinal" illumination.

Unlike the photocells of Noddack and Meier [1] our photocell had both front and back electrodes consisting of translucent metallic films (Pt, Au and Rh) deposited on quartz plates. Rearrangement of the plates made it possible to investigate the photo emf during illumination with both clamped and natural contacts between the dye and the electrodes. The thickness of the dyes deposited on the electrodes from alcohol solutions was of the order of 30-50mμ. We shall distinguish the photocells as follows: Type I with the dye deposited only on the front electrode; Type II with the dye only on the back electrode; and Type III with the dye on both electrodes.** The photocell was illuminated with light from a 300- or 1000-watt incandescent lamp. For measurements of the photo emf (E_{∞}) we used a dc amplifier with an input resistance of $R_{in} = 10^8$ ohms. E_{∞} was determined from the voltage produced by the photocell across the resistance $R_{in} \gg R$, where R is the internal resistance of the photocell. The sensitivity of the arrangement was 10^{-4}v/mm. The short-circuit current (I_0) was measured by a galvanometer of 10^{-9} amp/mm sensivity.

For detailed investigation we selected pinacyanol, orthochrome T and crystalline violet. Under illumination of about 1000 lux E_{∞} frequently reaches 0.1 to 0.2 v. The settling time for a stationary photo emf under this illumination was of the order of a few seconds or tenths of seconds; with 10 lux the time was measured in minutes.

Figure 1 shows typical dependence of E_{∞}, I_0 and R on the illumination L. The dependence of E_{∞} on L is described by the equation $E_{\infty} = A \ln (1 + BL)$, where A and B are constants. The dependence of I_0 on L in a

---

* Article being printed in the Journal of Physical Chemistry (USSR).

** Noddack and Meier also studied the photo emf for Type II.

1 : 100 range of illumination is satisfactorily approximated by $I = kL^n$, in which $\underline{n}$ is usually from 0.4 to 0.8. Measurements with interference filters showed that the maxima of E and I_0 coincide approximately with the absorption maxima of the dyes in the solid state.

Figure 2 shows the current-voltage characteristics of the dark current and photocurrent for a Type I photocell with pinacyanol (curves 1 and 2). Curve 1 indicates the existence of a barrier layer. Curve 2 shows that the photocurrent in the forward direction increases with the voltage and approaches saturation, but that it drops to zero in the back direction.

From the current-voltage characteristic of the dark current for a Type II photocell (curve 3), which was obtained from a Type I cell by exchanging electrodes, it follows that the forward direction of Type I here becomes the back direction and vice versa. But the photocurrent (curve 4) flows in the previous direction, which is now the reverse direction.

A photocell of Type III, obtained from a photocell of Type I by replacing the back electrode (not covered with dye) with a dye-covered electrode, does not reveal rectifying properties, and the dark current at low voltages obeys Ohm's law (curve 5). This result definitely shows the absence of a barrier layer rather than the compensation of two barrier layers as might be imagined. This is also shown by the fact that the resistance of a Type III photocell is several times smaller than that of the Type I and Type II photocells which are obtained from it. The existence of a barrier layer in the latter and its absence in the Type III photocell signifies that the effective barrier layer is formed at the clamped contact between the dye and the metal electrode which is absent in Type III. It is noteworthy that for all three types in which the same layer of dye was illuminated the direction of the photocurrent (curves 2, 4 and 6) was preserved and the photo emf (E_∞) is almost the same.

These results, which are also obtained from photocells with orthochrome T and crystalline violet, can hardly be reconciled with the concept of a barrier-layer photo emf. A comparison of Types I, II and III shows that there is no causal relationship between the photo emf and a barrier layer, because neither the position of the latter with respect to the illuminated electrode nor its presence or absence (see the photocell diagrams in Fig. 2) affects the direction of the photocurrent and the magnitude of the photo emf. We regard a photocell with a layer of dye as a source of a nonbarrier-layer photo emf in series with a rectifier. The action of the latter affects only the shapes of the current-voltage characteristics of the dark current and the photocurrent.

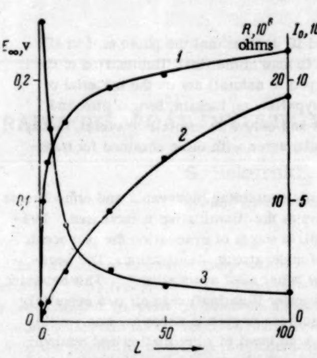

Fig. 1. Dependence of E_∞ (1), I_0(2) and R (3) on the intensity of illumination: 1) E_∞, 2) I_0, 3) R (L = 100 corresponds to about 1000 lux).

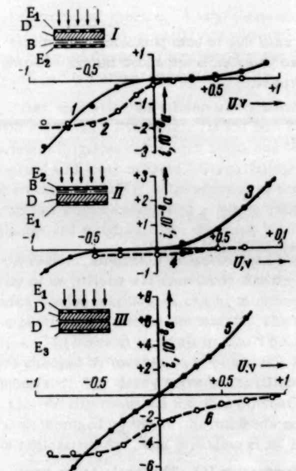

Fig. 2. Current-voltage characteristics of the dark current and photocurrent for photocells of Types I, II and III with pinacyanol: 1, 3, 5) dark current; 2, 4, 6) photocurrent. E) Electrodes; D) layer of dye; B) barrier layer. The horizontal axis gives the external voltage applied to the front electrode.

The structure of the barrier layer and the rectifying mechanism at the dye-to-metal contact are still not understood. It can only be stated that the rectification takes place at an incomplete clamped contact between a dye and a metal electrode when the conductivity of the dye is practically entirely electrolytic.* The presence of a film of adsorbed gas also is a possibly important factor.

The preservation of the photocurrent direction for Types I, II and III denotes that the photo emf in all three cases is of the "front-wall" type. The photo emf is entirely due to nonsymmetrical illumination of the two electrodes and does not depend on the nature of the contact (clamped or natural) nor on the material of the electrodes. With pinacyanol, orthochrome T, eosin, erythrosine, trypaflavine, fuchsin, Bengal pink and some other dyes the photo potential on the front electrode was positive and only with crystalline violet, methyl blue and phenosafranine was a negative potential observed. These results agree with those obtained for transverse illumination of the layers.

It must, of course, be noted that the positive photo emf of the cells containing pinacyanol and orthochrome T under illumination of the order of 2000 to 3000 lux begins to decrease as the illumination is increased. Evacuation of the air changes the direction of the photo emf. At intermediate stages of evacuation the photocells show a positive photo emf under weak illumination and a negative emf under strong illumination. The negative photo emf of cells containing crystalline violet is multiplied a few times after evacuation.** This behavior of the photo cells when evacuated can be understood if we assume that under illumination in air two oppositely oriented photo emfs are imposed — a positive photo emf for whose appearance oxygen is necessary and possibly also moisture, and a negative photo emf which can be observed with a high level of illumination and removal of the oxygen (air). The creation of the positive photo emf is associated with photo-oxidation of the dyes in the presence of oxygen. The negative photo emf is probably of purely photoelectric origin and is associated, for example, with the diffusion of light current carriers. The diffusion photo emf of powders of a number of dyes, and particularly pinacyanol, has already been investigated by Putseiko [5, 6] using a condenser technique. In our experiments the dye is in contact with metal electrodes, so that the diffusion photo emf phenomenon may be more complicated due to fields at the contacts.

There are probably also dyes for which the directions of the photo emfs due to both photoelectrochemical and photoelectric processes are reversed, as well as dyes for which the two photo emfs are added instead of being subtracted as in the cases of pinacyanol, orthochrome T and crystalline violet.

LITERATURE CITED

[1] W. Noddack and H. Meier, Z. Elektrochem. 57, 691 (1953).

[2] H. Meier, Z. Wiss. Phot. 2, 50, 301 (1955).

[3] H. Meier, Z. Elektrochem. 59, 1029 (1955).

[4] A. N. Terenin, The Photochemistry of Dyes [in Russian] (Izd. AN SSSR, 1947), p. 319.

[5] E. Putseiko, Doklady Akad. Nauk SSSR 59, 471 (1948).

[6] E. K. Putseiko, J. Phys. Chem. (USSR) 22, 1172 (1948).

Received May 24, 1957

---

* The presence of moisture in layers of dye salts results in electrolytic conduction [4]. This explains the unusually high conductivity of such layers in air. Following careful evacuation of the photocells their conductivity is reduced by a factor of 10^2 to 10^4 and ceases to depend on the direction of the applied field.

** After prolonged outgassing the negative photo emf of pinacyanol, orthochrome T and crystalline violet also begins to decrease. But this reduction is due to a considerable extent if not entirely to increased resistance of the cells by a factor of 10^3 to 10^4 following removal of the moisture and excess dye. Thus we no longer have the condition $R_{in} >> R$.

A RADIOCHEMICAL INVESTIGATION OF THE REACTION Si^{30}(p,π^+)Si^{31}

S. Sekerskii and A. K. Lavrukhina

(Presented by Academician A. P. Vinogradov July 8, 1957)

In 1950 one of us showed the presence of the radioactive isotope Ni^{65} in the products from the bombardment of Cu^{63,65} by fast protons [1]. The production of this isotope was then explained by a secondary reaction with neutrons, Cu^{65}(n, p)Ni^{65}. However, a study of the dependence of the Ni^{65} yield on the energy of the incident protons showed that the reaction involved in the production of the isotope is Cu^{65}(p, pπ^+)Ni^{65} [2]. This revealed the possibility of using a radiochemical method to detect π^+-mesons.

In the present work we attempted to detect the reaction Si^{30}(p, π^+)Si^{31} by a radiochemical method. Since all other radioactive isotopes of silicon have a very small half-life it is possible to detect Si^{31} (T = 2.65 hrs) even when the cross section for its production is small. For proof of the existence of this reaction we studied the dependence of the cross section for Si^{31} production on proton energies from 120 to 660 Mev.

Experimental method. A target consisting of 60-80 mg of spectrally pure powdered silicon and measuring 8 × 8 mm was wrapped in two layers of aluminum foil and irradiated with protons of different energies in the internal beam of the synchrocyclotron at the Laboratory for Nuclear Problems of the Joint Nuclear Research Institute. The irradiation lasted 1 to 2 hours.

After irradiation the silicon was dissolved in a few milliliters of a 3 M solution of NaOH. The solution was filtered through filter paper for the removal of undissolved silicon. To the solution were added 2 M HCl and a few milligrams of the salts $BeCl_2$ and $MgCl_2$; the solution was then boiled down until dry. The residue was treated with concentrated HCl, centrifuged, washed 3 to 4 times with the same acid and then dissolved in a 3 M solution of NaOH; after addition of the Be and Mg salts all operations were repeated two more times, with the last evaporation taking place in concentrated H_2SO_4. The separated SiO_2 was dried, baked at 900° for 45 minutes and weighed. The chemical yield of silicon was 20%. The separation required 4 hours.

A definite amount of SiO_2 (usually 18 mg) was placed on tracing paper weighing 8 mg/cm^2 and the radioactivity of the silicon was measured. For this purpose a TM-20 end-window counter was used; the diameter of the mica window was 20 mm and its thickness 4 mg/cm^2. The counter was placed in a standard lead housing with a plexiglas support for the targets. The radioactivity was measured 23 mm from the counter window during a period of 24 hours at intervals of 1 to 2 hours. The statistical error of the count was less than 3%. The counter was checked by measurement of a RaD + RaE standard source during the entire time that the silicon activity was measured. The decay curve of the silicon which was constructed shows one component with T = 2.6-2.7 hrs (Fig. 1). We also measured the absorption of beta radiation from silicon in aluminum. The energy of this radiation as determined by the Feather method was 1.47 Mev. These values are in good agreement with the literature [3] for radioactive Si^{31}, thus providing proof of the radiochemical purity of the separated silicon.

The cross section for the production of Si^{31} ($\sigma_{Si^{31}}$) was calculated from the well-known formula [4]. In order to determine the proton current the aluminum foil wrapper was weighed and dissolved in 5 ml of a 50% of HCl. The radioactive parts of this solution (usually 0.15 ml) were deposited on tracing paper and their activity was measured under the same conditions as for Si^{31}. The proton current was computed from the activity of the Na^{24} formed in the reaction Al^{27}(p, 3pn)Na^{24}. The cross section for this reaction is $(10.8 \pm 1.1) \cdot 10^{-27}$ cm^2 over a wide range of proton energies [5]. In the calculation of $\sigma_{Si^{31}}$ the value 10^{-26} cm^2 was taken. In calculating $\sigma_{Si^{31}}$ we took into account the Si^{30} content of a natural mixture of silicon isotopes.

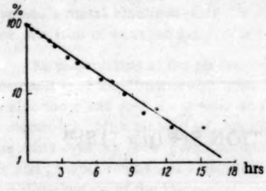

Fig. 1. Decay curve of the silicon.

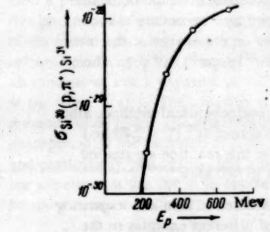

Fig. 2. The $Si^{30}(p, \pi^+)Si^{31}$ cross section as function of proton energy.

Results. The values obtained for $\sigma_{Si^{31}}$ at various proton energies are given in Table 1. It is seen that $\sigma_{Si^{31}}$ is almost constant in the range 120-220 Mev but increases considerably from 220 to 680 Mev. For the explanation of this curve let us consider all possible reactions for the production of Si^{31} when silicon is irradiated by protons.

TABLE 1

E_p Mev	$\sigma_{Si^{31}}$ (10^{-28} cm²) obs.	av.	$\sigma_{Si^{30}}(p, \pi^+)Si^{31}$ (10^{-28} cm²) average
120	0.60 0.52	0.56	
220	0.54 0.55 0.67	0.59	0.03
340	0.85 0.72	0.78	0.22
480	1.31 1.17	1.24	0.68
660	1.87 1.60	1.74	1.18

The production of Si^{31} with the disintegration of impurities in the silicon. An analysis of the activity showed the presence of about 10^{-4} % of Cu, Zn and Ga in the irradiated silicon. The disintegration of these elements should not add more than $1 \cdot 10^{-33}$ cm² to the Si^{31} yield, so that no essential contribution is made to the value obtained for $\sigma_{Si^{31}}$. The amounts of K and Ca were not determined but their presence (also about 0.1%) cannot provide the increased Si^{31} yield as the proton energy is increased, since their disintegration cross sections do not change in the indicated higher energy interval.

Reactions with secondary deuterons and neutrons. A reaction with secondary deuterons $Si^{30}(d, p)Si^{31}$ undoubtedly plays an important part in the formation of Si^{31}. The reactions with secondary deuterons have thus far not been investigated, but there is ground for believing that the secondary (d, p) reaction has a cross section of the same order as the reaction with secondary alpha particles (α, n). This follows, first, from the fact that the cross section for the (α, n) reaction is practically identical with the cross section for the (d, p) reaction at 10-15 Mev, which according to data in [6] is the maximum of the energy spectrum of the alpha particles (and apparently of the deuterons) that are evaporated from Ag and Br nuclei excited to 170 Mev. For example, the cross section for $Ni^{60}(\alpha, n)Zn^{63}$ is $2 \cdot 10^{-25}$ cm² [7], while the cross section for $Cu^{63}(d, p)Cu^{64}$ is $1.5 \cdot 10^{-25}$ cm² [8].

Secondly, the number of secondary deuterons according to Le Couteur's calculations [9] is only 2 to 2.5 times smaller than the number of alpha particles from nuclei with A = 100 at an excitation energy of 170 Mev.

Several investigators have established [10, 11] that the cross section for the secondary (α, n) reaction is $(3\text{-}9) \cdot 10^{-29}$ cm² and independent of the atomic number of the irradiated nucleus. The fact that $\sigma_{Si^{31}}$ for 120-Mev protons is in good agreement with this value is evidence that Si^{31} is produced for this proton energy in a reaction with secondary deuterons. However, it must be pointed out that the cross section of the secondary (α, n) reaction is almost independent of the energy of the bombarding protons. For example, the cross section for $Cu^{63}(\alpha, n)Ga^{66}$ in the case of 190-Mev protons is $2.4 \cdot 10^{-29}$ cm² and is $3.1 \cdot 10^{-29}$ cm² for 480-Mev protons [1]. Therefore, the marked increased of $\sigma_{Si^{31}}$ with proton energy cannot be explained by the production of Si^{31} in the secondary reaction $Si^{30}(d, p)Si^{31}$.

The reaction with secondary neutrons $Si^{30}(n, \gamma)Si^{31}$ makes a negligibly small contribution. The cross section for this secondary reaction can be estimated by comparing the cross sections for (α, n), (n, γ) and secondary (α, n)reactions. Considering the above-mentioned (α, n) cross section, the (n, γ) cross section which in the given nuclear region is $1 \cdot 10^{-27}$ cm^2 for neutrons of ≈ 1 Mev [12], and the ratio of the numbers of emitted neutrons and alpha particles, which is 2.5 for 170-Mev excitation [10], we arrive at a value not above $1 \cdot 10^{-30}$ cm^2 for the secondary (n, γ) reaction of the silicon.

The reaction $Si^{30}(p, \pi^+)Si^{31}$. When from $\sigma_{Si^{31}}$ we subtract $0.56 \cdot 10^{-28}$ cm^2 corresponding to the secondary reaction $Si^{30}(d, p)Si^{31}$ the difference will evidently represent the cross section for $Si^{30}(p, \pi^+)Si^{31}$ (Table 1). The values of the latter cross section show a large increase with increasing proton energy, being multiplied by a factor of 22 in the range from 220 to 480 Mev. This is in good agreement with the increase of the cross section for π^+ production in carbon with increasing proton energy [13]. According to these data the π^+ yield at 90° increases 25 times as the proton energy is increased from 240 to 440 Mev. This agreement is a proof of the existence of the $Si^{30}(p, \pi^+)Si^{31}$ reaction.

The dependence of this cross section on proton energy (Fig. 2) has made it possible to determine the reaction threshold. The value obtained for the threshold is ≈ 200 Mev, which corresponds to the threshold for meson production in medium-weight nuclei [14].

The foregoing provides proof, for high energies of the bombarding particles, of the (p, π^+) reaction, which is characterized by the emission of high-energy π^+-mesons. In this reaction the incident proton transfers all of its energy to the nucleus, and this energy is used only for the production of a π^+-meson and for the kinetic energy of the latter. Therefore, the $Si^{30}(p, \pi^+)Si^{31}$ cross section can be used to estimate the pion yield with maximum energy for a given proton energy in the interaction between protons and silicon nuclei.

An attempt to detect the (p, π^+) reaction radiochemically in heavier nuclei such as germanium and bismuth was unsuccessful because of the much greater yield (≈ 100 times greater than $\sigma(p, \pi^+)$) of other radioactive isotopes of these elements from various nuclear reactions.

LITERATURE CITED

[1] A. K. Lavrukhina, Doctoral dissertation, GEOKhI [in Russian] (Inst. Geochem. and Anal. Chem.) (Acad. Sci. USSR, 1955).

[2] S. -C Fung and A. Turkevich, Phys. Rev. 95, 176 (1954).

[3] G. T. Seaborg, I.Perlman and J. M. Hollander, Tables of Isotopes [Russian translation] (IL, 1956).

[4] A. P. Vinogradov, I. P. Alimarin et al., Conference of the Academy of Sciences USSR on the Peaceful Uses of Atomic Energy, June 1-5, 1955, Div. Chem. Sci. [in Russian] (1955), p. 97.

[5] J. Hudis, R. Wolfgang, N. Sugarman, and G. Friedlander, Phys. Rev. 94, 775 (1954).

[6] J. Wilson, Progress in Physics. Cosmic Rays (1952), p. 34.

[7] J. Blatt and V. Weisskopf, Theoretical Nuclear Physics (John Wiley and Sons, New York, 1952) [Russian translation, IL, 1954, p. 387].

[8] Ibid., p. 401.

[9] K. Le Couteur, Proc. Roy. Soc. A63, 259, 489 (1950).

[10] R. Batzel, D. Miller, and G. Seaborg, Phys. Rev. 84, 671 (1951).

[11] B. V. Kurchatov, V. N. Mekhedov et al., Abstracts of Reports at the All-Union Conference on High-Energy Physics [in Russian] (Acad. Sci. USSR Press, 1956), p. 83.

[12] E. Segre (Ed.), Experimental Nuclear Physics (John Wiley and Sons, New York, 1953) [Russian translation, IL, 1955, p. 287].

[13] S. Passman, M. Block, and W. Haveus, Phys. Rev. 88, 1247 (1952).

[14] A. Migdal and Ia. Smorodinskii, Uspekhi Fiz. Nauk 41, 133 (1950).

Received March 3, 1957

V. I. Vernadskii Institute of Geochemistry and Analytic
Chemistry, Academy of Sciences, USSR and Nuclear
Research Institute, Polish Academy of Sciences

ON THE THEORY OF NONSTATIONARY DISCONTINUITIES IN RELAXING FLUIDS

E. V. Stupochenko and I. P. Stakhanov

(Presented by Academician M. A. Leontovich June 3, 1957)

In supersonic flow, as a fluid passes through surfaces of discontinuity there arise states of incomplete statistical equilibrium which require additional parameters for their description. The hydrodynamical equations must in this case be supplemented by equations which describe the relaxational processes. One-dimensional stationary flows including relaxation were considered in [1 and 2]. A theoretically interesting case is that in which the speed of propagation of a very weak shock wave with respect to the undisturbed fluid is less than the velocity c_∞ of high-frequency sound calculated on the assumption that the relaxational processes are "frozen." From simple considerations connected with the characteristics of the Hugoniot adiabat it follows that in this case discontinuity surfaces are not present and that the state of the fluid changes smoothly in a transition region.

However, initial conditions can be realized under which a weak discontinuity arises in a relaxing fluid. In connection with the indicated impossibility of the existence of a stationary pattern of the motion there arises the question of the behavior of such discontinuity and of its degeneration into a smooth transition region. This problem will be examined here analytically.

The hydrodynamical equations supplemented by the equations of the relaxational processes have solutions for small disturbances of the type

$$u(x, t) \simeq e^{i(kx-\omega t)}, \tag{1}$$

where

$$k^2 = \omega^2 \frac{1 - i\omega\tau}{c_0^2 - c_\infty^2 i\omega\tau}; \tag{2}$$

u is the velocity of the fluid in the x direction; ω is the frequency; τ is the relaxation time (considering a single relaxation parameter for simplicity); c_0 and c_∞ are the velocities of sound for extremely small ($\omega t \ll 1$) and extremely large ($\omega\tau \gg 1$) frequencies, respectively [3].

Let us consider a disturbance u(x, t) which satisfies the following initial conditions

$$u(x, 0) = 0 \quad \text{for} \quad x \geqslant 0; \tag{3}$$

$$u(0, t) = \begin{cases} 0 & \text{for} \quad t < 0, \\ u_0 = \text{const} & \text{for} \quad t \geqslant 0. \end{cases} \tag{4}$$

These conditions represent a disturbance propagated in a fluid at rest in a cylindrical tube placed parallel to the x axis, if a piston in the plane x = 0 at time t = 0 instantaneously changes its speed from zero to u_0.

Representing u(0, t) in the form

$$u(0, t) = -\frac{1}{2\pi i}\int\limits_{\Omega} \frac{d\omega}{\omega} e^{i\omega t}, \tag{5}$$

where the integration in the plane of the complex variable ω is taken along the real axis from $-\infty$ to $+\infty$ with a circuit around the origin from above, we obtain on the basis of (1) a solution which satisfies (4), as follows:

$$u(x, t) = -\frac{u_0}{2\pi i}\int_{\frown} \frac{d\omega}{\omega}\, e^{i(kx-\omega t)}. \tag{6}$$

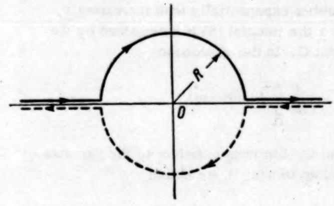

Fig. 1.

In the positive imaginary half plane $k(\omega)$ and the integrand in(6) have no singularities. Therefore, the path of integration in (6) can be moved to infinity in the positive imaginary direction. We then have asymptotically

$$\exp\{i(kx-\omega t)\} \simeq$$
$$\simeq \exp\left\{i\omega\left(\frac{x}{c_\infty} - t\right)\right\}$$

and for $x/c_\infty - t > 0$ the integrand in (6) diminishes exponentially. Thus $u(x, t) \doteq 0$ for $x/c_\infty - t > 0$. Hence we see that the solution of (6) also satisfies (3). Let us consider a disturbance near the line $x - c_\infty t = 0$ and considering the variable $t' = t - x/c_\infty$ to be positive and very small. The path of integration in (6) will be deformed into a semicircle of large radius R, with its center at the point O, and the two parts of the real axis (Fig. 1).

The same integral taken along the path represented by the dashed line vanishes, because as the path of integration is removed to infinity in the downward direction the integrand diminishes exponentially ($t' > 0$). Therefore in (6) the path of integration can be a circle of radius R with its center at O. Expanding $k(\omega)$ in a series with respect to $1/\omega\tau$, assuming $|\omega\tau| \gg 1$ and confining ourselves to terms of the order $1/(\omega\tau)^2$, we obtain

$$u(x,\ t) = u_0 e^{-\frac{1}{2}\frac{\alpha}{c_\infty\tau}x} J_0(-2i\sqrt{\zeta t'}). \tag{7}$$

where $J_0(z)$ is the zero-order Bessel function and

$$\zeta = \frac{1}{2}\,\frac{\alpha}{c_\infty\tau^2}\left(1 - \frac{3}{4}\alpha\right)x, \quad \alpha = 1 - \frac{c_0^2}{c_\infty^2} > 0. \tag{8}$$

It can be shown that (7) is valid for $t' \ll \tau$.

Thus a discontinuity is propagated in the fluid with the velocity c_∞, with its intensity decreasing as the distance x increases according to $e^{-x/l}$, where

$$l = \frac{2c_\infty^2}{c_\infty^2 - c_0^2}\, c_\infty\tau. \tag{9}$$

In the limiting case $c_\infty^2 - c_0^2 = 0$, as would be expected, a stationary shock wave is propagated from the piston.

We shall now change the path of integration of (6) as shown in Fig. 2. The branch points ω_1 and ω_2 of $k(\omega)$ lie on the negative imaginary axis:

$$\omega_1 = -\frac{i}{\tau}; \quad \omega_2 = -\frac{i}{\tau}\,\frac{c_0^2}{c_\infty^2}. \tag{10}$$

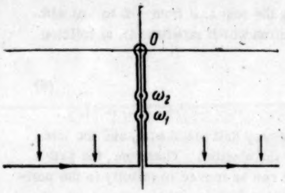

Fig. 2.

When t' is very large the value of $e^{-i\omega t'}$ at the branch points is very small. Therefore the residue of the integral at the pole O is unity. Thus, far from the shock front ($e^{-t'/\tau} \ll 1$)

$$u(x,\ t) = u_0. \tag{11}$$

Let us consider the disturbance at a great distance from the piston. The integrand of (6) for real and nonvanishing ω diminishes exponentially with increasing x, and for very large x the integral (6) is determined by the vicinity of the point O. In the expression

$$\frac{\partial u}{\partial t} = \frac{1}{2\pi} \int_{\Omega} d\omega e^{i(kx - \omega t)} \tag{12}$$

the path of integration can be replaced by the real axis including the point O. Limiting ourselves to the first two terms in the expansion of k in powers of ω, integrating in (12) and proceeding to u(x, t), we obtain

$$u(x,\ t) = \frac{u_0}{2} \Phi\left(\beta \frac{c_0 t - x}{\sqrt{x}}\right) + \frac{u_0}{2}, \tag{13}$$

where

$$\beta = \sqrt{\frac{c_0}{(c_\infty^2 - c_0^2)\tau}} \tag{14}$$

and $\Phi(z)$ is the probability integral.

The result (13) is valid when

$$\frac{c_\infty}{\sqrt{c_\infty^2 - c_0^2}} \sqrt{\frac{c_0 \tau}{x}} \ll 1. \tag{15}$$

We thus see that the region in which the disturbance increases from 0 to u_0 possesses a width Δ of the order

$$\Delta \simeq \frac{1}{\beta} \sqrt{x} \tag{16}$$

and is propagated in the fluid with the speed c_0. The maximum values of $\partial u / \partial x$ lie on the line $x - c_0 t = 0$.

Thus the general picture of the propagation of a disturbance sent out by a piston is as follows: the generated discontinuity is propagated with the velocity c_∞, is damped exponentially with distance and gradually gives way to a smoothly increasing disturbance propagated along the line $x - c_0 t = 0$.

The present analysis was carried through with linearized equations for extremely small disturbances. Inclusion of nonlinear terms is known to lead in the stationary case to a finite width Δ which becomes indefinitely large with disappearing u_0 in accordance with (16).

An analysis from the point of view of the hydrodynamical equations of relaxing fluids (which will be published later) shows that in plane supersonic flow there exist stationary solutions for discontinuities of unlimited smallness of intensity. The absence of stationary discontinuity solutions for small intensities is characteristic only of one-dimensional flows.

LITERATURE CITED

[1] Ia. B. Zel'dovich, J. Exptl.. Theoret. Phys. (USSR) 16, 365 (1946).

[2] S. P. D'iakov, J. Exptl. Theoret. Phys. (USSR) 27, 6, 728 (1954).

[3] L. I. Mandel'shtam and M. A. Leontovich, J. Exptl. Theoret. Phys. (USSR) 7, 438 (1937).

Received May 5, 1957

M. V. Lomonosov Moscow State University

ON THE FLUCTUATIONS OF THE PARAMETERS OF CERTAIN LINEAR SYSTEMS

V. I. Bespalov

(Presented by Academician M. A. Leontovich June 8, 1957)

1. A specific characteristic of the scattering of waves propagated in a shielded transmission line containing random inhomogeneities is the fact that the secondary waves (re-emitted by the inhomogeneities) are channeled along the same route as the primary wave. For sufficiently large wavelength the secondary field (i. e., the amplitudes of the reflected wave and of other modes arising through retransformation) can be comparable with the field of the primary wave. For this reason the perturbation method which is usually employed in scattering problems [1, 2], and which neglects the secondary re-emission of scattered waves, is inadequate for the solution of some problems concerning the influence of random inhomogeneities on the characteristics of a transmission line.

Similar difficulties arise in some other problems concerning the effect of random variations of the parameters on the performance of a linear system. Examples are: a filter (or delay line) where the parameters of the sections exhibit a certain random spread around their rated values; a traveling wave tube with a retarding system containing random imperfections; an oscillatory circuit whose parameters vary in jumps of random magnitude, etc. The solutions of such problems can be reduced under certain assumptions (see [3], for example) to the investigation of a set of linear difference equations:

$$Y_j(n) = A_{jk}(n)\, Y_k(n-1), \quad j, k = 1, 2, \ldots, L, \tag{1}$$

where the coefficients are random functions of n.

It is very difficult to determine the most complete characteristics of the random process $Y_j(n)$, the distribution of the probability density $W(Y_j, n)$. This can be done only by investigating the general solution of (1) or by solving the corresponding differential-difference equations for W. However, in many cases the required information concerning a random process is given by correlation functions and moments.

The present paper gives a general solution of (1) and a relatively simple method of calculating correlation functions and moments. As an example we shall consider a network of simple L sections and an oscillatory circuit with fluctuating parameters.

2. For the purpose of solving a set of linear difference equations with variable coefficients we can use the method of successive approximations. In distinction from differential equations, which in each case require proof of the convergence of a series of approximations, we can here select a zero approximation such that in each bounded interval a finite number of successive approximations leads to an exact solution. It is evident that an initial assumption of small perturbations of the coefficients becomes unnecessary.

Let us write the coefficients of (1) in the form

$$A_{jk}(n) = A^0_{jk} + \mu a_{jk}(n). \tag{2}$$

The solution of (1) which satisfies the initial conditions

$$Y_j(n)|_{n=0} = C_j, \tag{3}$$

will be sought as a series in powers of μ, as follows:

$$Y_j(n) = \sum_{s=0}^{\infty} \mu^s Y_j^{(s)}(n). \tag{4}$$

Then, substituting (4) into (1) and grouping powers of μ, we obtain

$$Y_j^s(n) = A_{jk}^0 Y_k^{(s)}(n-1) + a_{jk}(n) Y_k^{(s-1)}(n-1). \tag{5}$$

If we require that $Y_j^{(0)}(n)$ satisfy the initial conditions (3) it can easily be seen that the series terminates with s = n, because all $Y_j^{(s)}$ with s > n vanish identically. Indeed, $Y^{(s)}(0) \equiv 0$ for s > 0 from the choice of the zero order approximation. It is seen from (5) that $Y_j^{(s)}(n) = 0$ when $Y_j^{(s-1)}(n-1) = 0$ and $Y^{(s)}(n-1) = 0$. It follows by induction that $Y^{(s)}(n) \equiv 0$ for s > n.

By suitably selecting C_j we can satisfy any boundary conditions (not necessarily for n = 0).

For example, the general solution of the second-order equation with a single variable coefficient,*

$$Y(n+1) - \{\Phi_0 + P(n)\} Y(n) + Y(n-1) = 0, \tag{6}$$

as obtained by successive approximations, is

$$\begin{aligned} Y(n) = Ae^{j\varphi_0 n} &\times \\ \left\{1 + \sum_{s=1}^{n-1} (2j\sin\varphi_0)^{-s} \sum_{f_s=1}^{n-1} \sum_{f_{s-1}=1}^{f_s-1} \cdots \sum_{f_1=1}^{f_2-1} \prod_{m=1}^{s} P_{f_m} \left[e^{j2\varphi_0(f_m - f_{m+1})} - 1\right]\right\} &+ \\ + Be^{-j\varphi_0 n} &\times \\ \left\{1 + \sum_{s=1}^{n-1} (2j\sin\varphi_0)^{-s} \sum_{f_s=1}^{n-1} \sum_{f_{s-1}=1}^{f_s-1} \cdots \sum_{f_1=1}^{f_2-1} \prod_{m=1}^{s} P_{f_m} \left[1 - e^{-j2\varphi_0(f_m - f_{m+1})}\right]\right\}&, \end{aligned} \tag{7}$$

where A and B are arbitrary constants and $\varphi_0 = \arccos(\Phi_0/2)$.

When the P(n) are relatively small ($\mu \ll 1$) it is possible in many cases to stop at the first [3] or second approximation.

An increase of the order of a difference equation (or of the set of equations) and complication of the coefficients further complicates the solution and limits its applicability to random processes. However, when the number of sections is small (as in filters) a general solution such as (7) can be used successfully to investigate perturbations caused by random variations of the parameters of the sections.

3. The average characteristics** of the quantities described by (1) can be found simply when the $Y_j(n)$ process is a simple Markoff chain. This occurs when

a) The random functions $A_{jk}(n)$ are uncorrelated;*** i. e.,

---

* Such an equation is obtained in the investigation of a network of four-pole sections with variable series resistance or with variable shunt capacitance.

** Here and hereinafter averaging over the ensemble is intended.

*** When correlation exists in a finite region, i. e., when (8) is fulfilled only for $|m - n| \geq \nu \neq 0$, the $Y_j(n)$ process is a complex Markoff chain. This can be reduced to a simple chain [4], but the equations become considerable more complicated.

$$\overline{A_{jk}(n)\,A_{lp}(m)} = \overline{A_{jk}(n)}\;\overline{A_{lp}(m)}\,; \tag{8}$$

b) The boundary (initial) conditions are given for the same value of n, such as n = 0,

$$Y_j(n)\,|_{n=0} = Y_j^0. \tag{9}$$

The equations and initial conditions for $\overline{Y_j(n)}$ are then obtained immediately by averaging (1) and (9), i. e.,

$$\overline{Y_j(n)} = \overline{A_{jk}(n)}\;\overline{Y_k(n-1)}; \quad \overline{Y_j(n)}\,|_{n=0} = Y_j^0. \tag{10}$$

Thus the average values of the $\overline{Y_j(n)}$ in networks with random parameters subject to conditions (8) and (9) are distributed like the values of $Y_j(n)$ in a network with average values of the parameters $\overline{A_{jk}(n)}$ and averaged initial conditions.*

Under the same conditions (8) and (9) the equations for the average values of the products $\overline{Y_j(n)\,Y_k^*(n)} = \xi_{jk}(n, 0)$ are obtained after averaging the products of the equations (of the right and left sides, respectively) in (1) by the conjugate complex equations.** We thus obtain the L^2 equations

$$\xi_{jk}(n, 0) = \overline{A_{jl}(n)\,A_{kp}^*(n)}\,\xi_{lp}(n-1, 0). \tag{11}$$

If the elements of the matrix of the coefficients in (11) are independent of n, then, assuming*** $\xi_{jk}(n, 0) = \xi_{jk}(0, 0)\,\alpha^n$, from the condition that a nontrivial solution exists we have

$$\det\left|\overline{A_{jl}(n)\,A_{kp}^*(n)} - \alpha\delta_{jl}\delta_{kp}\right| = 0, \tag{12}$$

where δ_{qf} is the Kronecker symbol. Equation (12) determines the L^2 values of α and thus L^2 linearly independent solutions of $\xi_{jk}(n, 0)$ which can be used to satisfy the initial conditions

$$\xi_{jk}(n, 0)\,|_{n=0} = \overline{Y_j^0 Y_k^{0*}}. \tag{13}$$

Multiplying (1) by $Y_k^*(n-m)$ and averaging, for the correlation functions $\xi_{jk}(n, m) = \overline{Y_j(n)\,Y_k^*(n-m)}$ we obtain L sets of equations (since the subscript k takes values from 1 to L), each consiting of L difference equations:

$$\xi_{jk}(n, m) = \overline{A_{jl}(n)}\,\xi_{lk}(n-1, m-1). \tag{14}$$

The solution of (14) with known $\xi_{jk}(n, 0)$ is obtained simply. It is similarly possible to calculate moments of higher orders.

4. The distribution of the mean square modulus of the voltage in a network of simple L sections with fluctuating series resistances ($X_n = X_0\left\{1 + P(n)\right\}$), which is obtained by the foregoing method upon the asumption

---

* We note that, generally speaking, the average values of the voltage and current in an ensemble of networks of quadripoles which are lossless can increase or decrease exponentially.

** The equations for second moments (or other average quantities) can also be derived otherwise. Specifically, we can use differential-difference equations, which will here be of infinite order, for the transition probabilities, or go over from the difference equation (1) to a summation equation (the analog of an integral equation), and employ the method used in [5] to investigate an integral equation with a random kernel. The method employed here obtains the required result more briefly.

*** When the statistical properties of the A_{jk} depend on n (for example, random perturbations are imposed on a given $A_{jk}(n)$), then $\overline{A_{jl}(n)\,A_{kp}^*(n)} \neq \text{const}$ and the solution of (11) has the form of a finite number of multiple sums (§ 2). The difficulty of investigating the solution in each specific case will be determined by the way in which A_{jk} depends on n.

that P (n) P (m) = $p^2\delta_{nm}$, $p^2 \ll 1$, and that the output load is matched, is as follows:*

$$\overline{|V(n)|^2} \simeq |V_0^2| \left\{ \left(1 - p^2 \operatorname{tg}^2 \frac{\varphi}{2}\right) \exp\left(2p^2 n \operatorname{tg}^2 \frac{\varphi}{2}\right) - - p^2 \operatorname{tg}^2 \frac{\varphi}{2} \frac{\sin(2n-1)\varphi}{\sin\varphi} \cdot \exp\left(-p^2 n \operatorname{tg}^2 \frac{\varphi}{2}\right) \right\}, \tag{15}$$

where φ is the phase shift for one quadripole. It follows from (15) that for large n the value of $\overline{|V^2(n)|}$ increases exponentially. Similarly, the mean square modulus of the current in an oscillatory circuit with a capacitance fluctuating according to $C(t) = C_0\{1 + P(n)\}^{-2}$, where t is the time and n is the integral part of t/τ, is given by

$$\overline{|I^2(n)|} \simeq I_0^2 \left\{ \left[1 - p^2 \left(\sin^2 \omega\tau - \frac{\omega\tau \sin 2\omega\tau}{2\sin^2 \omega\tau}\right)\right] \exp(2p^2 n \sin^2 \omega\tau) - - p^2 \left[\frac{\sin^2 \omega\tau \cdot \sin 2(n-1)\omega\tau}{\sin 2\omega\tau} + \frac{\omega\tau \cos(2n+1)\omega\tau}{\sin \omega\tau}\right] \exp(-p^2 n \sin^2 \omega\tau) \right\}, \tag{16}$$

where ω is the resonance frequency of an ideal circuit and τ is the time during which the capacitance varies.

Equation (16) shows that due to the fluctuations of the capacitance the stored energy in the ensemble of circuits increases with time, and that as $t \to \infty$ the maxima of $\left.{}^1/_2 L \overline{|I^2(t,\ \tau)|}\right|_{t=\mathrm{const}}$ are observed for τ satisfying the equation $2\omega\tau \cot \omega\tau = 1$. The latter equation coincides with the condition for the maximum of the mean square density of the spectral amplitude of C (t) at one of the frequencies corresponding to parametric resonance [6]. The results can easily be extended to systems with randomly varying integrals of τ.

5. The foregoing method of calculating average values can be used not only to study systems with stepped changes of the parameters, but can also be applied to systems with continuous fluctuations if the form of the latter (in space or time) can with some accuracy be regarded as repeating itself. For example, the method can be used to estimate the effect of inhomogeneities in cylindrical transmission lines [7].

In conclusion the author wishes to thank A. V. Gaponov for suggestions.

LITERATURE CITED

[1] S. M. Rytov, Izv. Akad. Nauk SSSR, Ser. Fiz. 2, 223 (1937).

[2] H. Booker and W. Gordon, Proc. Inst. Radio Engrs. 38, 4, 401 (1950).

[3] V. I. Bespalov and A. V. Gaponov, Radiotekhnika i Elektronika 1, 6, 772 (1956).

[4] T. A. Sarymsakov, Elements of the Theory of Markovian Processes [in Russian] (Moscow, 1954).

[5] A. Rosenbloom, J. Heilfron and D. L. Trautman, Inst. Radio Engrs. Convent. Rec. 3, 4, 106 (1955).

[6] A. A. Andronov and M. A. Leontovich, J. Russ. Phys.-Chem. Soc., Physics Section 59, 5-6, 429 (1927).

[7] M. D. Didlandis and H. Kaden, Elektrische Nachr. Tech. 14, 1, 13 (1937); P. Mertz and W. Pfleger, Bell System Tech. J. 16, 541 (1937).

Received May 3, 1957

Radio-Physical Research Institute, (N. I. Lobachevskii)
Gorky State University

---

* 'tg' ≡ 'tan' – Publisher.

THE THERMODYNAMICS OF ALMOST PERFECTLY ORDERED SOLID SOLUTIONS

M. A. Krivoglaz

(Presented by Academician M. A. Leontovich June 8, 1957)

The statistical theory of solid solutions makes use of a number of crude hypothetical models. However, the results pertaining to certain portions of the phase diagram can be obtained with greater confidence from a thermodynamical theory which does not employ a specific model of the solution. When the order-disorder transition is a second-order phase transition, for temperatures close to the transition temperature these results are obtained in Landau's theory of second-order phase transitions [1, 2]. A thermodynamical examination can also be carried through considerably below the transition temperature when the solution is in almost perfectly ordered state. In this case "strange" atoms at the sites of each sublattice form a corresponding weak solution and the free energy can easily be determined from considerations of the same kind as in the calculation of the free energy of weak solutions (see [2], for example). For binary (A–B) solutions with n_1 sites of the first kind and n_2 sites of the 2nd kind in a unit cell, with the proportions close to the stoichiometric constitution $A_{n_1}B_{n_2}$, we obtain

$$F = F' + \frac{n_1}{n} N\chi_1 p_{B1} + \frac{n_2}{n} N\chi_2 p_{A2} + kT\frac{N}{n}[n_1(p_{A1}\ln p_{A1} + p_{B1}\ln p_{B1}) + n_2(p_{A2}\ln p_{A2} + p_{B2}\ln p_{B2})] + N(p_{B1}^2 e_{11} + 2p_{B1}p_{A2}e_{12} + p_{A2}^2 e_{22}). \qquad (1)$$

Here N is the total number of atoms in the crystal; $n = n_1 + n_2$; $p_{\alpha i}$ is the probability that sites of the i-th kind will be replaced by α atoms, which can be expressed in terms of the atomic concentration c_A of A atoms and the degree of long-range order η by means of the relations $p_{A1} = c_A + \frac{n_2}{n}\eta = 1 - p_{B1}$; and $p_{A2} = c_A - \frac{n_1}{n}\eta = 1 - p_{B2}$; F', χ_1, χ_2 and e_{ij} depend only on the temperature and volume and are independent of the composition and degree of long-range order.

In Eq. (1) F' denotes the free energy of a perfectly ordered solution at temperature T' in a metastable state; the 2nd and 3rd terms account for the change of free energy when "strange" atoms are "localized" at definite sites of the lattice; the 4th term allows for the possibility of permutating the atoms of each kind; and, finally, the last term is determined by the interactions of atoms at strange locations. We ignore higher terms in the expansion of F in powers of p_{B1} and p_{A2}. When T ⟶ 0 the values of χ_1 and χ_2 approach the finite limits χ_1^0 and χ_2^0.

Applying the Nernst heat theorem to a metastable state of a solid solution in which atoms at "strange" sites are "frozen" and "localized" (in the free energy of such a system the first three terms of (1) are unchanged, the 4th term disappears and the small last term changes), it is easily seen that the derivatives $\partial\chi_1/\partial T$ and $\partial\chi_2/\partial T$ approach zero as T ⟶ 0. In order to have perfect ordering of a solution of stoichiometric constitution at absolute zero, the products $p_{B1}e_{1i}$ and $p_{A2}e_{i2}$ (i = 1, 2) must be negligibly small at very low temperatures. Therefore, considerably below the order-disorder transition temperature in deriving the equation for the degree of long-range order the last term in (1) may be neglected. This equation is determined by the extremum of the free energy with respect to changes of η and is given by

$$\frac{\left(c_A - \frac{n_1}{n}\eta\right)\left(c_B - \frac{n_2}{n}\eta\right)}{\left(c_A + \frac{n_2}{n}\eta\right)\left(c_B + \frac{n_1}{n}\eta\right)} = \exp\left[-\frac{\chi_1 + \chi_2}{2kT}\right]. \qquad (2)$$

It follows from (2) that for a solution of stoichiometric constitution ($c_A = n_1/n$) the degree of long-range order at low temperatures approaches unity exponentially:

$$1 - \eta = \frac{n}{\sqrt{n_1 n_2}} \exp\left[-\frac{\chi_1^0 + \chi_2^0}{2kT}\right]. \tag{3}$$

The fact that the exponential in (3) is multiplied by exactly $n/\sqrt{n_1 n_2}$ results from the absence of linear terms in the T expansions of χ_1 and χ_2 and is a consequence of Nernst's theorem. Equation (3) is also approximately valid for solutions in which the departure $|\Delta c_A|$ from stoichiometric proportions is considerably smaller than the departure $\Delta\eta$ of the degree of long-range order from the maximum possible in a solution of the given constitution. When the opposite inequality $\Delta\eta \ll |\Delta c_A|$ is satisfied the degree of long-range order again varies exponentially with the temperature but with an exponent which is twice as large at any given temperature and a considerably larger coefficient:

$$\eta = 1 - \frac{n}{n_2}\Delta c_A - \frac{1 - \frac{n}{n_2}\Delta c_A}{\Delta c_A} \exp\left[-\frac{\chi_1^0 + \chi_2^0}{kT}\right] \quad \text{for} \quad \Delta c_A > 0,$$

$$\eta = 1 + \frac{n}{n_1}\Delta c_A + \frac{1 + \frac{n}{n_2}\Delta c_A}{\Delta c_A} \exp\left[-\frac{\chi_1^0 + \chi_2^0}{kT}\right] \quad \text{for} \quad \Delta c_A < 0. \tag{4}$$

When the transition temperature is very high the solution is almost perfectly ordered even at relatively high temperatures (of the same order as the Debye temperature or higher), when the consequences of Nernst's theorem cannot be utilized. In (3) and (4), instead of the constant quantity $\chi_1^0 + \chi_2^0$ the function $\chi_1 + \chi_2$ appears, which is slightly temperature dependent, whereas in the usual approximation of statistical ordering theory it is entirely independent. Since at temperatures different from zero the derivative of this function with respect to T is generally not zero, the expressions before the exponentials in (3) and (4) can differ from $n/\sqrt{n_1 n_2}$ and $1/|\Delta c_A|$, respectively, by some factors which are usually of the order of unity.

In the general case, when the inequalities $|\Delta c_A| \ll \Delta\eta$ and $|\Delta c_A| \gg \Delta\eta$ are not satisfied, the temperature and concentration dependence of η considerably below the transition temperature and close to stoichiometric composition is given by (2). For a given temperature the degree of long-range order in solutions whose composition is close to AB must be a maximum for stoichiometric proportions. It is interesting that the elementary ordering theory of Gorskii, Bragg and Williams does not hold true at high temperatures but rather at low temperatures. (In an almost perfectly ordered solution as well as considerably above the ordering temperature the correlation in the solution becomes unimportant.)

It must be noted that for a nonstoichiometric solution the foregoing discussion is unsuitable at very low as well as at very high temperatures, because in the former case when deriving the equation for η it is also impossible to neglect the last term in (1). (One of the probabilities p_{B_1} and p_{A_2} for nonstoichiometric solutions approaches a constant value while at lower temperatures e_{ij} can increase.) At such temperatures the solution must begin to separate into an ordered phase which is closer to stoichiometric constitution than the initial solution, and a disordered phase (or an ordered phase of different superstructure). As absolute zero is approached the equilibrium composition of the ordered phase must evidently approach the stoichiometric value, while the precipitated phase will be a pure metal or a perfectly ordered phase of different constitution. The quantitative investigation of these questions requires special study. The lower temperature limit for the applicability of the foregoing approximation is lowered as $|\Delta c_A|$ is reduced and becomes zero for stoichiometric solutions. This limit is considerably below the limit for (3).

Substituting (3) and (4) into (1), it is easily seen that at low temperatures the configurational part of the free energy $F - F'$ is proportional to the exponential factor $\exp\left[-\frac{\chi_1^0 + \chi_2^0}{2kT}\right]$ or $\exp\left[-\frac{\chi_1^0+\chi_2^0}{kT}\right]$, subject to the condition $\Delta\eta \gg |\Delta c_A|$ or $\Delta\eta \ll |\Delta c_A|$, respectively. This kind of exponential temperature dependence is possessed by the configurational parts of the energy, entropy, specific heat and the two thermodynamical functions.

Since F' and the analogous terms in the other thermodynamical functions, for a perfectly ordered solution, at low temperatures increase with temperature according to a power law, the configurational parts of the thermodynamical quantities at very low temperatures play a very unimportant part in the thermal effects. The exponential temperature dependence in these instances will appear in those properties of the solutions which depend essentially on the arrangement of the different kinds of atoms at lattice sites. In an investigation of the residual electrical conductivity of an ordered alloy quenched from different temperatures that are low compared with the transition temperature, this will apply to the intensities of diffuse x-ray and neutron scattering, etc.

It must be emphasized that all of the results above apply to the equilibrium state. They can be tested experimentally (with sufficient annealing times) in alloys which while almost perfectly ordered at low temperatures retain high atomic mobility, such as β-brass (especially after irradiation with fast particles, which greatly accelerates various processes in the crystal) and also in alloys with high order-disorder transition temperatures (above the melting point), such as AuZn and some intermetallic compounds.

LITERATURE CITED

[1] L. D. Landau, J. Exptl. Theoret. Phys. (USSR) 7, 19 (1937).

[2] L. D. Landau and E. M. Lifshits, Statistical Physics [in Russian] (Moscow, 1951).

Received January 7, 1957

Institute of Metal Physics, Academy of Sciences,
Ukrainian SSR

ON THE RELATIONSHIP BETWEEN FLUORESCENCE FREQUENCIES AND THE EFFECTIVENESS OF CERTAIN QUENCHERS

V. V. Zelinskii, V. P. Kolobkov and N. I. Kondaraki

(Presented by Academician A. N. Terenin June 6, 1957)

In [1] it is noted that some compounds show a relationship between the location of their fluorescence spectrum and their liability to quenching by potassium iodide and aniline. The discovery of this relation is of fundamental importance in questions concerning the mechanism of fluorescence quenching in solutions by foreign substances and in the spectroscopy of complex organic molecules. In [1] the quantity used to characterize fluorescence quenching by impurities was the ratio between the fluorescence yields of an unquenched solution and a solution containing a specific concentration of the impurity. No account was taken of the duration of the excited state nor of the viscosity of the solvent as factors which could influence the quenching.

In the present paper we have undertaken a quantitative study of the relation between the influence of impurities on the duration of the excited state and the location of the fluorescence spectrum. The effectiveness of the quencher is expressed by*

$$k = \frac{(\tau_1 - \tau_2)\,\eta}{\tau_1 \tau_2 c}; \qquad (1)$$

where τ_1 is the duration of the excited state in the absence of the quencher, τ_2 is the duration after a given concentration of the quencher is added, c is the concentration of the quencher in moles/liter and η is the viscosity of the solvent in poises.

The duration of the fluorescence was determined by a GOI (State Optical Institute) phase fluorometer [2].** Only τ_1 was measured directly. For the determination of τ_2 the vessel containing the quenched solution replaced the scatterer of exciting light which is ordinarily used in determining fluorescence duration. Thus the quantity measured directly was the phase difference of modulated flourescent light of quenched and unquenched solutions. By subtracting this quantity from the phase difference between unquenched modulated fluorescence and the exciting light we found the phase lag which corresponds to the fluorescence duration of the quenched solution. This method of determining τ_2 and $\Delta\tau = \tau_1 - \tau_2$ considerably improves the accuracy of the determination of the quenching effectiveness.

The accuracy of this determination of the effectiveness can be exemplified by 4-acetylamino-N-methylphthalimide in methyl alcohol acted on by potassium iodide. As is seen from Table 1, over a broad range of quencher concentrations the value of the effectiveness is fairly constant from measurement to measurement. In the cases of low fluorescence intensities or short durations and also when the radiation is too far in the red or ultraviolet regions of the spectrum, where the photomultiplier was relatively insensitive, the effectiveness was determined with considerably less accuracy.

---

* The probability q_2 of nonradiative deactivation of an excited state by a quencher is proportional to the concentration of the quencher and in first approximation is proportional to the viscosity of the solvent (η), i. e., $q_2 = kc/\eta$. In this equation the coefficient k is the effectiveness of the quencher; q_2 can be expressed in terms of the durations of the excited states $\tau_1 = 1/p + q$, $\tau_2 = 1/p + q_1 + q_2$, where p is the probability of a radiative transition from an excited state to the ground state and q_1 is the probability of nonradiative deactivation of the excited state in the absence of a quencher.

** The authors are very grateful to A. M. Bonch-Bruevich for making the fluorometer available and to G. A. Tishchenko, V. I. Shirokov and V. A. Molchanov for assistance in the use of the fluorometer.

TABLE 1

Effectiveness of Potassium Iodide on the Fluorescence of 4-Acetylamino-N-methylphthalimide in Methyl Alcohol at Various Quencher Concentrations ($\tau_1 = 19.8 \cdot 10^{-9}$ sec)

c mole/l	$\tau_2 \cdot 10^9$ sec	$\Delta\tau \cdot 10^9$ sec	$k \cdot 10^{-9}$	$\Delta k \cdot 10^{-9}$ from av.	Δk, % from av.
0 55	4.45	15.35	5.09	0.04	1
0.215	8.55	11.25	4.95	0.10	2
0.140	11.25	8.55	4.41	0.64	12.5
0.105	11.9	7.9	5.00	0.05	1
0.037	15.6	4.2	5.82	0.77	15
			5.05		

As quenching impurities we used triethylamine iodide and potassium iodide, aniline and diethylaniline. We investigated the influence of these impurities on the fluorescence duration of a number of 3-, 4- and 3, 6-derivatives of phthalimide in various solvents: water, acetone, methyl, ethyl and butyl alcohol, ethyl acetate, pyridine, anisole, benzene, chlorobenzene and n-octane. The results are shown in Table 2. Figures 1 and 2 show the dependence of the quenching effectiveness on the location of the fluorescence spectra of the various solvents and different phthalimide derivatives. In all cases the effectiveness increases with the frequency of the fluorescence peak. Most of the points which characterize the relation between the effectiveness and the location of the fluorescence spectrum for each substance in different solvents fit on a single almost straight line. Thus this relation between the effectiveness and the spectrum not only exists but is determinative; the influence of other solvent properties on the effectiveness is relegated to the background.

TABLE 2

Effectiveness of Aniline and Triethylamine Iodide on the Fluorescence of Phthalimide Derivatives. The Solvents are Numbered as Follows for Aniline Quenching: 1) ethyl acetate, 2) pyridine, 3) chlorobenzene, 4) benzene, 5) n-octane. For quenching by triethylamine iodide the solvents are numbered as follows: 1) butyl alcohol, 2) ethyl acetate, 3) pyridine, 4) acetone, 5) anisole

	Aniline					Triethylamine iodide				
Substance	solvent	$\tau_1 \cdot 10^9$, sec	$\Delta\tau \cdot 10^9$, sec	c, mole/l	$k \cdot 10^9$	solvent	$\tau_1 \cdot 10^9$, sec	$\Delta\tau \cdot 10^9$, sec	c mole/l	$k \cdot 10^{-9}$
3-Amino-N-methylphthalimide	1	14.1	9.3	1.835	3.29	1	13.25	0.55	2.29	0.97
	2	12.65	5.40	1.60	3.35	2	12.3	3.75	1.835	2.0
	3	11.35	6.80	1.70	5.95	3	12.65	3.55	2.265	2.92
	4	15.05	8.60	1.925	4.8	4	13.6	6.05	2.125	2.03
	5	—	—	—	—	5	13.15	3.15	1.14	6.39
4-Amino-N-methylphthalimide	1	18.0	10.9	1.835	2.0	1	11.1	0.4	2.28	1.0
	2	17.35	6.95	1.60	2.19	2	18.0	6.35	1.89	1.65
	3	18.30	13.15	1.70	6.3	3	17.35	6.5	2.08	3.58
	4	19.7	15.15	1.92	5.3	4	17.5	9.15	2.125	2.17
	5	12.75	9.35	1.42	7.85	5	18.1	8.1	1.315	8.50
3,6-Diacetylamino-N-methylphthalimide	1	12.0	8.05	1.835	3.97	1	10.3	3.05	2.28	1.22
	2	10.9	3.75	0.74	5.56	2	11.25	2.85	1.78	2 27
	3	10.6	6.4	1.70	6.5	3	10.9	3.3	2.285	3.79
	4	—	—	—	—	4	10.9	5.3	2,125	3.01
	5	10.8	7.25	1.42	6.8	5	12.85	3.10	1.315	4.95
3-Monomethylamino-N-methylphthalimide	1	11.9	6.8	1.835	2.62	1	—	—	—	—
	2	9.75	3.15	1.60	3 65	2	11.9	1.95	0.97	2.1
	3	13.05	7.95	1.70	5.4	3	8.75	2.55	2.08	2.48
	4	14 1	9 5	1.925	4.75	4	—	—	—	—
	5	2.7	0.95	1.42	7.3	5	14.0	3.65	1.42	5.3

From the relations thus far obtained we distinguish the values of the quenching effectiveness of potassium iodide on the fluorescence of aqueous solutions (Fig. 2A). This probably results from the considerably greater dissociation of potassium iodide in water than in other solvents. In some instances the effectiveness of the quencher in acetone solutions is lower than could be expected.

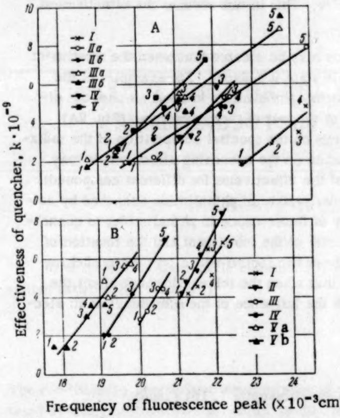

Fig.1. Dependence of the quenching effectiveness of aniline on the location of the fluorescence spectrum. A: I) 4-acetylamino-N'-methylphthalimide; IIa, b) 4-amino-N-methylphthalimide (b – quenching by diethylaniline); IIIa) 4-monomethylamino-N-methylphthalimide; IIIb) 4-dimethylamino-N-methylphthalimide; IV) 3-amino-N-methylphthalimide; V) 3-monomethylamino-N-methylphthalimide.
B: I) 3,6-diacetylamino-N-methylphthalimide; II) 3-methylacetylamino-6-acetylamino-N-methylphthalimide; III) 3-methylacetylamino-6-amino-N-methylphthalimide; IV) 3-acetylamino-6-amino-N-methylphthalimide; Va) 3-dimethylamino-6-methylacetylamino-N-methylphthalimide; Vb) 3-dimethylamino-6-acetylamino-N-methylphthalimide. For the numerals 1-5 see Table 2.

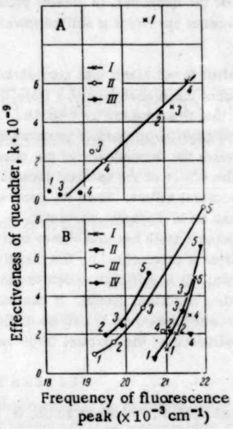

Fig. 2. Dependence of the quenching effectiveness of potassium iodide and triethylamine iodide on the location of the fluorescence spectrum. A. Quencher – potassium iodide: I) 3,6-diacetylamino-N-methylphthalimide; II) 3-acetylamino-6-amino-N-methylphthalimide; III) 3,6-diamino-N-methylphthalimide. Numbering of the solvents: 1) water, 2) methyl alcohol, 3) ethyl alcohol, 4) acetone. B. Quencher – triethylamine iodide: I) 3,6-diacetylamino-N-methylphthalimide; II) 3-amino-N-methylphthalimide; III) 4-amino-N-methylphthalimide; IV) 3-monomethylamino-N-methylphthalimide. For the numerals 1-5 see Table 2.

The identical character of the relation between the quenching effectiveness and fluorescence spectrum in the cases of potassium iodide, triethylamine iodide* and aniline indicates that the quenching effect of aniline as well as of the iodides [3] lies in an increase of the probability of a transition into a metastable state, despite the fact that when aniline was added no increase of the absolute fluorescence yield could be observed.

The slopes of the straight lines which express the relation between the effect of a quencher on an excited state and the location of the fluorescence spectrum are almost identical in all 4-derivatives, in all 3-derivatives and in all 3,6-derivatives. In the 4-derivatives the angles are smallest and in the 3,6-derivatives the angles are greatest. This appears most clearly in quenching by aniline and less clearly in the case of triethylamine iodide. The same order of effectiveness is shown by aniline, potassium iodide and triethylamine iodide.

In 3- and 4-derivatives the straight lines lie higher as the substituent becomes a better electron donor, i. e., at the same frequency the effectiveness for amino-derivatives of phthalimide is greater than for acetylamino derivatives, and is greater in methyl and dimethylamine derivatives than in amino derivatives. This rule is less consistently followed in 3,6 substitution derivatives, but even in this case at a given frequency the effectiveness for 3,6-diacetylamino-N-methylphthalimide is less than for 3-methylacetylamino-6-acetylamino-N-methylphthalimide, and for the latter is less than for 3-acetylamino-6-amino-N-methylphthalimide. Thus two opposing tendencies are clearly revealed: greater electron-donating capacity of a substituent leads to a greater effectiveness of the quencher, to greater probability of a transition to a metastable state, and at the same time the fluorescence spectrum is shifted toward lower frequencies. This in turn reduces the effectiveness of the quencher.

---

* Because of the low solubility of potassium iodide in the majority of organic solvents we used triethylamine iodide as a quencher.

If the spectral shift is not taken into consideration the impression may be created that when the substituent is a better electron donor the probability of a transition to a metastable state is reduced. For example, in the series 3,6-diacetylamino, 3-acetylamino-6-amino, 3,6-diamino-N-methylphthalimide in ethyl alcohol the effectiveness of potassium iodide diminishes successively from the first to the last of these substances (Fig. 2A). In actuality this expresses the dependence of the quenching effectiveness on the spectral composition of the radiation. In other cases the effect of the spectral location of the fluorescence on the quenching effectiveness may be disguised by a structural effect. Then the succession of changes of the effectivenss for different compounds in the same solvent can be of different character, as in the case of 4-derivatives of phthalimide quenched by aniline (Fig. 1A). The present work has thus shown that the susceptibility of fluorescence in phthalimides to quenching by various impurities is determined by the electron-donating capacity of the substituent and the location of the fluorescent spectrum. It is difficult to determine to what extent these two factors will affect the quenching of compounds from other chemical groups. It can only be mentioned that when the solvent does not affect the location of the fluorescence spectrum it will be difficult to distinguish the influence of the substituent as an electron donor from the influence of the spectral frequency.

LITERATURE CITED

[1] V. V. Zelinskii, V. P. Kolobkov and L. G. Pikulik, Optika i Spektroskopiia 1, 161 (1956).

[2] A. M. Bonch-Bruevich, Uspekhi Fiz. Nauk 58, 85 (1956).

[3] V. V. Zelinskii and V. P. Kolobkov, Optika i Spektroskopiia 1, 560 (1956).

Received May 28, 1957

CALCULATION OF THE ELECTRICAL CONDUCTIVITY OF SEMICONDUCTORS WITH HIGH IMPURITY CONTENT

R. Zigenlaub

(Presented by Academician N. N. Bogoliubov, July 3, 1957)

The method of the kinetic equation is only applicable, as we know [1], when the relaxation time of the system satisfies the inequality

$$\tau \gg h / \varkappa T. \tag{1}$$

The condition(1) greatly restricts the range of applicability of this method; for example, when carriers are scattered by charged impurities according to the Conwell-Weisskopf formula [2] low temperatures and high impurity contents are excluded. At concentrations of the order of 10^{18} cm^{-3} (1) is not fulfilled even at room temperature! It is therefore advantageous to employ a new method of calculating electrical conductivity [3-5], which is not dependent on the use of the kinetic equation.

It can easily be shown that the electrical conductivity of an isotropic system in a constant field is given by

$$\sigma = \int_0^\infty \varphi(\tau) d\tau, \quad \varphi(\tau) = \beta \operatorname{Re} \operatorname{Sp}[\rho j j(\tau)], \tag{2}$$

where $\varphi(\tau)$ is the relaxation function of the system and

$$\rho = \exp(-\beta H) / \operatorname{Sp}(\exp(-\beta H)), \quad j(\tau) = \exp(i\tau H / \hbar)\, j \exp(-i\tau H / \hbar). \tag{3}$$

Here H is the Hamiltonian of the system in the absence of the field; $\underline{j}$ is the current operator; $\beta = 1/\kappa T$. The volume of the system is taken as unity.

However, in [3, 4] for specific calculations limitations are imposed which are equivalent to (1). In the present paper the method of [3-5] is used to investigate the scattering of current carriers by charged impurities. It is important that restrictions such as (1) can be avoided.

§1. General equations. Let there be current carriers of one kind, which to be specific we shall call electrons. The Hamiltonian of the system is

$$H = H_0 + H', \quad H_0 = \sum_{\mathbf{k}} \varepsilon_{\mathbf{k}} a_{\mathbf{k}}^+ a_{\mathbf{k}}, \quad H' = \sum_{\mathbf{k}, \mathbf{k}'} V_{\mathbf{k}\mathbf{k}'} a_{\mathbf{k}}^+ a_{\mathbf{k}'}. \tag{4}$$

H' represents the interaction between electrons and charged impurity centers; **k** is the wave number vector of an electron in the conduction band; $a_{\mathbf{k}}^+$ and $a_{\mathbf{k}}$ are Fermi operators.

The current operator is (with the field in the Ox direction)

$$j = -\frac{e}{\hbar} \sum_{\mathbf{k}} \frac{d\varepsilon}{dk_x} a_{\mathbf{k}}^+ a_{\mathbf{k}}. \tag{5}$$

We shall assume that H' is small compared with H_0 and shall use perturbation theory. We emphasize that we thus neglect bound states of the electrons; this can evidently be done with almost fully ionized impurities.

Expanding the exponentials in (3) in powers of H' and inserting these into (2) we obtain

$$\varphi(\tau) = \beta \langle j^2 \rangle \exp\left[B - \mu(\tau)\right], \tag{6}$$

where

$$B = \langle j^2 \rangle^{-1} \int_0^\beta d\lambda \, (\beta - \lambda) \left\{ \langle j^2 H'_\lambda H' \rangle - \langle j^2 \rangle \langle H'_\lambda H' \rangle \right\},$$

$$\mu(\tau) = \hbar^{-2} \langle j^2 \rangle^{-1} \left\{ \operatorname{Im} \hbar \int_0^\tau d\theta \int_0^\beta d\lambda \, \langle H'_\lambda j \, [j, \, H'(\theta)] \rangle + \right. \\ \left. + \int_0^\tau d\theta \, (\tau - \theta) \, \langle j \, [[j, \, H'(\theta)], \, H'] \rangle \right\}. \tag{7}$$

Here

$$\langle A \rangle = \mathrm{Sp}\,(e^{-\beta H_0} A) / \mathrm{Sp}\,(e^{-\beta H_0}), \quad H'_\lambda = e^{\lambda H_0} H' e^{-\lambda H_0}, \quad H'(\theta) = e^{\frac{i}{\hbar} H_0 \theta} H' e^{-\frac{i}{\hbar} H_0 \theta}.$$

The first order terms in H' drop out because $V_{\mathbf{k}\mathbf{k}} = 0$ (see (13)). All of the averaging can easily be performed when (4) and (5) are substituted into (7) and we go over to the H_0 representation. As a result we have

$$\mu(\tau) = \frac{e^2}{\hbar^4 \langle j^2 \rangle} \sum_{\mathbf{k}, \mathbf{k}'} \left(\frac{d\varepsilon}{dk_x} - \frac{d\varepsilon}{dk'_x} \right)^2 |V_{\mathbf{k}\mathbf{k}'}|^2 f_{\mathbf{k}} (1 - f_{\mathbf{k}'}) \frac{2 \sin^2 (\omega_{\mathbf{k}\mathbf{k}'} \tau / 2)}{\omega^2_{\mathbf{k}\mathbf{k}'}}. \tag{8}$$

Here $f_{\mathbf{k}} = \langle a^+_{\mathbf{k}} a_{\mathbf{k}} \rangle$ is the Fermi distribution function and $\omega_{\mathbf{k}\mathbf{k}'} = (\epsilon_{\mathbf{k}} - \epsilon_{\mathbf{k}'}) / \hbar$.

We shall hereinafter confine ourselves to an investigation of nondegenerate semiconductors for which $f_{\mathbf{k}} = \exp[\beta(\zeta - \epsilon_{\mathbf{k}})] \ll 1$ where ζ is the Fermi level.

§2. Approximation of the δ-function. Let us consider the case of the integral in (2) when only large values of τ* play an appreciable part. Then

$$2 \sin^2 (\omega\tau / 2) / \omega^2 \approx \pi\tau\delta(\omega) \tag{9}$$

and thus $\mu(\tau)$ retains only terms corresponding to transitions between states of the same energy. We recall that (1) results from energy conservation for transitions.

Using (9) we obtain

$$\sigma = \beta \langle j^2 \rangle \exp(B) / \nu, \tag{10}$$

where

$$\nu = \frac{\pi e^2}{\hbar^4 \langle j^2 \rangle} \sum_{\mathbf{k}, \mathbf{k}'} |V_{\mathbf{k}\mathbf{k}'}|^2 \left(\frac{d\varepsilon}{dk_x} - \frac{d\varepsilon}{dk'_x} \right)^2 f_{\mathbf{k}} \delta\left(\frac{\varepsilon_{\mathbf{k}} - \varepsilon_{\mathbf{k}'}}{\hbar} \right). \tag{11}$$

---

* As will be shown hereinafter, this is equivalent to (1).

On the basis of (2) we hence obtain an expression which differs from that of Conwell and Weisskopf [2] by a numerical coefficient of the order 3. This difference apparently results from the greater consistency of the Kubo-Tomita-Nakano method compared with the kinetic equation.

The superiority of this method appears especially in the improvement of the form of the interaction between electrons and impurity centers. The field potential of an impurity center taking plasma screening into account is [6]

$$V(r) = -\frac{Ze^2}{\varepsilon r}\frac{2}{\pi}\int\limits_{k_0 r}^{\infty}\frac{\sin u}{u}\,du \tag{12}$$

and the matrix elements are thus

$$V_{\mathbf{kk'}}|^2 = \begin{cases} \dfrac{16\pi^2 Z^2 e^4}{\varepsilon^2(\mathbf{k}-\mathbf{k'})^4}\left\{N + 2\sum\limits_{l<i=1}^{N}\cos(\mathbf{k'}-\mathbf{k},\ \mathbf{R}_l-\mathbf{R}_i)\right\}, & \text{when}\quad (\mathbf{k}-\mathbf{k'})^2 > k_0^2;\\ 0, & \text{when}\quad (\mathbf{k}-\mathbf{k'})^2 < k_0^2. \end{cases} \tag{13}$$

Here N is the concentration of impurity centers; $\mathbf{R}_i$ and eZ are their coordinates and charge, respectively; ϵ is the dielectric constant of the semiconductor. k_0 is subject to the condition [7]

$$n^{4/3} \ll k_0^4 \ll \lambda^{-4} = (2m\varkappa T/h^2)^2$$

where $\underline{n}$, λ, and $\underline{m}$ are, respectively, the concentration, average de Broglie wavelength and effective mass of electrons in the conduction band.

When in (13) we neglect the interference of individual impurity centers, we have

$$\sigma_0 = \frac{3}{2\sqrt{2\pi}}\,\frac{\varepsilon^2 n}{Z^2 e^2\sqrt{m}\,N}\,\frac{(\varkappa T)^{3/2}}{[-\mathrm{Ei}(-\alpha)]}, \tag{14}$$

where

$$\mathrm{Ei}(-x) = -\int\limits_{x}^{\infty}\exp\left[\frac{-t}{t}\right]dt, \qquad \alpha = \frac{\hbar^2 k_0^2}{8m\varkappa T}. \tag{14a}$$

Equation (14) does not contain the factor exp(B), which gives only higher order corrections. In this approximation our condition of small H' becomes

$$n^{1/3} \ll \varepsilon\varkappa T/Ze^2. \tag{15}$$

Equation (14) must be compared with the analogous formula obtained in [6] by the kinetic equation method. Whereas the latter method, when the scattering probability is calculated in the Born approximation, requires simultaneous consideration of a second scattering mechanism in order to obtain a finite conductivity, the method which we have used here does not lead to such difficulties.

Taking the interference terms in (13) into account, we can investigate the effect of the impurity center configuration on the electrical conductivity of a semiconductor. We obtain

$$\sigma = \sigma_0\left\{1 + \frac{12}{N[-\mathrm{Ei}(-\alpha)]}\sum_{l<i=1}^{N}\int\limits_{k_0 R_{li}}^{\infty} e^{-\alpha_{li}y^2}\left[(\cos^2\theta_{li} - 1)\left(\frac{\cos y}{y} - \frac{\sin y}{y^2}\right) + \right.\right.$$
$$\left.\left. + \cos^2\theta_{li}\sin y\right]\frac{dy}{y^2}\right\}^{-1}. \tag{16}$$

Here $R_{li} = |\mathbf{R}_l - \mathbf{R}_i|$, θ_{li} is the angle between $(\mathbf{R}_l - \mathbf{R}_i)$ and the electric field direction; $\alpha_{li} = \hbar^2\beta/8mR_{li}^2$.

Unfortunately, experimental data still do not give sufficient information concerning the distribution of an impurity in a semiconductor. In the simplest case of random distribution, with the minimum separation of centers equal to the lattice constant d, we obtain

$$\sigma = \sigma_0 (1 - N/N_a)^{-1}, \tag{17}$$

where N_a is the number of atoms of the base material per unit volume. It follows from (17) that for the distribution of impurity centers indicated above, in cases of practical interest the interference of waves scattered by different centers plays an insignificant part; therefore this will be neglected hereinafter.*

§3. Low temperatures and high impurity concentrations. Let us calculate σ without the limitation (9). To terms of the third order in H'

$$\int_0^\infty e^{-\mu(\tau)}\,d\tau = \frac{2}{\nu} - \int_0^\infty e^{-\nu\tau}\mu(\tau)\,d\tau, \tag{18}$$

where ν and $\mu(\tau)$ are defined by (11) and (8), respectively. Using (2), (6), (8), (13), (14), and (18), we obtain

$$\sigma = \sigma_0 e^B \left\{ 2 - \frac{b}{[-\mathrm{Ei}(-\alpha)]\sqrt{\alpha}} \int_0^\infty \frac{\Phi\sqrt{gx(1+x)}}{\sqrt{gx(1+x)}} \cos bx\,dx \right\}, \tag{19}$$

where

$$b = \frac{2\sqrt{2\pi}}{3}\,\frac{Z^2 e^4 \hbar}{\varepsilon^2 \sqrt{m}}\,\frac{N}{(\varkappa T)^{5/2}}\,[-\mathrm{Ei}(-\alpha)], \quad g = \frac{b^2}{4\alpha}, \quad \Phi(x) = \frac{2}{\sqrt{\pi}}\int_0^x e^{-x^2}dx,$$

$$B = \frac{b}{2\sqrt{\alpha}\,[-\mathrm{Ei}(-\alpha)]} \Big\{ e^{-\alpha}\Phi(\sqrt{\alpha}) + \frac{1}{\sqrt{\pi}}(2e^{-\alpha} - 1) - 2\sqrt{2\alpha}\,(1 - \Phi(\sqrt{2\alpha})) - \tag{20}$$
$$- \sqrt{\alpha} \int_{\sqrt{\alpha}}^\infty e^{-y^2}\Phi(y)\frac{dy}{y} \Big\}.$$

When $\alpha \ll 1$,** we have

$$B \approx (4Z^2 e^4/3\varepsilon^2)(N/k_0 \varkappa^2 T^2). \tag{21}$$

When

$$g \ll 1, \quad b \ll 1, \tag{22}$$

that is, for low impurity concentrations and high temperatures, (19) reduces to (14). Consequently, (22) is the condition for applicability of the kinetic equation method. We note that the second inequality in (22) coincides with (1).

---

* It may be important to take interference into account for a different type of distribution of the impurity.

** For a resonable choice of the parameters this condition is always satisfied in the region defined by (15).

In the opposite asymptotic case of large N and small T

$$g \gg 1, \tag{23}$$

and for σ we obtain an expression which differs considerably from the Conwell-Weisskopf formula:

$$\sigma = \sigma_0 e^B \left\{2 - \frac{\pi}{[-\mathrm{Ei}(-\alpha)]}\left[\sin\frac{b}{2}J_0\left(\frac{b}{2}\right) - \cos\frac{b}{2}N_0\left(\frac{b}{2}\right) - \frac{8\sqrt{\alpha}}{\pi^{3/2}b}\right]\right\}, \tag{24}$$

where J_0 and N_0 are the zero-order Bessel and Neumann functions, respectively. For a reasonable choice of the parameters (ϵ = 20, m = 10^{-28} g) with N = 10^{18} cm^{-3} Condition (23) is satisfied for T < 100°K; with N = 10^{16} cm^{-3} it is satisfied for T < 70°K.

The author is very grateful to V. L. Bonch-Bruevich for proposing the problem and for several valuable suggestions, and to Academician N. N. Bogoliubov for valuable comments during a discussion of the results.

LITERATURE CITED

[1] L. E. Gurevich, Elements of Physical Kinetics [in Russian] (1940).

[2] E. Conwell and V. F. Weisskopf, Phys. Rev. 77, 388 (1950).

[3] H. Nakano, Progr. Theoret. Phys. 15, 77 (1956).

[4] H. Nakano, Progr. Theoret. Phys. 17, 145 (1957).

[5] R. Kubo and K. Tomita, J. Phys. Soc. Japan 9, 888 (1954).

[6] V. L. Bonch-Bruevich, J. Exptl.-Theoret. Phys. (USSR) 32, 4 (1957).*

[7] V. L. Bonch-Bruevich, Physics of Metals and Metallurgy (USSR) 4, 546 (1957).

Received June 26, 1957

M. V. Lomonosov Moscow State University

---

* [See Soviet Physics – JETP].

ON THE MOBILITY OF ELECTRONS AND HOLES IN A LIQUID SEMICONDUCTOR

I. Z. Fisher

(Presented by Academician M. A. Leontovich June 12, 1957)

We shall consider the problem of a single "excess electron" or of a single hole in an atomic semiconductor from the point of view of the theory of tight binding. Let $\mathbf{R}_k$ (k = 1, 2, . . ., N) be the instantaneous coordinates of the atomic nuclei of the system as numbered in some order. Let Ψ_k be the wave function of a nonstationary state of the entire system constructed out of single-atom wave functions and antisymmetric in the coordinates of all electrons, where the kth atom is either a (+) or (−) ion and the remaining N − 1 atoms are neutral. Then any state of the system with a single excess electron or a single hole will be

$$\Psi = \sum_{k=1}^{N} a_k(t)\,\Psi_k, \tag{1}$$

so that $a_k(t) \equiv a(\mathbf{R}_k, t)$ can be regarded as the wave function of the excess electron or hole and

$$dW(\mathbf{R}_k;\, t) = |a_k(t)|^2\, dV \tag{2}$$

is the probability of observing the excess electron or hole at time t in the vicinity of the point $\mathbf{r} = \mathbf{R}_k$.

At t = 0 let $a_1 = 1$, $a_k = 0$ with $k \geq 2$ and $\mathbf{R}_1 = 0$. If the medium is not perfectly ordered and its structural defects (of thermal, chemical or mechanical origin) are uniformly and isotropically distributed on the average, then for sufficiently large t and not too small dV with $N \rightarrow \infty$ we must have asymptotically

$$dW(\mathbf{R};\, t) \sim (4\pi Dt)^{-3/2} e^{-\mathbf{R}^2/4Dt}\, dV. \tag{3}$$

For example, when a mean free path l exists the distribution (3) is established at distances $|\mathbf{R}| \gg l$. We then have the diffusion coefficient $D \sim {}^1/_3\, lv$, where v is the average velocity of the electron or hole.

We shall be interested here in the diffusion of electrons or holes in a liquid semiconductor. We then have no mean free path, which exists upon the assumption that the wave function of an electron or hole is a plane wave to a good approximation and that $l \gg \lambda$, where λ is the wavelength. For many semiconductors this condition is not satisfied even at room temperature, and near the melting point of all semiconductors we have $l \lesssim \lambda$ or even $l \ll \lambda$. Consequently, we have here no plane waves and no "free path." The expression "free path" has even less meaning after melting of the semiconductor.

In order to determine the diffusion coefficient D in our problem we shall begin by noting that a distribution such as (3) can be obtained in the subsidiary and purely formal problem of the wandering of a classical particle through a given set of points $\mathbf{R}_k$ with a given a priori probability of the transition $\mathbf{R}_k \rightarrow \mathbf{R}_l$. It is possible to give different detailed forms of the probability process which describes the wandering, with different degrees of aftereffects (the influence of previous motion on the probabilities of later motions). In this set of probability processes there is one process which gives exactly the same value of the diffusion coefficient that is derived in the quantum mechanical problem of the behavior of an electron or hole in a real liquid semiconductor. We shall designate this as the equivalent probability process.

It is reasonable to assume that for real liquids, with the possible exception of the immediate vicinity of the melting-crystallization line, the equivalent probability process is close to being Markovian. In actuality the problem evidently amounts to the question, how good an integral of the motion is the quasi-momentum of the electron or hole ? The smaller its indeterminacy Δp the greater is its after-effect on the probabilities of subsequent transitions $\Psi_i \rightarrow \Psi_k$; for $\Delta p = 0$ we would have strict determinacy of the process. On the other hand, the greater Δp becomes, the more likely is the electron or hole to depart from its original direction of motion. But the degree of conservation or nonconservation of the quasi-momentum as an integral of the motion depends on the invariance of the Hamiltonian of the electronic subsystem with respect to the translational group. In our case, unlike that of crystals, such invariance is completely absent for the liquid as a whole and is practically absent in small regions. Indeed, our information from x-ray studies of the short range order of simple liquids shows no repetition of the instantaneous liquid structure through rectilinear translations even within the limits of a few assumed "unit cells."

But only such repetition could result in the existence of a quasi-momentum for an electron or hole and in its existence in small regions. Therefore in a real liquid the probabilities of successive quantum transitions $\Psi_i \rightarrow \Psi_k$ are practically independent of each other, and this makes the above-introduced equivalent probability process Markovian or almost Markovian.

For the diffusion coefficient of an electron or hole we then obtain [1]

$$D = {}^1/_6 \langle \nu \rangle \langle R^2 \rangle, \tag{4}$$

where $\langle \nu \rangle$ is the average number of transitions per unit time and $\langle R^2 \rangle$ is the mean square displacement of the electron or hole in a single transition. For the mobility we obtain from Einstein's relationship

$$u = \frac{e}{kT} D = \frac{e}{6kT} \langle \nu \rangle \langle R^2 \rangle. \tag{5}$$

The unknown quantities in (4) and (5) can be computed as follows. We first consider the atoms to be fixed in position. Then the probability per unit time w_{ik} of a transition $\Psi_i \rightarrow \Psi_k$ is proportional to the absolute value of the "transfer integral" L_{ik} from the Shubin-Vonsovskii polar model [2] of an electron conductor. If only two atoms were present L_{ik} would coincide with the "exchange integral" in the theory of a (±) ion of a diatomic molecule, which determines the propotionality coefficient between L_{ik} and w_{ik} [3]:

$$w_{ik} = \frac{2}{\pi\hbar} | L_{ik} |. \tag{6}$$

Hence, for the total number of transitions per unit time from Ψ_i to all possible Ψ_k with subsequent averaging over all Ψ_i we obtain

$$\langle \nu \rangle = \frac{1}{N} \sum_{i=1}^{N} \left(\sum_{\substack{k=1 \\ (k \neq i)}}^{N} w_{ik} \right) = \frac{2}{\pi\hbar N} \sum_{i=1}^{N} \sum_{\substack{k=1 \\ k \neq i}}^{N} | L_{ik} |. \tag{7}$$

Similarly, for $\langle R^2 \rangle$ we obtain

$$\langle R^2 \rangle = \langle | \mathbf{R}_i - \mathbf{R}_k |^2 \rangle = \frac{\sum\limits_{i=1}^{N} \sum\limits_{\substack{k=1 \\ (k \neq i)}}^{N} | \mathbf{R}_i - \mathbf{R}_k |^2 \, | L_{ik} |}{\sum\limits_{i=1}^{N} \sum\limits_{\substack{k=1 \\ k \neq i}}^{N} | L_{ik} |}, \tag{8}$$

and thus for the mobility of an electron or hole, with fixed atoms, we obtain from (5), (7) and (8)

$$u_1 = \frac{e}{3\pi\hbar kT}\,\frac{1}{N}\sum_{i=1}^{N}\sum_{\substack{k=1\\(k\neq i)}}^{N} |\mathbf{R}_i - \mathbf{R}_k|^2 |L_{ik}|. \tag{9}$$

For real values of u and D we must take into account the thermal motion of the atoms in the liquid and the probabilities of their configurations. All of this is apparently accomplished by averaging the result in (9) over the Gibbsian distribution $dW(\mathbf{R}_1, \mathbf{R}_2, \ldots, \mathbf{R}_N)$ for the atomic configurations. If $L_{ik} = L(|\mathbf{R}_i - \mathbf{R}_k|)$ were a strictly binary quantity this averaging would be easily performed by using the radial function $g(r)$ of the atomic distribution, which can be regarded as known from x-ray studies, since

$$dW(\mathbf{R}_1, \mathbf{R}_2) = g(|\mathbf{R}_1 - \mathbf{R}_2|)\,\frac{d^3\mathbf{R}_1 \cdot d^3\mathbf{R}_2}{V^2}, \tag{10}$$

where V is the volume of the system. Then from (9) and (10) it would follow that

$$u = \frac{4e}{3v\hbar kT}\int_0^\infty |L(r)|\, g(r)\, r^4 dr, \tag{11}$$

where $v = V/N$ is the average volume per atom of the liquid.

But in reality L_{ik} has a more complex structure of the form

$$L_{ik} = L^{(0)}(\mathbf{R}_i, \mathbf{R}_k) + \sum_{\substack{j=1\\(j\neq i,k)}}^{N} L^{(1)}(\mathbf{R}_i, \mathbf{R}_k; \mathbf{R}_j). \tag{12}$$

For example, for a hole in the model of monovalent atoms in an s state, we obtain [2]

$$\begin{aligned} L_{ik} &= \int \varphi_i(\mathbf{r})\, G(\mathbf{r} - \mathbf{R}_k)\, \varphi_k(\mathbf{r})\, d^3\mathbf{r} + \\ &= \sum_{j\neq i,k} \int \varphi_i(\mathbf{r}) \left\{ G(\mathbf{r} - \mathbf{R}_j) + e^2 \int \frac{\varphi_j^2(\mathbf{r}')\, d^3\mathbf{r}'}{|\mathbf{r} - \mathbf{r}'|} \right\} \varphi_k(\mathbf{r})\, d^3\mathbf{r} + \\ &+ \sum_{j\neq i,k} e^2 \iint \frac{\varphi_i(\mathbf{r})\, \varphi_j(\mathbf{r})\, \varphi_j(\mathbf{r}')\, \varphi_k(\mathbf{r}')}{|\mathbf{r} - \mathbf{r}'|}\, d^3\mathbf{r}\, d^3\mathbf{r}', \end{aligned} \tag{13}$$

where $\varphi_i(\mathbf{r}) = \varphi(\mathbf{r} - \mathbf{R}_i)$ is the electronic wave function in the ith atom and $G(\mathbf{r} - \mathbf{R}_i)$ is the potential of the ith atom core (see also [4]). Therefore (11) is valid only when by L_{ik} we mean the result of averaging (12) over all possible values of $\mathbf{R}_j$ (with $\mathbf{R}_i$ and $\mathbf{R}_k$ fixed):

$$L_{ik} = L^{(0)}(\mathbf{R}_i, \mathbf{R}_k) + (N-2)\,\overline{L^{(1)}(\mathbf{R}_i, \mathbf{R}_k; \mathbf{R}_j)}^{(\mathbf{R}_j)}. \tag{14}$$

It is difficult to perform this averaging exactly because the ternary atomic distribution function is unknown. However, an approximate and sufficiently accurate method is the "superposition approximation" from the theory of liquids [5], which gives

$$\overline{L_{ik}^{(1)}} = \frac{1}{V}\int L^{(1)}(\mathbf{R}_i, \mathbf{R}_k; \mathbf{R}_j)\, g(|\mathbf{R}_j - \mathbf{R}_i|)\, g(|\mathbf{R}_j - \mathbf{R}_k|)\, d^3\mathbf{R}_j. \tag{15}$$

Then from (11), (12), (14), and (15) we finally obtain

$$u = \frac{4e}{3\hbar vkT}\int\limits_0^\infty g(r)\,|L^{(0)}(r) + \frac{1}{v}\overline{L^{(1)}(r)}\,|\,r^4\,dr. \qquad (16)$$

It must be kept in mind here that g(r) depends parametrically on T and $\underline{v}$, so that the temperature and density dependence of electron or hole mobility in an atomic liquid semiconductor is more complex than is indicated by the coefficient of the integral in (16).

A preliminary numerical estimate of the results of the theory using hydrogen $\varphi(r)$ functions in a completely disordered liquid with $g(r) \equiv 1$, with typical values of $\underline{v}$ for real liquids, gives $D \sim 1$ cm^2/sec for the diffusion coefficient, which we consider entirely satisfactory and encouraging.

LITERATURE CITED

[1] S. Chandrasekar, Stochastic Problems in Physics and Astronomy, Rev. Mod. Phys. 15, 1 (1943) [Russian translation, IL, 1947].

[2] S. Shubin and S. Vonsovskii, Sow. Phys. 7, 292 (1935).

[3] D. I. Blokhintsev, Principles of Quantum Mechanics [in Russian] (1949).

[4] S. V. Vonsovskii, Uspekhi Fiz. Nauk 48, 289 (1952).

[5] N. N. Bogoliubov, Problems of Dynamical Theory in Statistical Physics [in Russian] (1946).

Received June 10, 1957

V. I. Lenin Belorussian State University

INELASTIC PROTON-PROTON CROSS SECTION ABOVE 7 Bev

K. I. Alekseeva and N. L. Grigorov

(Presented by Academician D. V. Skobel'tsyn June 29, 1957)

Our measurement of the inelastic proton-proton cross section (as the difference between proton interactions in paraffin and graphite) was obtained during an expedition in 1955 under conditions that were similar to those which existed during the measurement of the proton-carbon cross section [1-3]. The measurements were obtained in the stratosphere at 20-25 km, at 31°N latitude, for protons with an average energy of the order of 20 Bev.

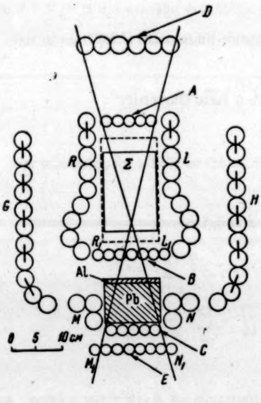

Fig. 1. Arrangement of counters and absorbers.

The apparatus that was used consisted (Fig. 1) of a telescope (counter trays D, A, B, and C) which defined a vertical beam of charged particles and a system of counters for registration of the products that resulted from interactions between protons and the matter of the absorbers placed in the telescope. All of the counters including the telescope counters were connected to a vacuum-tube hodoscope. During measurements involving the penetrating component of cosmic radiation an absorber consisting of 8 cm Pb and 0.9 cm Al was placed between trays B and C of telescope counters. Filters Σ consisting of paraffin and graphite [*] were placed on a carriage; every three minutes during the entire flight they were alternately moved automatically into the space between trays A and B of the telescope, so that measurements for paraffin and graphite were constantly being alternated. A detailed description of the construction of the instruments and their characteristics, as well as a description of the methods used to determine the inelastic cross section, is given in [2, 3].

The inelastic proton-proton cross section was determined by two methods: 1) by the variation in shower production in lead when the telescope contained substances which included hydrogen (the attenuation of the flux of single shower-producing particles due to interactions in hydrogen); 2) by direct measurement of the number of mixed showers from paraffin and graphite. Showers from paraffin and graphite were registered by counters K, K_1, B, L_1, L, which were placed in the upper part of the apparatus immediately surrounding the absorber Σ under investigation.

It should be noted that in a proton-proton interaction the production of a shower consisting only of fast neutral particles is much less likely than in a collision between a proton and a complex nucleus. It can therefore be assumed that the method of direct observation of showers in hydrogen is practically free of erroneous counts resulting from the production of only fast neutral particles. In our measurement of the proton-carbon nucleus cross section the situation was exactly the opposite [3].

---

[*] In the drawing the graphite filter is outlined by a solid line and the paraffin filter by a dashed line.

For the purpose of determining the inelastic proton-proton cross section we used data from flights with two sets of apparatus (Nos. 3 and 5) including a lead filter and one (No. 7) without a lead filter.

In order to create approximately identical conditions for the registration of showers in paraffin and graphite we used powdered graphite (the density of the graphite powder was 1.0-1.1 g/cm^3; that of the paraffin was ~ 0.95 g/cm^3). The thickness of the graphite absorber in g/cm^2 was always such that it was equal to the amount of carbon per g/cm^2 contained in the paraffin absorber. The difference between the thickness of the paraffin (18.8 g/cm^2) and graphite (16.0 g/cm^2) absorbers gave the quantity of hydrogen in the paraffin (2.8 g/cm^2).

Absorbers Σ, of paraffin and graphite, were placed in the telescope in such a way that their centers coincided (Fig. 1). Therefore the distance between the lower surface of the investigated filter and tray B of telescope counters was 2 cm greater for graphite than for paraffin. This circumstance resulted in different conditions for the registration of δ-showers from paraffin and graphite. Therefore, in order to determine the contribution of δ-showers to our registration of showers from paraffin and graphite and to make a suitable correction of the results we determined the actually recorded percentage of δ-showers in the total number of registered single particles at sea level subject to the same geometry as the flights. In measurements with the hard component these results were: for paraffin (6.45 ± 0.13)%, and for graphite (7.10 ± 0.15)%. The correction to the measured number of showers in hydrogen is the difference between these two percentages (0.65 ± 0.20)%. The corrections for the production of δ-electrons (for paraffin 6.45% and for graphite 7.10%) were applied both to measurements with the hard component* and with the total intensity of cosmic radiation** at sea level and in the stratosphere.***

---

* Visual examination of the hodoscopic diagrams of δ-showers from the hard component at sea level showed an insignificant number of nonlocal showers (not above 2%). We regarded a shower as nonlocal if it was impossible to draw a straight line representing the path of the particle producing the δ-shower, through the triggered showers among those within the solid angle of the apparatus.

** We also investigated the production of δ-showers at sea level for the total flux of cosmic radiation particles without using a lead absorber. In these experiments the fraction of showers registered by the counters that surrounded the graphite (or paraffin) was (10.23 ± 0.24)% for the graphite and (9.63 ± 0.24)% for the paraffin out of the total number of single particles registered. However, an analysis of the hodoscopic diagrams of these showers showed that the increase in the percentage of showers for the total flux with an identical difference of (0.60 ± 0.34)% (between the data for graphite and paraffin, resulting from the arrangement of the absorbers) was due principally to the presence of nonlocal showers, which are present in considerably greater numbers than during measurements with the hard component. Therefore, in making corrections for δ-showers in the variation with the total intensity of cosmic radiation we used the percentage of δ-showers compared with registered single particles which had been obtained for the hard component, that is, 6.45% for paraffin and 7.10% for graphite.

*** In 1949-1950 K. I. Alekseeva and S. N. Vernov performed special experiments to observe δ-electron production by the total flux of cosmic radiation at various altitudes, using a graphite absorber of 20 × 20 cm^2 area and 1.0 g/cm^2 thickness. The telescope consisted of 3 counter trays placed one above the other to form the solid angle. A row of counters under the graphite filter at a distance of ~ 15 cm, which registered δ-electrons, consisted of 10 thin-walled counters (of ~ 1.8 cm diameter, 20 cm length and 0.2-0.3 mm wall thickness). Due to the thinness of the graphite absorber there was only a small admixture of electron-nucleon and electron-photon showers among the δ-showers. Because of the absence of vertical rows of hodoscope counters the apparatus registered a relatively small number of lateral nonlocal showers. The δ-showers were selected visually through examination of the hodoscope records of triggered counters. It was found that the percentage of δ-showers (mostly showers which did not trigger more than 3 counters) with reference to the number of registered single particles at all altitudes from sea level to 20 km remains practically unchanged. The observed small increase of the relative number of δ-showers (about 20%) above 20 km could be explained mainly by the small fraction of electron-nucleon showers from graphite and of nonlocal showers.

On the basis of the approximate equality of the percentage of δ-showers for the hard component and for the total intensity of cosmic radiation at sea level and in the described experiments on δ-shower production in the atmosphere, we have concluded that there is no appreciable change in the ratio of δ-showers to the number of registered single particles throughout the range from sea level to the stratosphere.

The percentage of δ-showers from a lead absorber, as registered by counters M, M_1, C, E, N_1, N, immediately surrounding the lead, within the limits of statistical accuracy of our measurements, did not change when absorber Σ was placed in the telescope, and amounted on the average to $(6.85 \pm 0.12)\%$ of the single particles registered.

We calculated the inelastic proton-proton cross section from the ratio of the fluxes of single shower-producing particles when the telescope contained paraffin (I_p) and graphite (I_{gr}), which is associated with the mean free path L_p^H of the inelastic proton-proton interaction by the ratio

$$\frac{I_p}{I_{gr}} = e^{-2.8/L_p^H}.$$

TABLE 1

Apparatus	Method	Average depth of atmosphere x, g/cm²		Flux ratio, I_p/I_{gr}		Mean free path for inelastic proton-proton interaction L_p^H, g/cm²	Inelastic proton-proton cross section σ_p^H, mb
No. 3, with 8 cm Pb + 0.9 cm Al absorber	Direct measurement of no. of showers from paraffin and graphite	36.4	34.0	0.905± ± 0.033	0.947± ± 0.016	51^{+23}_{-12}	32± 10
No. 5 with Pb + + Al absorber	The same	25.9		0.948± ± 0.030			
No. 7 without Pb absorber	The same	42.5					
No. 3 with 8 cm Pb + 0.9 cm Al absorber	Attenuation of flux of single shower-producing particles due to interactions in hydrogen (from the change of the no. of showers from Pb when graphite is replaced with paraffin)	36.4		0.981± ± 0.028			
No. 5 with Pb + + Al absorber	The same	25.9		1.000± ± 0.060			

The quantity of hydrogen in the paraffin was 2.8 g/cm². The correction for interactions with primary α-particles was very small and was therefore not introduced. In the method of direct observation of showers from paraffin (N_s^p) and from graphite (N_s^{gr}) the ratio of the fluxes is obtained from measurements of $\frac{N_s^p - N_s^{gr}}{I_{gr}}$ because $\frac{I_p}{I_{gr}} = 1 - \frac{N_s^p - N_s^{gr}}{I_{gr}}$, where I_{gr} is the flux of single shower-producing particles at a given altitude, reduced through interactions with carbon nuclei in the paraffin absorber. For the purpose of determining I_{gr} we used: 1) our data for the flux I_0 of charged particles at the boundary of the atmosphere at latitude 31°N, which was 2.0 particles $\text{cm}^{-2} \cdot \text{min}^{-1} \cdot \text{sterad}^{-1}$ [2]; 2) the absorption coefficient of the shower-producing component in air, $L_{abs}^{air} = 150$ g/cm² [2] and 3) the mean free path of the inelastic interaction between protons and carbon nuclei, $L_p^C = 63$ g/cm² [3]. In the method of reducing the flux of the single shower-producing particles the ratio of the fluxes is obtained by measuring the number of showers from lead, $N_{s\,Pb}^p$ and $N_{s\,Pb}^{gr}$ for paraffin and graphite, respectively, in the telescope; thus $I_p/I_{gr} = N_{s\,Pb}^p/N_{s\,Pb}^{gr}$.

Table 1 contains the ratio of the fluxes of single shower-producing particles I_p/I_{gr} obtained with different apparatus and different methods; in each instance the mean square statistical error is given. The data were corrected for chance coincides and δ-showers. In addition, the recorded number of showers from hydrogen contained corrections for: a) a lead absorber; this correction for the change of the background of showers from lead with particles directed upward, when the change is made from graphite to paraffin [2, 3], amounts to around 6% of the cross section; b) noncounting due to incidence of the shower particles in the space between counters, amounting to ~ 6%; c) for electron-photon showers, which affect the paraffin-graphite difference in the absence of lead, amounting to ~ 15% of the cross section.

After averaging all of the tabulated data and taking account of the statistical weights we obtained the following values for the mean free path L_p^H and the cross section σ_p^H of inelastic proton-proton interactions:

$$L_p^{\mathrm{H}} = 51^{+23}_{-12}\ \mathrm{g/cm^2};\quad \sigma_p^{\mathrm{H}} = 32 \pm 10\ \mathrm{mbarns.}$$

Walker et al. [4], using a cloud chamber at mountain altitudes, measured the inelastic proton-proton interaction in paraffin. Taking the inelastic proton-carbon cross section as equal to the geometric cross section of carbon, they calculated the mean free path and cross section of proton-proton interactions, obtaining $L_p^H = 31^{+35}_{-7}$ g/cm² and $\sigma_p^H = 54^{+15}_{-29}$ mb. In a brief communication by Fowler et al. [5] the inelastic proton-proton cross section was given as 29.5 ± 5.5 mb; this was obtained with a 5.3-Bev bevatron beam. In the proceedings of the April 1956 Rochester Conference on High-Energy Physics ~ 25 mb (with no indication of the statistical accuracy) was given for the inelastic proton-proton interaction at 5.3 Bev. For an average proton energy ~ 20 Bev we obtained 32 ± 10 mb. Considering the large statistical error of the experiment, it can be assumed that in the energy range from 1.5-2.0 to ~ 20 Bev no appreciable increase is observed for the inelastic proton-proton interaction.

This work was assisted by S. I. Brikker and M. M. Dubrovin.

LITERATURE CITED

[1] K. I. Alekseeva and N. L. Grigorov, J. Exptl.-Theoret. Phys. (USSR) 32, 404 (1957).*

[2] K. I. Alekseeva, S. I. Brikker, N. L. Grigorov, F. D. Savin, and N. A. Shcherbakov, Doklady Akad. Nauk SSSR 115, 71 (1957).**

[3] K. I. Alekseeva and N. L. Grigorov, Doklady Akad. Nauk SSSR 115, 259 (1957).***

[4] W. D. Walker, N. M. Duller, and J. D. Sorrels, Phys. Rev. 86, 865 (1952).

[5] R. W. Wright, G. Saphir et al., Phys. Rev. 100, 1802 (1955).

Received June 28, 1957

M. V. Lomonosov Moscow State University

---

* Soviet Physics – JETP, p. 339.

** Soviet Physics – "Doklady," p. 303.

*** Soviet Physics – "Doklady," p. 317.

SOME CHARACTERISTICS OF THE K EMISSION SPECTRUM OF TITANIUM IN TITANATES

E. E. Vainshtein, M. N. Bril', and I. B. Staryi

(Presented by Academician A. P. Vinogradov, June 27, 1957)

In a recent study of the K-emission spectrum of titanium in certain compounds [1] it was suggested that the appearance of the satellite $K_{\beta''}$ is associated with a "cross-over" transition to a K-level of the metal on the part of certain electrons of an anion. Subsequently, [2] the correctness of this hypothesis was confirmed in special experiments.

This hypothesis [1] enables us to explain very simply many properties of the line, specifically its absence in the metal spectrum and the strong dependence of its relative intensity on the valency of the atoms in the compound.

"Cross-over" transitions of electrons in compounds are also apparently associated with a number of other effects observed in x-ray [3, 4] and optical [5] absorption spectra. Since the relative intensity of selective x-ray absorption lines as a result of "direct" and "cross-over" transitions of electrons of the absorbing atom depends strongly on the polarization of this atom in the compound [6], it could be concluded that the same factor influences the relative intensity of the corresponding emission lines.

The present work was intended to obtain an experimental verification of this conclusion. We investigated the K_{β}-emission lines of titanium in brookite, anatase and a number of other titanates — Mg, Ca, Sr, Ba, Fe, and Zn.* Mono- and tetratitanates of barium were also studied ($BaO \cdot TiO_2$ and $BaO \cdot 4\,TiO_2$). In all of these compounds the titanium atoms are at the centers of regular or deformed and variously interlinked octahedrons of TiO_6. In brookite and anatase each octahedron is linked with others on several edges, and zigzag chains of octahedrons containing titanium alternate with similar chains of unoccupied octahedrons. In perovskite structures ($CaTiO_3$, $SrTiO_3$ and $BaTiO_3$) the TiO_6 octahedrons are joined at their vertices and form an endless tridimensional anion with interstitial ions of the alkali earth metals. Linking of TiO_6 octahedrons at opposite vertices also apparently occurs in the structure of barium tetratitanate [7]. Thus in all of these compounds the nearest circle of titanium ions consists of six octahedronally arranged oxygen ions, and a direct interaction between atoms of different metals in the compound is impossible. On the other hand, in the ilmenite structure ($FeTiO_3$, $MgTiO_3$) both metals are located approximately alike. The occupied hexagons of the octahedrons are each divided into pairs of triangles containing Fe and Ti ions alternately. In the vertical columns of the structure the octahedrons occupied by Fe and Ti ions alternate with others which are vacant. It is evident that the polarization conditions and the nature of the interaction between titanium and other atoms in these compounds differ from the corresponding conditions in perovskite compounds.

TABLE 1

Titanium K_{β_1}-Lines in Compounds

Substance	Energy in ev	Substance	Energy in ev
Ti (metal)	4931.5	$SrTiO_3$	4931.1
$MgTiO_3$	4931.2	$BaTiO_3$	4931.2
$CaTiO_3$*	4931.3	$BaO \cdot 4TiO_2$	4931.3
$ZnTiO_3$	4931.3	TiO_2 (anatase)	4931.3

---

* In [1] the energy of K_{β_1} in this compound was determined incorrectly.

In this work wer used a focusing x-ray spectrograph tube [8] with a quartz crystal as analyzer. The reflecting surfaces were prism surfaces with d = 3.33 A. The radius of curvature of the crystal was 2.5 m; the effective portion of the crystal was 15 mm in extent and the linear dispersion of the spectrograph in the investigated spectrum was ~ 2.5 Xu/mm. For investigation of fluorescent spectra the materials were placed outside the x-ray tube at a distance of 26 mm from its anode. The copper anode was chromium plated. The x-ray tube was operated at 35 kv and 50 ma, with exposures from 15 to 25 hours and photographic recording of the spectra. We studied the positions, shapes and relative intensities of the K_{β_1}, K_{β_5}, $K_{\beta'}$ and $K_{\beta''}$ lines of titanium in the aforesaid compounds. The maxima of the titanium K_{β_1} and K_{β_5} lines in all of the compounds were slightly shifted towards longer waves than in the metal spectrum [1]. For the first of these lines the shift was small and fell within the limits of accuracy (± 0.2 ev) (Table 1). The K_{β_5} maximum was shifted by the larger amount ~ 0.6 ev. The energy and shape (width

---

* Prof. G. I. Skanavi kindly provided us with some of the titanates studied here.

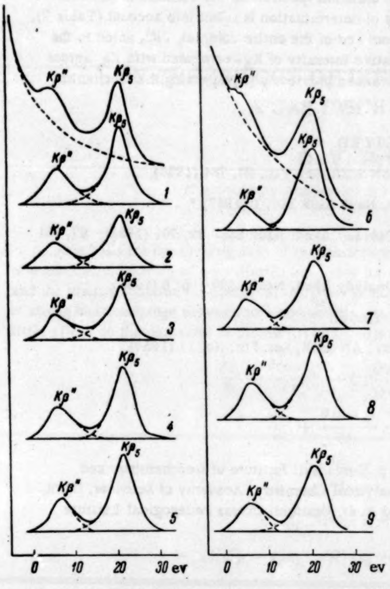

Fig. 1. $K_{\beta''}$- and K_{β_5}-lines of the x-ray spectrum of titanium in various compounds: 1) $CaTiO_3$; 2) $SrTiO_3$; 3) $BaTiO_3$; 4) $BaO \cdot 4TiO_2$; 5) TiO_2 (anatase); 6) $FeTiO_3$; 7) $ZnTiO_3$; 8) $MgTiO_3$; 9) TiO_2 (brookite).

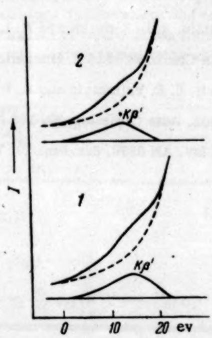

Fig. 2. Titanium $K_{\beta'}$ line in two titanates: 1) $CaTiO_3$, 2) $SrTiO_3$.

TABLE 2

The Relative Intensity of Titanium $K_{\beta''}$ and K_{β_5} in Various Compounds

Substance	$IK_{\beta''}/IK_{\beta_5}$	Substance	$IK_{\beta''}/IK_{\beta_5}$	Substance	$IK_{\beta''}/IK_{\beta_5}$
$FeTiO_3$	0.24	$BaO \cdot 4TiO_2$	0.48	$CaTiO_3$*	0.56
$ZnTiO_3$	0.40	TiO_2 (rutile)	0.49	$SrTiO_3$	0.58
TiO_2 (brookite, anatase)	0.41	$MgTiO_3$*	0.51	$BaTiO_3$	0.56

---

* We investigated a few different specimens of these compounds which differed in chemical purity and in dielectric properties. The titanium x-ray spectra were practically identical. Table 2 gives the average values of the ratio $IK_{\beta''}/IK_{\beta_5}$ for these substances.

and index of asymmetry) of the diagram emission lines of titanium (K_{β_1} and K_{β_5}) in different compounds do not exhibit appreciable variation beyond the limits of error. The same applies to the satellites $K_{\beta'}$ and $K_{\beta''}$ (Figs. 1 and 2). At the same time the relative intensity of $K_{\beta''}$ in the emission spectrum of the element in different compounds is not constant even if the relatively low accuracy of determination is taken into account (Table 2), and evidently depends on the polarization of the absorbing atom and of the entire complex TiO_6 anion in the compound. The experimentally observed variation of the relative intensity of $K_{\beta''}$ compared with K_{β_5} agrees qualitatively with expectations [6] based on the hypothesis advanced previously [1] regarding the mechanism which produces these lines.

LITERATURE CITED

[1] E. E. Vainshtein, I. B. Staryi and M. N. Bril', Izv. AN SSSR, Ser. Fiz. 20, 784 (1956).

[2] E. E. Vainshtein and Iu. N. Vasil'ev, Doklady Akad. Nauk SSSR 114, 1 (1957).*

[3] E. E. Vainshtein, R. L. Barinskii and K. I. Narbut, Doklady Akad. Nauk SSSR 82, 701 (1952); 87, 381 (1952).

[4] E. E. Vainshtein, R. L. Barinskii and K. I. Narbut, Doklady Akad. Nauk SSSR 105, 6 (1955).

[5] A. Kiss, Acta Chem. Acad. Sci. Hungarical 10, 1-3 (1956).

[6] R. L. Barinskii, E. E. Vainshtein and K. I. Narbut, Izv. AN SSSR, Ser. Fiz. No. 11 (1957).

[7] F. W. Harrison, Acta Cristallogr. 9, 198 (1956).

[8] I. B. Staryi, Izv. AN SSSR, Ser. Fiz. 20, 798 (1956).

Received June 11, 1957

V. I. Vernadskii Institute of Geochemistry and
Analytical Chemistry, Academy of Sciences, USSR,
and K. D. Ushinskii Odessa Pedagogical Institute

---

* Soviet Physics – "Doklady," p. 207.

ON THE THEORY OF DIFFUSION OSCILLATIONS IN A GAS DISCHARGE PLASMA

O. V. Prudkovskaia

(Presented by Academician N. N. Bogoliubov June 18, 1957)

As a basis for our investigation of oscillations in a gas discharge plasma we shall employ the usual [1] set of equations, consisting of the diffusion equations for electrons and ions, Poisson's equation for the electric field and the energy equation for electrons. Analysis of the most general set of equations has shown that, as a result of strong heat exchange between ions and neutral gas atoms the temperature perturbations of the ions have very little effect on the character of the oscillations. We thus have

$$\frac{\partial n_1}{\partial t} - \frac{\partial (n_1 u_{\alpha_1})}{\partial x_\alpha} - D_1 \frac{\partial^2 n_1}{\partial x_\alpha^2} - D_T \frac{\partial^2 T_1}{\partial x_\alpha^2} = \beta n_1 - R; \tag{1}$$

$$\frac{\partial n_2}{\partial t} + \frac{\partial (n_2 u_{\alpha_2})}{\partial x_\alpha} - D_2 \frac{\partial^2 n_2}{\partial x_\alpha^2} = \beta n_1 - R, \tag{2}$$

$$\frac{\partial E_\alpha}{\partial x_\alpha} = 4\pi e (n_2 - n_1); \tag{3}$$

$$\frac{\partial}{\partial t}(n_1 c_{v1} T_1) + \frac{\partial}{\partial x_\alpha}(c_{v1} T_1 S_{\alpha_1}) =$$
$$= - eE_x S_{\alpha_1} - (\beta n_1 - R)(\varepsilon_u + c_{v1} T_1) - \gamma_1 \frac{m}{M} c_{v1} \frac{T_1}{T_0}(T_1 - T_0) n_1. \tag{4}$$

Here the subscript 1 refers to electrons and subscript 2 refers to ions; u_{α_1} and u_{α_2} are the drift velocities of electrons and ions, respectively; D_1 and D_2 are diffusion coefficients; D_T is the thermal diffusion coefficient for electrons; M is the atomic mass of the neutral gas; T_1 is the electron temperature; $c_{v_1} T_1$ is the internal energy of the electron gas; T_0 is the temperature of the neutral gas; γ_1 is the number of elastic collisions between electrons and neutral gas atoms (of the same order as the total number α_1 of collisions); ϵ_u is the ionization energy; and S_{α_1} designates the electron flux which results from diffusion, thermal diffusion and drift in the electric field:

$$S_{\alpha_1} = - n_1 u_{\alpha_1} - D_1 \frac{\partial n_1}{\partial x_\alpha} - D_T \frac{\partial T_1}{\partial x_\alpha}. \tag{5}$$

The energy equation takes into account the transport of energy with the electron flux S_{α_1}, the removal of energy as electrons move in the electric field, heat exchange with neutral gas atoms and, finally, energy expended in the process of stripping electrons from neutral gas atoms and the transfer to these electrons of energy which amounts to the mean electron energy per unit volume.

In the central part of the tube we can regard the problem as one-dimensional. We assume

$$n_1 = n_0 + \nu_1 e^{i(\omega t + kx)}\ \nu_1 \ll n_0; \quad n_2 = n_0 + \nu_2 e^{i(\omega t + kx)}\ \nu_2 \ll n_0;$$
$$T_1 = T_{10} + \tau_1 e^{i(\omega t + kx)}\ \tau_1 \ll T_{10}. \tag{6}$$

Substituting into (1)-(4) we find that the condition for the existence of a nontrivial solution is a dispersion equation of the form

$$D_T k^2 \Big[(\beta + 4\pi e n_0 \mu_2) 2u_1 \frac{4\pi e n_0 \mu_1}{ik} - \\ - (i\omega + u_2 ik + D_2 k^2 + 4\pi e n_0 \mu_2) \Big(2u_1 \frac{4\pi e n_0 \mu_1}{ik} - D_1 u_1 ik \Big) \Big] + \\ + \frac{c_{v1} n_0}{m \alpha_1} \Big(i\omega + 2\gamma_1 \frac{m}{M} - \frac{c_{p1}}{c_{v1}} u_1 ik \Big) [(i\omega - u_1 ik + D_1 k^2 + 4\pi e n_0 \mu_1 - \beta) \times \\ \times (i\omega + u_2 ik + D_2 k^2 + 4\pi e n_0 \mu_2) - (\beta + 4\pi e n_0 \mu_2) 4\pi e n_0 \mu_1] = 0. \quad (7)$$

Hence, if it is assumed that the external electric field is not too large, that is,

$$u_1 / c_1 < \lambda_1 / l, \quad (8)$$

where u_1 is the electron drift velocity in the electric field; c_1 is their mean thermal velocity; λ_1 is the mean free path of electrons, and l is the wavelength ($l = 2\pi/k$) of the investigated process, we obtain the simpler dispersion equation

$$(i\omega + D_1 k^2 - u_1 ik + 4\pi e n_0 \mu_1 - \beta)(i\omega + D_2 k^2 + u_2 ik + 4\pi e n_0 \mu_2) = \\ = (\beta + 4\pi e n_0 \mu_2) 4\pi e n_0 \mu_1. \quad (9)$$

This form of the equation can be derived without using the energy equation, which means that in this case the temperature perturbations of the electrons have little effect on the character of the process.

In a weakly charged plasma where the Debye radius d_1 is larger than or of the same order of magnitude as the wavelength l, the electrons and ions are very weakly bound and can move independently. Thus, with $d_1 > l$ or $D_1/d_1^2 = 4\pi e n_0 \mu_1 \ll D_1 k^2 \approx \omega \approx \beta$ the right-hand side of Eq. (9) can be neglected and we obtain the following equations for the electronic and ionic waves:

$$i\omega - u_1 ik + D_1 k^2 - \beta = 0; \quad (10)$$

$$i\omega + u_2 ik + D_2 k^2 = 0, \quad (11)$$

where the terms $u_1 k$ and $u_2 k$ are small compared with the diffusion terms according to (8). When $k^2 = \beta/D_1$ an undamped electronic wave is possible, propagating with the electron drift velocity u_1; while in other cases the dispersion equation (10) describes the damped electronic wave. The ionic wave described by (11) is practically nonexistent because of very strong damping.

In plasmas with a higher concentration of charged particles nonquasineutral electron-ion waves are possible. Thus with $l \cong d_1 \sqrt{\mu_1/\mu_2}$ by using the Thomson method [5] we obtain from (9) the following expression for the wave number of the ionic wave:

$$k^2 = \frac{4\pi e n_0 \mu_2 + \beta}{D_1} + \frac{4\pi e n_0 \mu_1}{D_1} \frac{(\beta - i\omega)(4\pi e n_0 \mu_2 - i\omega)}{(4\pi e n_0 \mu_2)^2 - \omega^2}, \quad (12)$$

the imaginary part of which is negative at low frequencies, when $\omega < 4\pi e n_0 \mu_2$, in which case we have damped waves. At frequencies of the order of $4\pi e n_0 \mu_2$ there is no clearly defined wave and the function $\underline{k}$ is discontinuous. At higher frequencies $\omega > 4\pi e n_0 \mu_2$ the imaginary part of (12) is positive and we have an increasing wave.

Finally, in real highly charged plasmas, where the Debye radius is smaller than the period of the process:

$$d_1 < l, \quad (13)$$

we obtain the dispersion equation of quasineutral waves

$$\Big(D_1 \frac{\mu_2}{\mu_1} + D_2 \Big) k^2 + (i\omega - \beta) \Big(1 + \frac{\mu_2}{\mu_1} \Big) = 0, \quad |\nu_1 - \nu_2| \ll |\nu_1|, \quad (14)$$

which we have identified with striations [2], since the physical conditions under which striations are observed agree with Conditions (8) and (13) for the validity of Eq. (14). Encouraging results are obtained when the theoretical dependence of the striation period on the tube radius and discharge current [2] are compared with experiment.

The velocity of moving striations is related to the space decrement* through the ratio

$$v = \frac{\omega}{k} = -\left(D_1\frac{\mu_2}{\mu_1} + D_2\right)\frac{2b}{1 + \mu_2/\mu_1}. \tag{15}$$

A. A. Zaitsev and Kh. A. Dzherpetov [3] have called attention to the relation between the velocity of moving striations and asymmetry of the discharge.

Simple special cases can be derived from the general dispersion equation (7) with a very high external electric field $u_1/c_1 > \lambda_1/l$. In this case, because of the strong effect which temperature disturbances of the electrons have on the character of the process, it is necessary to take into account the dependence on the average electron energy, of such terms in the equations as the diffusion and thermal diffusion coefficients, electron mobility μ_1, etc.

We shall take into account the temperature dependence of the ionization coefficient by setting, according to Killian's formula [4], $\beta = B\sqrt{\varkappa T_1}e^{-x_i}\left(1 + \frac{1}{x_i}\right)$, where κ is the Boltzmann constant and $x_i = \frac{\epsilon_u}{\kappa T_1}$.

In accordance with Eq. (6) instead of a constant ionization coefficient $\beta = \beta_0$ we must everywhere in the dispersion equation insert

$$\beta = \beta_0\left[1 + \frac{\tau_1}{T_{10}}\left({}^3/_2 + x_i + \frac{1}{x_i}\right)\right].$$

The dependence of the diffusion and thermal diffusion coefficients and of charged particle mobility on electron temperature is related to the dependence of the cross section for collisions between electrons and neutral gas atoms on electron velocity, and is different for different gases. Let the total number of electron collisions α_1 be proportional to some power g of the electron temperature T_1. The complete dispersion equation becomes

$$\begin{gathered}
\left(D_T k^2 + g u_1 ik\,\frac{n_0}{T_{10}} - \beta_x\frac{n_0}{T_{10}}\right)\left[2u_1\,\frac{4\pi e n_0\mu_1}{ik}(\beta_0 + 4\pi e n_0\mu_2) -\right.\\
\left.-(i\omega + u_2 ik + D_2k^2 + 4\pi e n_0\mu_2)\left(2u_1\,\frac{4\pi e n_0\mu_1}{ik} - D_1u_1ik\right)\right] +\\
+\beta_x\frac{n_0}{T_{10}}\left[(i\omega + D_1k^2 + 4\pi e n_0\mu_1 - u_1ik - \beta_0)\cdot 2u_1\frac{(-4\pi e n_0\mu_1)}{ik} -\right.\\
\left.-4\pi e n_0\mu_1\left(u_1D_1ik - 2u_1\,\frac{4\pi e n_0\mu_1}{ik}\right)\right] +\\
+\left\{\frac{c_{v_1}n_0}{m\alpha_1}\left[i\omega - \frac{c_{p_1}}{c_{v_1}}u_1ik + \beta_x + \beta_0 + 2\gamma_1\frac{m}{M}(1 + g)\right] +\right.\\
\left.+2u_1^2\frac{n_0}{T_{10}}g\right\}[(i\omega + D_1k^2 + 4\pi e n_0\mu_1 - u_1ik - \beta_0)(i\omega + D_2k^2 +\\
+4\pi e n_0\mu_2 + u_2ik) - 4\pi e n_0\mu_2(4\pi e n_0\mu_2 + \beta)] = 0,
\end{gathered} \tag{16}$$

where $\beta_x = \beta_0[{}^3/_2 + x_i + 1/x_i + (2g - 1)]$.

For a highly charged plasma in a strong external field (Condition (13)) we obtain from (16) a dispersion equation which for gases where the thermal diffusion coefficient is not zero and the mobility is not temperature dependent (corresponding to a collision cross section which is inversely proportional to electron velocity, such as has been observed for mercury) is of simple form, and in the stationary case

---

* The magnitude of the space decrement characterizes the degree of asymmetry of the charged particle distribution in space: $n = n_0 + \nu e^{i(kx+\omega t)}e^{-bx}$.

$$D_T \frac{T_{10}}{n_0} \frac{\mu_2}{\mu_1} k^2 = \beta_0 \left(1 + \frac{\mu_2}{\mu_1}\right)\left(\frac{3}{2} + x_l + \frac{1}{x_l} + g + 1\right) \quad (17)$$

agrees formally with dispersion equation (14) when account is taken of the fact that for a nonvanishing thermal diffusion coefficient we have $D_1 = D_T T_{10}/n_0$. Thus it is possible to have stationary striations which obey the same laws as the striations described by (14), but which are caused by thermal diffusion.

When the mobility depends on electron temperature, then, independently of the character of the thermal diffusion, in a high external electric field the wave is very similar in character to an ionic wave:

$$i\omega + u_2 ik = 0 \quad (18)$$

and is propagated with a velocity equal to the ionic drift velocity.

Thus an analysis of the total dispersion equation of diffusion oscillations shows that in real plasmas, in which the Debye radius is of the order of a hundredth or a thousandth of a centimeter and is thus smaller than the period of the processes being investigated, quasineutral waves are observed.

In high electric fields these oscillations are described by dispersion equations (17) and (18); in very weak fields (Condition (8)) they are described by Eq. (14). In an intermediate external field the dispersion equation is too complicated for direct analysis because of the high algebraic powers of the wave number.

In a very weakly charged plasma, where the Debye radius is of the same order or smaller than the period of the process under investigation, it is possible to have electronic waves propagating independently as well as ionic waves accompanied by electronic motion (12).

In conclusion I wish to thank Professor M. F. Shirokov for proposing this research and for valuable suggestions.

LITERATURE CITED

[1] J. Druyvesteyn, Physica 1, 273, 1003 (1934).

[2] O. V. Prudkovskaia and M. F. Shirokov, Doklady Akad. Nauk SSSR 112, 1023 (1957).*

[3] A. A. Zaitsev and Kh. A. Dzherpetov, Doklady Akad. Nauk SSSR 89, 825 (1953).

[4] I. J. Killian, Phys. Rev. 35, 1238 (1930).

[5] J. J. Thomson and G. P. Thomson, Conduction of Electricity in Gases 2 (Cambridge, 1933).

Received June 10, 1957

M. V. Lomonosov Moscow State University

---

* Soviet Physics – "Doklady," p. 96.

DURATION OF THE EXCITED STATE AND QUANTUM YIELD OF FLUORESCENCE FROM CHLOROPHYLL IN VITRO AND IN VIVO

L. A. Tumerman

(Presented by Academician M. A. Leontovich June 12, 1957)

We know that the quantum yield of fluorescence from chlorophyll in its natural state and in the cells of plants is about one order of magnitude smaller than in solutions. According to [1], for example, in the cells of various algae the yield is 1.5-3%, whereas in solutions it reaches 30%. Thus in plant cells some very effective quenching processes occur, which are apparently associated with the mechanism of the primary photochemical reaction and with the plant's utilization of the excitation energy of chlorophyll molecules for photosynthesis.

In order to determine the nature of these processes we obtained parallel measurements of the relative quantum yield and duration of fluorescence from chlorophyll in vitro and in vivo. An integrating sphere was used for the measurements of the yield, while the duration of the excited state was measured with a phase fluorometer [2], whose amplifying and phasometric parts were constructed according to the design of A. M. Bonch-Bruevich [3]. A. A. Krasnovskii provided us with solutions for in vitro study; these contained an unseparated mixture of chlorophylls a and b purified of carotinoids, as well as extracts of sugar beet leaves. Chlorophyll fluorescence in the cell was studied in suspensions of the one-celled alga Scenedesmus accuminatus, a culture of which was available through the kindess of N. S. Gaevskaia.* The Hg 436 mμ line was used for excitation, filtered from the radiation of a very-high-pressure mercury lamp.

TABLE 1

Object	ρ_{rel}	$\tau \cdot 10^9$ sec
Solutions of chlorophyll a and b		
in acetone	1.00	5.4
in ethyl alcohol	1.05	5.3
in ethyl ether	1.0	–
Leaf extract		
in acetone	–	5.7
in ethyl alcohol	–	5.5
in ethyl ether	0.98	5.1
Scenedesmus accuminatus	0.08	0.8-0.9

Our results are given in Table 1. The fluorescence yield of a solution of chlorophyll in acetone was arbitrarily taken as unity. The mean square error in the determination of τ, as computed by averaging 15-20 extensive sets of measurements performed on different days by three observers, was about $(0.1-0.2)\cdot 10^{-9}$ sec, but the spread of the average results of different days in the case of the alga exceeded this value by a factor of 2 or 3. This fact is possibly associated with the physiological state of the alga and with the intensity of photosynthesis within it, but no systematic study has yet been made of the influence of physiological conditions on fluorescence yield and duration. Our values of τ for solutions and the alga agree in absolute magnitude, within the limits of error, with those which E. Rabinowitch obtained by a different method [4].

A comparison of these values of the "actual" duration of the excited state of chlorophyll in solutions (τ) with the absolute values of the fluorescence quantum yield (ρ) and the values of the "natural" duration (τ_0) as calculated by different authors [5] from the integral of the first absorption band of chlorophyll (the integral of T. P. Kravets) shows that the relation $\tau = \rho\tau_0$ is satisfied quite accurately. Especially good agreement is obtained when Livingston's value of τ_0 in Table 2 is taken or $\tau_0 = 1.52\cdot 10^{-8}$ sec, which is given in the cited work of Rabinowitch.

---

* Note added in the proof. For a suspension in water of chloroplasts and their fragments obtained in the usual way from the leaves of various plants (sugar beets, tobacco, etc.) we obtained $\tau = (1.0-1.2)\cdot 10^{-9}$ sec, which is close to the values obtained for τ in vivo. When alcohol, acetone or pyridine is added to the medium τ increases and approaches its values in vitro. This increase parallels the increase of ρ which was noted in [9] and which was confirmed by ourselves.

TABLE 2

Values of $\tau_0 \cdot 10^8$ (sec)

	Prins (1934)	Livingston (1952)	Jacobs (1954)
Chlorophyll a	8.2	1.8	1.27
" b	8.9	4.4	1.62

This shows that the factor which limits the fluorescence yield of chlorophyll in solutions is the competition, occurring throughout the duration of the excited molecular state, between spontaneous emission by the excited molecule and nonradiative deactivation processes. In a solution which lacks the conditions for stimulation of photochemical reactions by chlorophyll these processes, regardless of whether they represent internal conversion, that is, the direct transformation of electronic excitation energy into vibrational energy, or are associated with the transformation of a molecule into another tautomeric form followed by the re-establishment of thermodynamic equilibrium, always represent the transformation of excitation energy into heat. The yield values ρ = 0.25-0.30 show that the probability of fluorescence in a solution is about 3 times smaller than the probability of these processes of transformation of excitation energy into heat. We have no grounds for assuming that the situation regarding these probabilities differs in the cell.

However, in the cell the aforesaid two possible methods of the deactivation of excited chlorophyll molecules are joined by a third possibility — the utilization of excitation energy for a primary photochemical reaction. The reduced fluorescence yield in the cell is evidently caused by this third method of deactivation, and the sharp reduction of fluorescence duration which accompanies the lower yield indicates that these three processes compete during the entire excitation period of the chlorophyll molecule. In other words, it can be stated that the specific fluorescence quenching processes in the live cell are mainly of a "second kind," using the terminology of S. I. Vavilov [6].

It is important to note, however, that in our case there is no strict proportionality between ρ and τ for solutions and cells; a 12-fold reduction of the yield is accompanied by a six- to seven-fold reduction of the duration. For comparison with the simplest case of quenching of the second kind, that is, quenching of fluorescence in solutions by additives, we measured ρ and τ for the quenching of acetone solutions of chlorophyll by quinone and of aqueous solutions of uranine by potassium iodide. In both instances the measurements showed strict proportionality between ρ and τ.

The absence of such proportionality in the comparison of ρ and τ for chlorophyll in solutions and in cells can be explained in two ways. It can be assumed that besides quenching of the second kind in the cell there occur processes of "instantaneous quenching" (quenching of the first kind, according to Vavilov) which do not shorten the duration of the fluorescence. This is equivalent to Rabinowitch's hypothesis that some of the molecules in a cell are in a nonfluorescing state.

A second possible explanation of the same facts would be that in the cell we are dealing with pure quenching of the second kind, but that, unlike fluorescence quenching in solutions by additives, in our case the probability of a photochemical reaction leading to quenching is not constant throughout the entire period of excitation and is gradually reduced. M. D. Galanin [7] has shown that this occurs in the concentration quenching of fluorescence from a number of dyes in viscous solutions.

It is also possible to assume that in the cell fluorescence quenching has the character of such complicated concentration quenching and is thus associated with the migration of excitation energy and with its transfer to "centers" of photosynthetic activity.

In our case we could assume that the probability of photochemical utilization of the excitation energy depends on the distance between an excited chlorophyll molecule and other molecules participating in the reaction, or on other statistically distributed factors which determine the state of the reacting system. Since the process is occurring in a very viscous medium, where the diffusive displacement of a molecule during time τ is very small and "interspersion" cannot establish a statistical equilibrium of molecular distribution, in the region close to an excited chlorophyll molecule there must take place a gradual "impoverishment" of easily reacting molecules, that is, the probability of a photochemical reaction must gradually diminish during the excited state. Predominantly short-lived molecules will be quenched and the duration of the excited state will be reduced more slowly than the yield.

At the present time we have no clear experimental proof of the correctness of any one of the foregoing hypotheses. The second hypothesis is favored by the fact that it most simply and without special assumptions provides a possibility of explaining the very high quantum yield of primary photochemical reactions. Indeed, if during the entire life of the excited state a photochemical process of utilization of the excitation energy competes both with the fluorescence process and with the transformation of this energy into heat, the plant can utilize for photosynthesis a considerable portion of both the energy which in a solution is emitted as fluorescence and that which in a solution is transformed into heat. The twelve-fold reduction of the fluorescence yield in vivo as compared with a solution shows that the probability of photochemical utilization exceeds by the same amount the combined probability of the other two processes; this means that photosynthesis has available the energy of more than 90% of the excited molecules.

On the other hand, if for the explanation of the discrepancy between ρ and τ we assume "instantaneous" quenching processes of the first kind we must ascribe the quenching of about 40% of the excited molecules to this cause. Thus, in order to explain the high quantum yield (near unity) of primary photochemical reactions in the cell we would have to introduce some special notions regarding the mechanism of this "instantaneous" absorption by the plant of the energy of these 40% of the excited molecules. Since no sufficient basis exists at present for such a model we can adopt the second explanation as a working hypothesis.

It is also a striking fact that our measurements of ρ and τ yielded practically identical values for fluorescence from a specimen which had been purified of carotinoids and for a leaf extract which evidently contained them. This conflicts with [8], according to which the migration of energy from carotinoids to chlorophyll occurs in the live cell but not in solutions. The entire problem requires more detailed investigation.

This paper was presented at the second All-Union Conference on Photosynthesis in January 1957 and will appear in more complete form in the proceedings of that conference.

LITERATURE CITED

[1] P. Latimer, T. T. Bannister, and E. Rabinowitch, Science 124, 585 (1955).

[2] L. A. Tumerman, J. Exptl.-Theoret. Phys. (USSR) 11, 515 (1941); Uspekhi Fiz. Nauk 33, 2, 218 (1947).

[3] A. M. Bonch-Bruevich, Izv. AN SSSR, Ser. Fiz. 20, 591 (1956); A. M. Bonch-Bruevich, V. A. Molchanov, and V. I. Shirokov, Izv. AN SSSR, Ser. Fiz. 20, 596 (1956).

[4] E. Rabinowitch, Science 125, 3248 (1957).

[5] J. A. Prins, Nature 134, 457 (1934); E. Rabinowitch, Photosynthesis 2, p. 2, 1798 (1956).

[6] S. I. Vavilov, Doklady Akad. Nauk SSSR 3, 271 (1936); Coll. Works 1, p. 424 (1954).

[7] M. D. Galanin, J. Exptl.-Theoret. Phys. (USSR) 28, 485 (1955).*

[8] H.J. Dutton, W. M. Manning, and B. M. Dugger, J. Phys. Chem. 47, 308 (1943).

[9] L. M. Kosobutskaia and A. A. Krasnovskii, Biochemistry (USSR) 18, 340 (1953).

Received June 10, 1957

---

* Soviet Physics – JETP, p. 317.

THE INFLUENCE OF "ENTRAINMENT" ON THERMOMAGNETIC EFFECTS IN BISMUTH SELENIDE

Academician Kh. I. Amirkhanov (Azerbaidzhan Academy of Sciences), R. I. Bashirov, A. Z. Daibov, and I. M. Tsidil'kovskii

Bismuth selenide is one of the good semiconductors which have been studied intensively in recent years because of their great practical value. The electrical properties of Bi_2Se_3 were studied by Cullity [1] and Konorov [2]. It will be shown below that an investigation of thermomagnetic effects enables us to understand certain new characteristics of the interaction between current carriers and the crystal lattice. We have studies the electrical conductivity, Hall effect, thermoelectric power and the transverse and longitudinal Nernst-Ettinghausen (N-E) effects in 10 polycrystalline specimens of bismuth selenide which were either hot pressed or from slowly cooled melts. The experimental method was similar to that described previously in [3, 4], and the measurements were taken between 120° and 700°K. We shall give the measurements for 6 specimens. The sign of the Hall effect and of the thermoelectric power at low temperatures shows specimens Nos. 1 and 3 to be p-type and the remaining specimens to be n-type. The concentration of holes (or electrons), as calculated from the Hall effect at $T < 200°K$ (in cm^{-3}) is as follows: No. 1 – $1.2 \cdot 10^{19}$, No. 2 – $1.6 \cdot 10^{18}$, No. 3 – $1.9 \cdot 10^{19}$, No. 4 – $1.2 \cdot 10^{18}$, No. 5 (cast) – $1.5 \cdot 10^{19}$, No. 6 – $1.7 \cdot 10^{19}$. Figure 1 shows the temperature dependence of the transverse N-E coefficient:

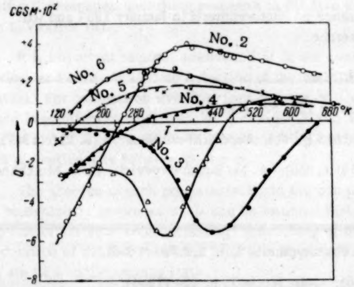

Fig. 1.

$$Q = E_y \Big/ \frac{\partial T}{\partial x} H_z$$

where E_y is the field of the N-E effect, $\partial T / \partial x$ is the temperature gradient and H_z is the magnetic field strength.

For specimen No. 2 (and two additional specimens for which the data are not given) in the range 120-200°K, $|Q| \sim T^{-1.3}$, and for No. 4 (and one more similar specimen) $|Q| \sim T^{1.3}$ (Fig. 2).* This temperature dependence of the N-E effect cannot be explained by the usual formula for weak magnetic fields ($uH/c \ll 1$, u is the carrier mobility and c is the velocity of light)

$$Q_e = \frac{1-n}{2} a_n \frac{k}{e} u, \tag{1}$$

with n determined by the relation between the carrier mean free path l and velocity v, as follows: $l = l_0(T)v^n$, $a_n \sim 1$.

In crystals with predominantly homopolar binding, among which bismuth selenide is evidently included, when carriers are scattered by acoustic lattice vibrations the theory gives $n = 0$ and the N-E effect should be positive. A negative sign at low temperatures could be attributed to scattering by ionized atoms of an impurity, for which $n = 4$. But here we encounter two difficulties:

---

* As in original—Publisher's note.

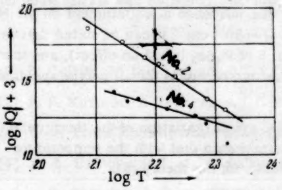

Fig. 2.

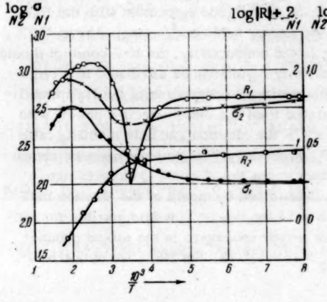

Fig. 3.

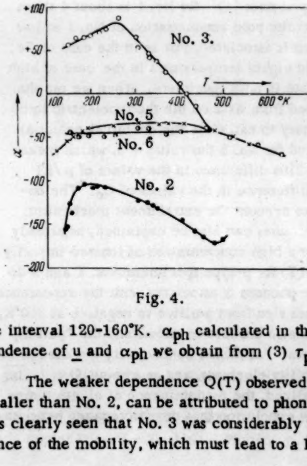

Fig. 4.

1) The mobilities calculated from Eq. (1) and from the Hall effect are quite different; for example, at 200°K, $u_x \sim 10u_{NE}$.

2) According to (1) the temperature dependence of Q is determined by the temperature dependence of the mobility. But from data on the Hall effect and electrical conductivity of Nos. 2, 4 and 5 below 450° we have $u \sim T^{-0.5} - T^{-1.0}$.

It can be assumed that in the investigated low-temperature region the N-E effect for specimen No. 2 of Bi_2Se_3 is determined principally by the fact that phonons entrain electrons [5]. According to calculations by Gurevich and Obraztsov [6] in nondegenerate semiconductors this entrainment should affect the N-E effect more strongly than it affects the thermoelectric power. This has been confirmed experimentally by Mochan, Obraztsov and Krylov [7], who thoroughly investigated highly resistant p-type Ge.

The hypothesis that entrainment influenced the N-E effect in specimen No. 2 was confirmed by measurements of the thermoelectric power (Fig. 4). From 120°K to 160°K the thermoelectric coefficient α decreases in absolute value according to the law $|\alpha| \sim T^{-1.5}$. A decrease of $|\alpha|$ with increasing T at low temperatures has been observed in single crystals of gray tin, Ge, Si and InSb by several investigators [9-13], who gave entrainmant as the explanation. The α(T) law in specimen No. 2 of polycrystalline Bi_2Se_3 can also be attributed to entrainment of electrons by phonons. When electrons are scattered only by phonons the thermoelectric power can be represented as the sum of an electronic part α_e and a phonon part (due to entrainment) α_{ph} [12]:

$$\alpha = \alpha_e + \alpha_{ph} = \pm \frac{k}{l}\left(2 - \frac{\mu}{kT}\right) \pm \frac{w^2\tau_{ph}}{uT}, \quad (2)$$

where μ is the chemical potential, τ_{ph} is the phonon relaxation time and w is the velocity of sound with the signs + and − referring to p-type and n-type semiconductors, respectively. From the experimental curve α(T) we obtained the temperature dependence of α_{ph}. Assuming that in the interval 170-300°K $\alpha \approx \alpha_e$, it is possible by using data on the Hall effect to compute the effective electron mass m_-; the value obtained was 0.18 m_0 (m_0 is the mass of a free electron). Having obtained the effective mass we can calculate α_e in the interval 120-160°K. α_{ph} calculated in this manner obeys the law $|\alpha_{ph}| \sim T^{-2.8}$. From the temperature dependence of u and α_{ph} we obtain from (3) $\tau_{ph} \sim T^{-2.3}$.

The weaker dependence Q(T) observed in specimen No. 4, which had an electron concentration somewhat smaller than No. 2, can be attributed to phonon scattering on grain boundaries (under × 15-20 magnification it was clearly seen that No. 3 was considerably finer grained than No. 2), and also to less steep temperature dependence of the mobility, which must lead to a lower power in the function $\tau_{ph} \sim T^{-r}$.

In [10] it is shown for Ge that at 100-150°K increase of the impurity concentration from $\sim 10^{14}$ cm^{-3} to $\sim 10^{18}$ cm^{-3} does not result in a decrease of α_{ph}. The same should, of course, be true for Q_{ph}. Our experiments with bismuth selenide show that at carrier concentrations $N \sim 10^{18}$ cm^{-3} the influence of entrainment on the N-E effect and on the thermoelectric power is decisive. For specimens with $N \sim 10^{19}$ cm^{-3} it can be stated that as the concentration increases the entrainment plays a smaller part (for No. 6 of Bi_2Se_3 it had no effect), and that in p-type specimens entrainment is more important than in n-type (at low temperatures for all p-type specimens only negative ranges of Q were observed).

For Bi_2Se_3 specimen No. 2 we also investigated the longitudinal N-E effect (variation of the thermoelectric power in a magnetic field). The effect was relatively small but it was established that with the temperature increasing from 120°K to 160°K $\Delta\alpha = \alpha(H) - \alpha(0)$ decreases in agreement with the theory [6].

The positive portion of the curve Q(T) for specimens 2, 5, and 6 is determined by ordinary carrier scattering on phonons and is described by Eq. (1). A calculation of electron mobility according to (1) for n = 0 (scattering by acoustic vibrations) near the maximum of Q(T), where neither entrainment nor the appearance of another kind of carrier seriously influences the N-E effect, leads to values of u_{NE} which are in good agreement with the Hall mobilities. For example, at 360°K in Bi_2Se_3 No. 2 $u_{NE} = 760$ cm^2/v·sec and $u_x = 780$ cm^2/v·sec. Above 450°K, where according to the data for R, σ and α holes begin to participate in the conductivity, the N-E constant should reverse its sign. The absence of a reversal of sign in the mixed conductivity region can be attributed to a large ratio between the electron and hole mobilities. This hypothesis is confirmed by a comparison of the Hall mobilities in n-type and p-type specimens and of the effective masses calculated from the thermoelectric power, with an evaluation of $\underline{b}$ from the N-E effect, etc. For temperatures below 200°K the electron and hole mobility ratio as calculated from the Hall effect for specimens Nos. 2 and 3, is ≈ 13. From the effective mass ratio we obtain $b \approx (m_+/m_-)^{5/2} \approx 12$. If it is assumed that at temperatures where in specimens Nos. 1 and 3 Q changes sign, $N_+ \approx N_-$, then using the width of the forbidden band $\Delta E = 0.27$ ev, as determined by means of the relation $\ln RT^{3/2}$ from 1/T to T = 800°K, we easily obtain $b \simeq 16$ for Bi_2Se_3 No. 3 and $b \approx 17$ for No. 1. It is also possible to compute $\underline{b}$ from the ratio between the maximum of the Hall coefficient for p-type specimens in the mixed conductivity region, and the value of R in the impurity region: $|R_{max}|/R_{imp} = (b-1)^2/4b$. For No. 1 we obtain $b \approx$ ≈ 13 and for No. 3 $b \approx 12$.

According to the data for R and σ, and also from the high-temperature portion of the Q(T) curves in No. 2 and other specimens above 450°K, the mobility law $u \sim T^{-0.5} - T^{-1.0}$ is replaced by $u \sim T^{-1.5}$. A stronger dependence u(T) for a narrower forbidden band leads to the fact that above ~ 500°K σ begins to decrease (Fig. 3).

The functions Q(T) for Nos. 1 and 3 are similar. A difference lies in the fact that the minimum of Q(T) for No. 3 is at a higher temperature than for No. 1, and that at low temperatures $|Q|$ for No. 1 is about 4 times greater than for No. 3. This difference can be explained by the fact that the hole concentration of No. 1 at low temperatures is 1.5-2 times smaller than in No. 3. The minimum, which is associated, just as in the case of Ge, with the appearance of a different type of carrier, must be shifted toward higher temperatures in the case of high carrier concentrations. At low temperatures the electron gas is degenerate in both specimens. When we use the estimate of the effective mass of holes ($m_+ = 0.5\ m_0$), which was obtained from data on the thermoelectric force in the 200-280°K region, where Pisarenko's formula is applicable, it is easy to calculate the chemical potential term μ/kT. At 130°K for No. 1 this potential term has the value ~ 3 and for No. 5 the value ~ 5, which means that in the second instance the electron gas is more highly degenerate. This difference in the values of μ/kT must, according to Wright's calculations [14], correspond to a two-fold difference in the values of Q_e. The observed difference in the values of Q can be explained if we also take into account the entrainment mechanism, which should be stronger in No. 1. The negative sign of Q at low temperatures can also be explained, as already mentioned, by entrainment. It should be noted that carrier scattering by a high concentration of ionized impurity atoms also leads to a negative sign for Q. The fact that the curves of Q(T) for p-type specimens Nos. 1 and 3 do not have a positive region corresponding to carrier scattering by acoustic phonons is associated with the appearance of conduction electrons at relatively low temperatures (in No. 1 R reverses sign from positive to negative at 300°K, and in No. 3 at 370°K), to which the N-E constant is very sensitive. It is also possible to understand the "pulling down" of the negative part of the Q(T) curves towards higher temperatures. For mixed conductivity the concentration of low-mobility holes is greater than the concentration of high-mobility electrons, and as a result $Q < 0$. In the transition to intrinsic conductivity, when the concentrations are equalized, the predominance of electron mobility over hole mobility leads to a reversal of the sign of Q. We note in conclusion that the discrepancy between the values of the mobilities according to the Hall and N-E effects, which is observed at low temperatures in PbS, PbSe and PbTe [15] is also evidently attributable to the influence of entrainment on the N-E effect.

LITERATURE CITED

[1] B. Cullity, Metals Technol. 15, 1 (1948).

[2] P. P. Konorov, J. Tech. Phys. (USSR) 26, 1126 (1956).*

[3] I. M. Tsidil'kovskii, Dissertation (Leningrad State Univ., 1956).**

[4] A. Z. Daibov and I. M. Tsidil'kovskii, J. Tech. Phys. (USSR) 25, 742 (1955).

[5] L. E. Gurevich, J. Exptl.-Theoret. Phys. (USSR) 16, 193, 416 (1946).

[6] V. L. Gurevich and Iu. N. Obraztsov, J. Exptl.-Theoret. Phys. (USSR) 32, 390 (1957).***

[7] I. V. Mochan, Iu. N. Obraztsov and T. V. Krylova, J. Tech. Phys. (USSR) 27, 242 (1957).****

[8] C. Herring, Phys. Rev. 96, 1163 (1954).

[9] H. P. R. Frederikse, Phys. Rev. 92, 248 (1953).

[10] T. H. Geballe and G. W. Hull, Phys. Rev. 94, 1134 (1954); 98, 940 (1955).

[11] H. P. R. Frederikse and E. V. Mielcrzarek, Phys. Rev. 99, 1839 (1955).

[12] J. Erdmann, H. Schulz, and J. Appel, Z. Naturforsch. 12a, 171 (1957).

[13] A. N. Goland and A. W. Ewald, Phys. Rev. 104, 948 (1956).

[14] R. W.Wright, Proc. Phys. Soc. A64, 984 (1951).

[15] I. M. Tsidil'kovskii, Doklady Akad. Nauk SSSR 102, 737 (1955).

Received June 11, 1957

Academy of Sciences, USSR, Dagestan Branch,
Makhachkala

---

* Soviet Physics — Technical Physics, p. 1100.

** In Russian.

*** Soviet Physics — JETP, p. 302.

**** Soviet Physics — Technical Physics, p. 213.

APPROXIMATE DISPERSION RELATIONS FOR NUCLEON-NUCLEON SCATTERING

V. Z. Blank[*] **and P. S. Isaev**

(Presented by Academician N. N. Bogoliubov July 15, 1957)

Dispersion relations for nucleon-nucleon scattering have been discussed by several authors [1-3]. The relations which they derived could not be compared with experiment because they contained unobservable quantities as well as unknown quantities associated with the scattering of antinucleons by nucleons.

The present article is concerned with approximate dispersion relations. We consider nucleon-nucleon scattering in the absence of antinucleons. We begin with dispersion relations which are obtained in the usual manner [4]:

$$D(E)-\frac{1}{2}\left(1+\frac{E}{M}\right)D(M)-\frac{1}{2}\left(1-\frac{E}{M}\right)D(-M)=$$

$$=\frac{E^2-M^2}{\pi}P\int\limits_0^\infty\frac{A(E')\,dE'}{(E'-E)(E'^2-M^2)}-\frac{E^2-M^2}{\pi}P\int\limits_0^\infty\frac{A(-E')\,dE'}{(E'+E)(E'^2-M^2)}. \tag{1}$$

Here D and A are the real and imaginary parts of the nucleon-nucleon scattering amplitude; E is the energy of the scattered nucleon in the coordinate system where the sum of the momenta of the scatterer before and after a collision is zero ($\mathbf{p}+\mathbf{p}'=0$). The nucleon-nucleon scattering amplitudes D(−M) and A(−E') can be expressed linearly in terms of antinucleon-nucleon scattering amplitudes for positive energies. Thus the dispersion relations (1) relate the amplitudes of nucleon-nucleon and antinucleon-nucleon scattering.

In the approximation under consideration (1) becomes

$$D(E)-\frac{1}{2}\left(1+\frac{E}{M}\right)D(M)=$$

$$=\frac{E^2-M^2}{\pi}P\int\limits_{\frac{M^2-\mathbf{p}^2}{\sqrt{M^2+\mathbf{p}^2}}}^\infty\frac{A(E')\,dE'}{(E'-E)(E'^2-M^2)}+C\,\frac{(E^2-M^2)\,\delta_{0T}\delta_{1S}}{E-\dfrac{M^2-\mathbf{p}^2-2M\epsilon}{\sqrt{M^2+\mathbf{p}^2}}}, \tag{2}$$

where the last term is the constribution of the intermediate deuteron state: δ_{0T} and δ_{1S} are Kronecker symbols which are nonvanishing for total isotopic spin T = 0 and total ordinary spin S = 1; C is an energy-independent constant which must be determined experimentally; and ϵ is the deuteron binding energy.

This approximation is satisfactory in the energy region where the integral is determined mainly by the behavior of the integrand for E' ~ E. For this purpose the function A(E') in the integrand must possess a large derivative in the given energy range, because the integration is performed in the sense of the principal value. The scattering amplitude A(E') under the integral sign in (2) is unobservable in the region

$$\sqrt{M^2+\mathbf{p}^2}>E'\geqslant\frac{M^2-\mathbf{p}^2}{\sqrt{M^2+\mathbf{p}^2}}. \tag{3}$$

---

[*] Deceased.

For forward scattering $\mathbf{p}^2 = 0$ and the unobservable region vanishes.

For nucleon-nucleon scattering it is necessary to take into account the identity of the particles and to consider not the scattering amplitude $f(\theta)$ at a certain angle θ, but rather the linear combination

$$f(\theta) \pm f(\pi - \theta), \tag{4}$$

where θ is the scattering angle in the center-of-mass system. For this amplitude the unobservable region (3) remains in effect at certain θ. For the purpose of symmetrization we write (2) in the center-of-mass system, as follows:

$$\begin{aligned} D(W, \mathbf{p}^2) - \frac{1}{2}\left(1 + \frac{W^2 - 2M^2 - 2\mathbf{p}^2}{2M\sqrt{M^2 + \mathbf{p}^2}}\right) D(2M, \mathbf{p}^2) = \\ = \frac{W^4 + 4(\mathbf{p}^2 - W^2)(M^2 + \mathbf{p}^2)}{\pi} P \int_{2M}^{\infty} \frac{2W' A(W', \mathbf{p}^2)\, dW'}{(W'^2 - W^2)[W'^4 + 4(\mathbf{p}^2 - W'^2)(W^2 + \mathbf{p}^2)]} + \\ + C' \frac{W^4 - 4(W^2 - \mathbf{p}^2)(M^2 + \mathbf{p}^2)}{W^2 - 4M(M - \epsilon)}, \end{aligned} \tag{5}$$

where W is the total energy of the two-nucleon system, $C' = \frac{c}{2\sqrt{M^2 + \mathbf{p}^2}}$ and $\mathbf{p}^2 = \frac{W^2 - 4M^2}{8}(1 - \cos\theta)$.

The unobservable region in (5) is given by $2M \leq W' < 2\sqrt{M^2 + \mathbf{p}^2}$. Here $\cos\theta' < -1$. The transition $\theta \rightarrow \pi - \theta$ is equivalent to the substitution $\mathbf{p}^2 \rightarrow \mathbf{p}'^2 = (W^2 - 4M^2)/4 - \mathbf{p}^2$ in (5). For symmetrization it is essential that

$$\frac{W^4 + 4(\mathbf{p}^2 - W^2)(\mathbf{p}^2 + M^2)}{W'^4 + 4(\mathbf{p}^2 - W'^2)(\mathbf{p}^2 + M^2)} - \frac{W^4 + 4(\mathbf{p}'^2 - W^2)(\mathbf{p}'^2 + M^2)}{W'^4 + 4(\mathbf{p}'^2 - W'^2)(\mathbf{p}'^2 + M^2)} \sim W'^2 - W^2. \tag{6}$$

In addition, the quantities $\cos\theta'$ and $\cos(\pi - \theta)'$ which enter into the integrand of (5) are given by

$$\begin{aligned} \cos\theta' &= 1 - \frac{8\mathbf{p}^2}{W'^2 - 4M^2}; \\ \cos(\pi - \theta)' &= -1 + \frac{8\mathbf{p}^2}{W'^2 - 4M^2} + 2\frac{W'^2 - W^2}{W'^2 - 4M^2}. \end{aligned} \tag{7}$$

Therefore, if in accordance with the assumption made previously, $A(W')$ varies very rapidly in the region $W' \sim W$, the integral which contains the difference (6) can be neglected compared with the integral that contains the corresponding sum and in (7) the last term of the expression for $\cos(\pi - \theta)'$ can be neglected. Then

$$\cos(\pi - \theta)' = \cos(\pi - \theta') = -\cos\theta',$$

and it becomes possible to carry out the operation (4). In this approximation for forward scattering ($\mathbf{p}^2 = 0$) the unobservable region disappears completely and we have

$$\begin{aligned} D(k) - \frac{1}{2}\left(\frac{3}{2} + \frac{k^2}{M^2} + \frac{\sqrt{k^2 + M^2}}{2M}\right) D(0) = \\ = \frac{2k^2(k^2 + M^2)}{\pi} P \int_0^{\infty} \frac{A(k')\, dk'}{k'(k'^2 - k^2)(k'^2 + M^2)} + C' \frac{3k^2(k^2 + M^2)}{k^2 + M\epsilon}, \end{aligned} \tag{8}$$

where $k^2 = \frac{W^2 - 4M^2}{4}$.

An experimental test of dispersion relation (8) is of interest. The existing experimental data on the total cross section $\sigma(k)$ and the angular distribution enable us to calculate the integral of the total cross section and to compare $D(k)$ obtained in this manner with experimental measurements. This test will determine the range of applicability of (8). For very low energies (up to 6 Mev) where scattering is well described by an S-wave we can use the expansion

$$k \cot \delta = -\frac{1}{a} + \frac{1}{2} r k^2 \tag{9}$$

and thus check (8), which in this case becomes

$$\frac{1}{k} \sin 2\delta_{0,1}(k) + \left(\frac{3}{2} + \frac{k^2}{M^2} + \frac{\sqrt{k^2 + M^2}}{2M}\right) a_{0,1} = \\ = \frac{4k^2 (k^2 + M^2)}{\pi} P \int_0^\infty \frac{\sin^2 \delta_{0,1}(k')\, dk'}{k'^2 (k'^2 - k^2)(k'^2 + M^2)} + C' \frac{3k^2 (k^2 + M^2)}{k^2 + M\varepsilon}, \tag{10}$$

where $a_{0,1} = \lim_{k \to 0} \left[\frac{1}{k} \sin 2\delta_{0,1}(k)\right]$, and δ_0 and δ_1 are the phase shifts of singlet and triplet S-scattering, respectively. Substituting (9) into (10), differentiating with respect to k^2 and setting $k^2 = 0$, we obtain an expression containing $\underline{r}$ and $\underline{a}$. These quantities are well known and have the following values [5]: $r_0 = 3 \cdot 10^{-13}$ cm, $r_1 = 1.704 \cdot 10^{-13}$ cm, $a_0 = -23.69 \cdot 10^{-13}$ cm, $a_1 = 5.38 \cdot 10^{-13}$ cm.

For singlet scattering the deuteron term is absent and the left-hand side of (10) agrees with the right-hand side to within 0.01%. But this does not enable us to obtain r_0 in terms of a_0, because r_0 is very sensitive to change of the total cross section $\sigma(k)$. The insertion of (9) instead of using the total cross section provides only a rough check of the dispersion relations.

For triplet scattering when the deuteron term is neglected the left-hand side of (10) agrees with the right-hand side to within 3%.

The authors are deeply grateful to N. N. Bogoliubov for valuable suggestions and to L. I. Lapidus, A. A. Logunov and D. V. Shirkov for fruitful discussions.

LITERATURE CITED

[1] V. Ia. Fainberg and E. S. Fradkin, Doklady Akad. Nauk SSSR 109, 507 (1956).*

[2] B. L. Ioffe, J. Exptl.-Theoret. Phys. (USSR) 31, 583 (1956).**

[3] F. M. Kuni, Doklady Akad. Nauk SSSR 111, 571 (1956).***

[4] N. N. Bogoliubov, B. V. Medvedev, and M. K. Polivanov, Problems in the Theory of Dispersion Relations [in Russian] (1957); N. N. Bogoliubov and D. V. Shirkov, Introduction to the Theory of Quantized Fields [in Russian] (1957).

[5] E. E. Lampi, G. D. Freier, and J. H. Williams, Phys. Rev. 80, 853 (1950).

Received June 28, 1957

Joint Nuclear Research Institute

---

* Soviet Physics – "Doklady," p. 455.

** Soviet Physics – JETP, p. 534.

*** Soviet Physics – "Doklady," p. 686.

ON THE THEORY OF PHASE TRANSITIONS

**Academician N. N. Bogoliubov, D. N. Zubarev
and Iu. A. Tserkovnikov**

It has been shown in [1, 2] that the theory of superconductivity can be developed advantageously through the use of a model with the Hamiltonian

$$H = H_0 + H_{int},$$
$$H_0 = \sum_{k,s} (E(k) - \lambda)\, a^+_{k,s} a_{k,s}, \quad H_{int} = -\frac{J}{V} \sum_{(k \neq k')} a^+_{-k,-1/2} a^+_{k,1/2} a_{k',1/2} a_{-k',-1/2}. \tag{1}$$

The summation in H_{int} extends over the momenta k,k' which pertain to the energy layer

$$E_F - \omega < E(k) < E_F + \omega. \tag{2}$$

We shall show that with this Hamiltonian it is possible to construct a thermodynamic potential

$$\Psi = F - \lambda N = -\theta \ln \mathrm{Sp}\, e^{-H/\theta}$$

which is exact asymptotically (for V → ∞). We shall show, moreover, that a similar calculation is possible with the more general expression

$$H = \sum_{k,s} (E(k) - \lambda)\, a^+_{k,s} a_{k,s} - \frac{1}{V} \sum_{(k,k')} J(k,k')\, a^+_{-k,1/2} a^+_{k,1/2} a_{k,1/2}\, a_{-k',-1/2}, \tag{3}$$

which contains the bounded real function J(k, k') that practically disappears outside of a certain finite region of the momenta k, k'.

In view of the fact that in the theory of phase transitions only very few examples have been solved exactly we believe it will be expedient to develop a method of calculating the thermodynamic potentials for Hamiltonian (3), and all the more so because we here obtain applications to the theory of superconductivity.

We perform our canonical transformation

$$\alpha_{k,1/2} = u_k \alpha_{k,0} + v_k \alpha^+_{k,1}, \quad \alpha_{-k,-1/2} = u_k \alpha_{k,1} - v_k \alpha^+_{k,0}$$

with the real functions u_k, v_k associated by the relation

$$u_k^2 + v_k^2 = 1.$$

We obtain

$$H = H^{(0)} + H',$$
$$H^{(0)} = U + \sum_k H_k, \quad H' = -\frac{1}{V} \sum_{(k,k')} J(k,k')\, B^+_k B_{k'}, \tag{4}$$

where

$$U = \mathrm{const} = 2\sum_{k} (E(k) - \lambda)\, v_k^2 - \frac{1}{V}\sum_{(k,k')} J(k,k')\, u_k v_k u_{k'} v_{k'},$$

$$\begin{aligned} H_k = &\left\{ (E(k) - \lambda)(u_k^2 - v_k^2) + 2u_k v_k \sum_{k'} \frac{J(k,k')}{V} u_{k'} v_{k'} \right\} (\overset{+}{\alpha}_{k0}\alpha_{k0} + \overset{+}{\alpha}_{k1}\alpha_{k1}) + \\ &+ \left\{ 2(E(k) - \lambda)\, u_k v_k - (u_k^2 - v_k^2) \sum_{k'} \frac{J(k,k')}{V} u_{k'} v_{k'} \right\} (\overset{+}{\alpha}_{k0}\overset{+}{\alpha}_{k1} + \alpha_{k1}\alpha_{k0}), \\ B_k = &\; u_k v_k (\overset{+}{\alpha}_{k0}\alpha_{k0} + \overset{+}{\alpha}_{k1}\alpha_{k1}) - u_k \alpha_{k1}\alpha_{k0} + v_k^2 \overset{+}{\alpha}_{k0}\overset{+}{\alpha}_{k1}. \end{aligned} \tag{5}$$

We note that all operators H_k, B_k, $\overset{+}{B}_k$ commute among themselves for different $\underline{k}$.

We now apply the statistical theory of perturbations to (4), and obtain

$$\frac{\mathrm{Sp}\, e^{-H/\theta}}{\mathrm{Sp}\, e^{-H^{(0)}/\theta}} = 1 + \sum_{(n>1)} (-1)^n \int_0^{1/\theta} dt_1 \int_0^{t_1} dt_2 \dots \int_0^{t_{n-1}} dt_n \frac{\mathrm{Sp}\{e^{-H^{(0)}/\theta} H'(t_1) \dots H'(t_n)\}}{\mathrm{Sp}\{e^{-H^{(0)}/\theta}\}},$$

where

$$H'(t) = e^{H^{(0)}t} H' e^{-H^{(0)}t}.$$

This relation can also be represented by

$$\ln \mathrm{Sp}\, e^{-H/\theta} - \ln \mathrm{Sp}\, e^{-H^{(0)}/\theta} = \ln\left\{ 1 + \sum_{(n>1)} \int_0^{1/\theta} dt_1 \int_0^{t_1} dt_2 \dots \int_0^{t_{n-1}} dt_n \mathfrak{A}_n \right\}, \tag{6}$$

where

$$\mathfrak{A}_n = \frac{1}{V^n} \sum_{\binom{k_1,\dots,k_n}{k_1',\dots,k_n'}} J(k_1, k_1'), \dots, J(k_n, k_n') \times$$

$$\times \frac{\mathrm{Sp}\{e^{-H^{(0)}/\theta} \widetilde{B}_{k_1}(t_1) B_{k_1'}(t_1) \dots \widetilde{B}_{k_n}(t_n) B_{k_n'}(t_n)}{\mathrm{Sp}\{e^{--H^{(0)}/\theta}\}}, \tag{7}$$

$$B_k(t) = e^{H^{(0)}t} B_k e^{-H^{(0)}t} = e^{H_k t} B_k e^{-H_k t}, \quad \widetilde{B}_k(t) = e^{H_k t} B_k^{+} e^{-H_k t}.$$

We shall show that if for all $\underline{k}$

$$\mathrm{Sp}\,(e^{-H_k/\theta} B_k) = 0, \tag{8}$$

then each $\mathfrak{A}_n$ remains bounded when we pass to the limit V ⟶ ∞.

In the summation (7) let us take any term for which at least one of the momenta k_q or k_q' is not equal to one of the other momenta k_j and k_j'. It is easily seen that this term will be proportional to

$$\mathrm{Sp}\{e^{-H_{k_q}/\theta} \widetilde{B}_{k_q}(t)\} = \mathrm{Sp}\{e^{-H_{k_q}/\theta} B_{k_q}^{+}\} = 0,$$

or

$$\mathrm{Sp}\,\{e^{-H_{k'_q}/\theta} B_{k'_q}(t)\} = \mathrm{Sp}\,\{e^{-H_{k'_q}/\theta} B_{k'_q}\} = 0.$$

Therefore in (7) we need take into account only the terms for which there are not more than n different momenta among $k_1, k'_1, \ldots, k_n, k'_n$. These lead to a quantity of the order V^n which is canceled by the factor $1/V^n$. Consequently, $\mathfrak{A}_n$ remains finite when $V \to \infty$. On the other hand, both terms in the left-hand side of (6) must be proportional to V when $V \to \infty$. If on this basis we neglect terms of finite order we can replace $\ln \mathrm{Sp}\, e^{-H/\theta}$ by $\ln \mathrm{Sp}\, e^{-H(0)/\theta}$ and obtain for the thermodynamic potential under consideration an expression of the form

$$\Psi = U - \theta \sum_k \ln \mathrm{Sp}\, e^{-H_k/\theta} \tag{9}$$

Thus, in order to solve our problem we must determine u_k, v_k from (8) and then use (9).

It is technically convenient to carry through this program by diagonalizing H by means of the canonical transformation

$$\alpha_{k0} = \lambda_k \beta_{k0} - \mu_k \beta^+_{k1}, \quad \alpha_{k1} = \lambda_k \beta_{k1} + \mu_k \beta^+_{k0} \tag{10}$$

with real coefficients related by

$$\lambda_k^2 + \mu_k^2 = 1.$$

These coefficients are determined by the vanishing of the nondiagonal part of the operator H_k, which is proportional to

$$\beta_{k1}\beta_{k0} + \beta^+_{k0}\beta^+_{k1}.$$

Then substituting (10) into (5) for B_k we develop Eq. (8). We thus obtain

$$u_k v_k = \frac{C(k)}{2\Omega(k)} \; \frac{1 - e^{-\Omega(k)/\theta}}{1 + e^{-\Omega(k)/\theta}},$$

$$C(k) = \frac{1}{} \sum_{k'} J(k, k')\, u_{k'} v_{k'}, \quad \Omega(k) = \sqrt{(E(k) - \lambda)^2 + C^2(k)}. \tag{11}$$

and hence obtain the following equation for the determination of C(k):*

$$C(k) = \frac{1}{2V} \sum_{k'} J(k, k')\, \mathrm{th}\, \frac{\Omega(k')}{2\theta} \frac{C(k')}{\Omega(k')}. \tag{12}$$

It is interesting to note that this equation, especially in the form

$$2\Omega(k)\, u_k v_k = \frac{\mathrm{th}\, \dfrac{\Omega(k)}{2\theta}}{V} \sum_{k'} J(k, k')\, u_{k'} v_{k'},$$

is somewhat analogous to the equation of the two-body problem in the momentum representation.

We note that (12) always possesses the trivial solution C(k) = 0.

Expanding (9), we obtain

---

* 'th' ≡ 'tanh', 'ch' ≡ 'cosh', 'sh' ≡ 'sinh' – Publisher.

$$\Psi = \sum_{k} \left\{ E(k) - \lambda + \frac{C^2(k)}{2\Omega(k)} \operatorname{th} \frac{\Omega(k)}{2\theta} - \Omega(k) - 2\theta \ln\left(1 + e^{-\Omega(k)/\theta}\right) \right\}. \tag{13}$$

This expression will be regarded as the function $\Psi(\ldots C^2(k) \ldots)$. Then

$$\frac{\partial \Psi}{\partial C^2(k)} = C^2(k) \frac{\partial \Omega(k)}{\partial C^2(k)} \left\{ \frac{\partial}{\partial \Omega(k)} \frac{1}{2\Omega(k)} \operatorname{th} \frac{\Omega(k)}{2\theta} \right\} = -\frac{C^2(k)}{4\theta^3} f\left(\frac{\Omega(k)}{\theta}\right),$$

where

$$f(x) = \frac{\operatorname{sh} x - x}{2x^3 \operatorname{ch}^2 \frac{x}{2}} > 0.$$

Therefore when $C^2 \neq 0$ the value of Ψ is always smaller than for the trivial solution.

Thus a phase transition will occur at the temperature for which Eq. (12) has a nontrivial solution.

Passing now to Bardeen's model, in which J and C are independent of k, we obtain for C the equation *

$$1 = \rho \int_{0}^{\omega} \frac{\operatorname{th} \frac{\sqrt{\xi^2 + C^2}}{2\theta}}{\sqrt{\xi^2 + C^2}} \, d\xi, \tag{14}$$

where

$$\rho = \frac{J}{2\pi^2} \left(\frac{k^2}{\partial E / \partial k} \right)_{k = k_F}.$$

We note that when $\theta = 0$ Eq. (13) gives for the gap the expression obtained in [1, 2].

It is easily seen that (14) has solutions only when $\theta < \theta_0$, where θ_0 is determined from (13) with $C = 0$:

$$1 = \rho \int_{0}^{\omega} \frac{\operatorname{th} \frac{\xi}{2\theta_0}}{\xi} \, d\xi, \tag{15}$$

whence

$$\theta_0 = 1.13\, \omega e^{-1/\rho}. \tag{16}$$

Equation (14) determines C as a function of θ. When $\theta = 0$ we have $C(0) = 2\omega e^{-1/\rho}$ [2].

Near $\theta = \theta_0$ the gap C approaches zero and becomes

$$C^2 = 9.39\, \theta_0 (\theta_0 - \theta). \tag{17}$$

From (13) when (17) is taken into account we see that at the point $\theta = \theta_0$ the entropy is continuous and the specific heat $\mathfrak{S}$ shows a finite jump given by

$$\frac{\Delta \mathfrak{S}}{\mathfrak{S}_0} = 1.43, \tag{18}$$

---

* Thermodynamical formulas in the simplest case J = const were also obtained by Bardeen, Cooper and Schrieffer [3] on the basis of different ideas and through the use of an approximate variational method.

where $\mathfrak{S}_0$ is the specific heat of an ideal Fermi gas at $\theta = \theta_0$. Therefore at the point $\theta = \theta_0$ we have a second-order phase transition.

LITERATURE CITED

[1] V. V. Tolmachev and S. V. Tiablikov, J. Exptl.-Theoret. Phys. (USSR) 34, 1 (1958). *

[2] N. N. Bogoliubov, J. Exptl.-Theoret. Phys. (USSR) 34, 1 (1958).*

[3] L. Cooper, Post-deadline Paper at March, 1957, AP3 A Meeting in Philadelphia, BCS (to be published).

[4] J. Bardeen, L. N. Cooper, and J. R. Schrieffer, Preprint, University of Illinois, Techn. Rep. No. 9, June 17 (1957).

Received November 13, 1957

---

* See Soviet Physics — JETP.

DISPERSION RELATIONS FOR VIRTUAL PROCESSES

A. A. Logunov

(Presented by Academician N. N. Bogoliubov July 18, 1957)

1. It is one of the tasks of quantized field theory to establish relations between observable quantities. This is the reason for the great interest in the so-called dispersion relations, which are derived from the general principles of local field theory and are not associated with any form of perturbation theory.

Dispersion relations have thus far been obtained for the processes of meson-nucleon scattering, photoproduction, the Compton effect on nucleons, etc. [1]. A very promising procedure is the determination of dispersion relations for vertex parts — "units" in the matrix elements of processes. Among the simplest examples are the "units" of photoproduction and of the Compton effect, which are shown diagrammatically in Fig. 1.

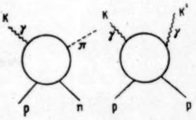

Fig. 1.

The photoproduction unit has one virtual photon, while that of the Compton effect may have either one virtual photon (with the second photon assumed to be real) or two virtual photons. The "units" depicted in Fig. 1 differ from real photoproduction and the real Compton effect in that here $k^2 \neq 0$. They are evidently component parts of the matrix elements of real physical processes. Thus the vertex part of the photoproduction can enter into the processes represented in Fig. 2, and the Compton effect into the processes represented in Fig. 3. Many other processes may be cited in which "units" of photoproduction and the Compton effect are components. Since all "unit" matrix elements can be studied in largely the same way, we shall confine ourselves to a study of the photoproduction "unit" with $k^2 \neq 0$.

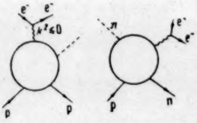

Fig. 2.

For the photoproduction "unit" it is possible to obtain dispersion relations which, as in the case of real photoproduction, can be used to obtain approximate equations. Since the "unit" is a component of the matrix elements of any processes these equations can give information concerning such processes.

2. According to the general theory of dispersion relations, in the coordinate system with $\mathbf{p} + \mathbf{p}' = 0$ the "Hermitian" part of the amplitude is equal to a certain integral of the "anti-Hermitian" part over the energy plus an arbitrary polynomial $P_n(E)$.

As in the case of real photoproduction, the "anti-Hermitian" part of the π-meson photoproduction amplitude by virtual photons (e. g., for $k^2 \leq 0$) can be written as

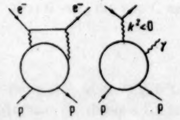

$$A_{\nu\rho}(E, \lambda\mathbf{e}) = \pi \sum_n \langle p', s' | j_\rho(0) | n, \lambda\mathbf{e} - \varepsilon\mathbf{p} \rangle \langle n, \lambda\mathbf{e} - \varepsilon\mathbf{p} \, | j_\rho(0) | p, s \rangle \times$$
$$\times \delta\left(\sqrt{M^2 + \mathbf{p}^2} + E - \sqrt{M_n^2 + \lambda^2 + \varepsilon^2\mathbf{p}^2}\right) -$$
$$- \pi \sum_n \langle p', s' | j_\nu(0) | n, -\lambda\mathbf{e} + \varepsilon\mathbf{p} \rangle \langle n, -\lambda\mathbf{e} + \varepsilon\mathbf{p} | j_\nu(0) | p, s \rangle \times$$
$$\times \delta\left(\sqrt{M^2 + \mathbf{p}^2} - E - \sqrt{M_n^2 + \lambda^2 + \varepsilon^2\mathbf{p}^2}\right), \qquad (1)$$

Fig. 3.

where $j_\rho(0)$, $j_\nu(0)$ are the "meson" and "electromagnetic" currents, E is the energy of the π-meson, $\epsilon = \frac{1}{4}\frac{m_\pi^2 + m_\gamma^2}{\mathbf{p}^2}$; $\lambda^2 = E^2 - (1-\varepsilon)^2\mathbf{p}^2 - m_\pi^2$; $k^2 = (q-q')^2 = -m_\gamma^2$.

The negative energy region in dispersion relations can be converted into a positive energy region by using the parity with respect to energy of a photoproduction "unit." We note that the parity properties of a photoproduction "unit" are analogous to those of a real photoproduction amplitude.

Making the usual assumption that between M and M + m_π there are no bound states of the meson-nucleon system, it is easily shown that the region of integration in the dispersion relations can be divided into two parts

$$0 < E' < \frac{Mm_\pi + {}^1/_4\,(m_\pi^2 + m_\gamma^2) - \mathbf{p}^2}{\sqrt{M^2 + \mathbf{p}^2}} \leqslant E' < \infty. \tag{2}$$

In the first region the nonvanishing portion of the integral is supplied by only one-nucleon states (n = 0). All states with n ≥ 1 contribute to the integral only in the second region. For scatterer momenta $\mathbf{p}^2 < {}^1/_4\,(m_\gamma^2 - m_\pi^2)$ the anti-Hermitian part of the "unit" in the first region will be

$$A_{\nu\rho}(E, \lambda\mathbf{e}) = \pi \sum_{s''} \langle p's' \,|\, j_\rho(0) \,|\, \lambda\mathbf{e} - \varepsilon\mathbf{p} \rangle \langle \lambda\mathbf{e} - \varepsilon\mathbf{p},\ s'' \,|\, j_\nu(0) \,|\, p, s \rangle \times$$
$$\times \frac{M^2 - {}^1/_4\,(m_\pi^2 - m_\gamma^2)}{M^2 + \mathbf{p}^2}\, \delta\left(E + \frac{\mathbf{p}^2 + {}^1/_4\,(m_\pi^2 - m_\gamma^2)}{\sqrt{M^2 + \mathbf{p}^2}}\right), \tag{3}$$

and for momenta ${}^1/_4\,(m_\gamma^2 - m_\pi^2) < \mathbf{p}^2 < {}^1/_2\,Mm_\pi + {}^1/_4 m_\gamma^2$

$$A_{\nu\rho}(E, \lambda\mathbf{e}) = -\pi \sum_{s''} \langle p', s' \,|\, j_\nu(0) \,|\, -\lambda\mathbf{e} + \varepsilon\mathbf{p},\ s'' \rangle \langle -\lambda\mathbf{e} + \varepsilon\mathbf{p},\ s'' \,|\, j_\rho(0) \,|\, p, s \rangle \times$$
$$\times \frac{M^2 - {}^1/_4\,(m_\pi^2 - m_\gamma^2)}{M^2 + \mathbf{p}^2}\, \delta\left(E - \frac{\mathbf{p}^2 + {}^1/_4\,(m_\pi^2 - m_\gamma^2)}{\sqrt{M^2 + \mathbf{p}^2}}\right). \tag{4}$$

From consideration of relativistic invariance the meson and electromagnetic currents can be written as

$$\langle p's' \,|\, j_\rho(0) \,|\, ps \rangle = g \langle \bar{u}_{s'}(p')\, \gamma_5 \tau_\rho u_s(p) \rangle;$$

g is the renormalized pseudoscalar coupling constant;

$$\langle p', s' \,|\, j_\nu(0) \,|\, p, s \rangle = \Big\langle \bar{u}_{s'}(p') \Big\{ e\,\frac{1+\tau_3}{2}\,\gamma^\nu F_1(k^2) +$$
$$+ \frac{1}{2}\left(\frac{1+\tau_3}{2}\,F_2^p(k^2) + \frac{1-\tau_3}{2}\,F_2^n(k^2)\right)[(k\gamma), \gamma^\nu] \Big\}\, u_s(p) \Big\rangle.$$

It must be emphasized that the invariant functions $F_1(k^2)$, $F_2^{p,n}(k^2)$ are form factors which characterize the electromagnetic structure of the nucleon. Information regarding these functions can be obtained from electron-nucleon scattering processes [2]. It is easily seen that the dispersion relations which have been obtained still contain a region of unobservable energies. When the recoil momentum of the nucleon is given by

$$\mathbf{p}^2 = \frac{1}{4}\,(m_\pi^2 + m_\gamma^2)\,\frac{M}{M + m_\pi},$$

the unobservable region is entirely absent, as in the case of real photoproduction.

An important application of dispersion relations is in the obtaining of a set of approximate equations for certain processes. For meson-nucleon scattering and photoproduction such equations have been obtained in the approximation of a fixed nucleon source as well as with account of nucleon recoil [3].

Similarly, equations can be obtained for "unit" elements, with the single difference that instead of the unitarity condition it is necessary to use (1). It is easily seen that (1) (like the unitary condition for photoproduction) makes it possible in the one-meson approximation to express the phases of the photoproduction "unit" in terms of the phases of meson-nucleon scattering.

We note that especially simple Low equations can be obtained in the approximation of a fixed nucleon source because in this case the unobservable energy region is entirely absent.

In conclusion I wish to express my deep gratitude to Academician N. N. Bogoliubov for his interest and for valuable suggestions.

LITERATURE CITED

[1] M. L. Goldberger, Phys. Rev. 97, 508 (1955); A. A. Logunov and A. N. Tavkhelidze, J. Exptl.-Theoret. Phys. (USSR) 32, 1393 (1957)* ; E. Corinaldesi, Nuovo cimento 4, 1384 (1956); M. Gell-Mann, M. L. Goldberger, and W. E. Thirring, Phys. Rev. 95, 1612 (1954); N. N. Bogoliubov and D. V. Shirkov, Doklady Akad. Nauk SSSR 113, 529 (1957).

[2] D. R. Yennie, M. M. Levy, and D. G. Ravenhall, Rev. Mod. Phys. 29, 144 (1957).

[3] L. D. Solov'ev, Nuclear Physics (in press).

Received July 6, 1957 Joint Nuclear Research Institute

---

* Soviet Physics – JETP, p. 1134.

X-RAYS FROM A STRONG PULSED DISCHARGE IN XENON

I. M. Podgornyi and S. A. Chuvatin

(Presented by Academician L. A. Artsimovich July 5, 1957)

It is known [1] that a powerful pulsed discharge through a gas in a certain pressure range is accompanied by both an x-ray pulse at the start and x-ray emission at a later stage of the pulse. This radiation appears at the instant when sharp bends ("singularities") appear in the curves of the discharge current and voltage at the discharge chamber electrodes. In light gas discharges under certain initial conditions the energy of the x-rays is considerably higher than the energy which can be acquired by electrons from the entire potential difference applied to the electrodes of the discharge chamber at the corresponding moment. In addition to its intrinsic interest this effect can be of importance in explaining the nature of cosmic radiation. The present article reports certain results of an investigation of gas discharge x-rays not associated with the start. The discharges occurred in xenon and in mixtures of hydrogen and xenon.

The porcelain discharge chamber was 175 mm in diameter and 1000 mm long. The discharge circuit included a condenser bank of 36μf capacity. A voltage divider was used to measure voltages between the discharge electrodes, while the discharge current was measured with a Rogovskii belt and RL integrating circuit. With an initial potential of 40 kv on the condensers the maximum discharge current reached 200 kiloamperes.

The experiments were performed under different initial gas pressures ranging from $5 \cdot 10^{-3}$ to $5 \cdot 10^{-1}$ mm Hg. Spectrally pure xenon was used, and had been chosen because of its large atomic weight compared with hydrogen and its chemical inertness. This latter factor can be important because of the possibility of a strong interaction between a heated gas and the chamber wall. A palladium absorber was used to purify the hydrogen. The discharge chamber was filled with gas from a calibrated volume in which the pressure was measured with an oil manometer. It was thus possible to eliminate errors in measuring the initial pressure due to heating of the walls by the preceding discharges.

In order to obtain the oscillograms of the pulses of x-rays, the discharge current and the voltage we used an OK-17 double pulsed oscilloscope. The discharge was initiated at the right moment by a pulse applied to an electrode in one of the spheres of the discharge tube. The same pulse triggered the oscilloscope sweep.

Openings covered with 7.5μ aluminum foil were used to extract soft x-ray beams, which could easily be absorbed by the chamber walls. The radiation was recorded on x-ray film as well as by a scintillation register. The method of recording was described in [1].

From oscillograms of potentials on the discharge chamber electrodes it is easily seen that the course of discharges differs in hydrogen and xenon under identical experimental conditions (initial gas pressure and condenser discharge voltage). Singularities of the current and voltage curves are clearly seen when the discharge occurs at low initial pressure in light gases (hydrogen, deuterium and helium). While the voltage curve of a discharge in hydrogen shows sharp peaks, these are absent in a xenon discharge even though the voltage curve in the latter case is far from a cosine curve. Just about the same can be stated with regard to the discharge current curves under the given conditions.

The x-ray pulse oscillograms in Figs. 1a and 1b show identical pulse lengths in hydrogen and xenon of about 1 μsec, although the energy of the x-rays in hydrogen reaches a few hundred kilo electron volts, while in xenon under similar conditions it does not exceed 10-15 kev. Hard x-rays were not observed in a mixture of light and heavy gases even when hydrogen at optimum pressure was mixed with 0.1% of xenon (by pressure).

The addition of small portions of xenon to hydrogen which is at such low pressure that the effect is just not observable leads to soft x-rays for the mass of gas which corresponds to pulses in a pure hydrogen discharge.

The oscillograms show a noteworthy absence of a starting x-ray pulse. In obtaining an oscillographic record of the x-ray pulse from a hydrogen discharge the scintillation register was placed behind a lead shield which completely absorbed the starting x-rays, whose energy limit was 40 kev. For xenon discharges, despite the fact that the apparatus was able to record low-energy photons down to 1 kev, the starting x-ray pulse at a xenon pressure $P_0 = 2 \cdot 10^{-2}$ mm is of such low intensity that its amplitude is negligibly small compared with the amplitude of a singular pulse.

The pressure dependence of x-radiation is also quite different (Fig. 2). In a xenon discharge it increases monotonically as the pressure is reduced down to $5 \cdot 10^{-3}$ mm, below which the gas did not break down. The same figure shows a curve obtained in hydrogen. The extreme difference of the curves shows that the intensity of x-ray emission is not determined by the number of atoms in the discharge chamber.

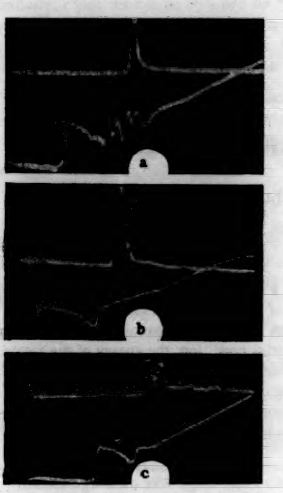

Fig. 1. Oscillograms of x-ray pulses and electrode potentials. Sweep period 22 μsec.

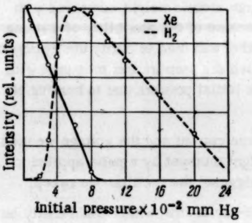

Fig. 2.

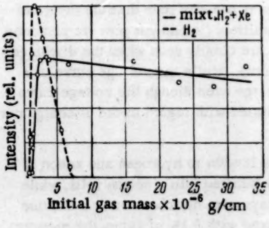

Fig. 3.

From the theory of inertial compression of a discharge [2] it follows that one of the principal parameters which determine the courses of different processes in a strong pulsed discharge with short pulse length is the total mass of gas in the chamber. This hypothesis was tested by experiments to determine x-ray intensities from discharges in mixtures of hydrogen and xenon. The admixture of small amounts of xenon in hydrogen does not appreciably affect the soft x-ray intensity at pressures ($6 \cdot 10^{-2}$ mm Hg) for which a discharge in pure hydrogen is accompanied by x-radiation in the singular range. The situation is otherwise when the initial hydrogen pressure is sufficient small, such as $2 \cdot 10^{-2}$ mm, under which conditions there is usually no pulse in the singular range. The addition of 1 % of xenon (by pressure) with the total pressure of the mixture amounting to $2 \cdot 10^{-2}$ mm, which means that the mass of the gas increases about 1.5 times while the number of particles remains practically unchanged, results in an x-ray pulse in the singular range. The amplitude of this pulse increases with the relative xenon content. The amount of hydrogen was reduced in such a way that the total number of atoms in the discharge chamber remained constant. When the mixture contains from 5% to 20% of xenon there is a double pulse in the singular region (Fig. 1c), the cause of which is still unknown. With further increase of the relative amount of xenon while maintaining the same total pressure the pulse resumes its usual shape. The dependence of the x-ray intensity on the total mass of the mixture is shown in Fig. 3. A study of this relation shows that x-rays appear in a mixture for the same mass of gas as in the case of a pure hydrogen discharge, and this indicates directly the essential role of inertial forces in the development of a powerful gas discharge.

LITERATURE CITED

[1] S. Iu. Luk'ianov and I. M.Podgornyi, J. Atomic Energy (USSR) 1, 3, 97 (1956).

[2] M. A. Leontovich and S. M. Osovets, J. Atomic Energy (USSR) 1, 3, 81 (1956).

Received July 5, 1957

DETERMINATION OF THE CHARACTER OF AN ELEMENTARY RADIATOR FOR NONPARALLEL ABSORBING AND EMITTING OSCILLATORS

Academician A. N. Sevchenko (Byelorussian Academy of Sciences)
and G. P. Gurinovich

The study of polarized luminescence at different angles with respect to the direction of the exciting light and with different directions of vibration for the electric vector of the exciting light makes it possible, as was shown by S. I. Vavilov [1], to determine the nature of the elementary acts of absorption and emission of light by matter. This method was developed in articles by P. P. Feofilov [2, 3], and it can be used to determine the character both of parallel absorbing and emitting oscillators and those forming any angle α.

In the coordinate system XYZ with the electric vector of the exciting light parallel to the OZ axis the degree of polarization observed parallel to the OY axis will be

$$P = \frac{I_z - I_x}{I_z + I_x}.$$

The subscripts on I denote the direction of vibration of the electric vector in the corresponding components of the luminescent flux.

We now turn the electric vector of the exciting light together with the coordinate system through the angle η with respect to the line of observation. Then the observed degree of polarization as a function of η has the form

$$P = \frac{I_Z \cos^2\eta + I_y \sin^2\eta - I_x}{I_Z \cos^2\eta + I_y \sin^2\eta + I_x}. \qquad (1)$$

The components I_x, I_y and I_Z differ for different multipoles.

A tedious but not complicated calculation yields an expression for the degree of polarization as a function of α and η for the case of absorbing and emitting electric dipoles:

e → e:

$$P = \frac{3\cos^2\alpha - 1}{3 + \cos^2\alpha} \frac{\cos^2\eta}{1 + \dfrac{3\cos^2\alpha - 1}{3 + \cos^2\alpha}\sin^2\eta}. \qquad (2)$$

Similarly for the cases: electric dipole and quadrupole

e → q:

$$P = \frac{3\cos^2\alpha - 1}{5 - \cos^2\alpha} \frac{\cos^2\eta}{1 + \dfrac{3\cos^2\alpha - 1}{5 - \cos^2\alpha}\sin^2\eta}; \qquad (3)$$

electric quadrupole and dipole

q → e:

$$P = -\frac{3\cos^2\alpha - 1}{5 - \cos^2\alpha} \frac{\sin^2\eta}{1 + \dfrac{3\cos^2\alpha - 1}{5 - \cos^2\alpha}\cos^2\eta}; \qquad (4)$$

electric quadrupoles

q → q:
$$P = -\frac{5\cos^4\alpha - 3\cos^2\alpha}{4\cos^4\alpha - 3\cos^2\alpha + 3}\,\frac{\sin^2\eta}{1 + \dfrac{5\cos^4\alpha - 3\cos^2\alpha}{4\cos^4\alpha - 3\cos^2\alpha + 3}\cos^2\eta}; \tag{5}$$

magnetic dipoles

m → m:
$$P = -\frac{3\cos^2\alpha - 1}{3 + \cos^2\alpha}\,\frac{\sin^2\eta}{1 - \dfrac{3\cos^2\alpha - 1}{3 + \cos^2\alpha}\cos^2\eta}; \tag{6}$$

magnetic dipole and electric dipole

m → e:
$$P = \frac{3\cos^2\alpha - 1}{3 + \cos^2\alpha}\,\frac{\sin^2\eta}{1 - \dfrac{3\cos^2\alpha - 1}{3 + \cos^2\alpha}\cos^2\eta}; \tag{7}$$

electric dipole and magnetic dipole

e → m:
$$P = -\frac{3\cos^2\alpha - 1}{3 + \cos^2\alpha}\,\frac{\cos^2\eta}{1 - \dfrac{3\cos^2\alpha - 1}{3 + \cos^2\alpha}\sin^2\eta}. \tag{8}$$

Assuming in Formulas (2), (3) and (8) that $\eta = 0$ and in (4), (5), (6) and (7) that $\eta = \pi/2$, which are the usual conditions for measurements of the degree of polarization, we obtain

$$e \to e\colon P_0 = \frac{3\cos^2\alpha - 1}{3 + \cos^2\alpha}, \tag{2'}$$

$$e \to q\colon P_0 = \frac{3\cos^2\alpha - 1}{5 - \cos^2\alpha}; \tag{3'}$$

$$q \to e\colon P_0 = -\frac{3\cos^2\alpha - 1}{5 - \cos^2\alpha}; \tag{4'}$$

$$q \to q\colon P_0 = -\frac{5\cos^4\alpha - 3\cos^2\alpha}{4\cos^4\alpha - 3\cos^2\alpha + 3}. \tag{5'}$$

The formula for m → e is the same as (2') and the formulas for m → m and e → m differ from (2') only in sign.

(2') is the familiar formula of F. Perrin [6] and V. L. Levshin [5] which relates the observed degree of polarization with the angle between the absorbing and radiating electric dipoles. Formulas (3'), (4') and (5') express the same relation for the dipole-quadrupole, quadrupole-dipole and quadrupole-quadrupole cases. These formulas when used for the polarization limits make it possible to calculate the angles between oscillators, but it is first necessary to determine the nature of the oscillator, which, to our knowledge, was not formerly done. This is especially important under the usual conditions of observation the degree of polarization is near zero, because in this case a quadrupole may possibly be responsible for the absorption.

As we know, the limit of the degree of polarization for horizontal observation in the case of parallel absorbing and emitting electric dipoles is $P_0 = {}^1/_2$; for mutual perpendicular dipoles $P_0 = {}^1/_3$. P_0 is always zero for vertical observation. In other cases, as can be seen from Table 1, P_0 has entirely different limits of variation depending on the conditions of observation.

Formulas (2) to (8) make it possible to extend S. I. Vavilov's method of polarization diagrams for determination of the character of elementary radiators to the case of nonparallel absorbing and emitting oscillators.

TABLE 1

P_0 for Different Multipoles and Different Values of Angle α

	$e \to e$		$q \to q$		$e \to q$		$q \to e$		$m \to m$		$m \to e$		$e \to m$	
Observation	$\alpha = 0$	$\alpha = \frac{\pi}{2}$	$\alpha = 0$	$\alpha = \frac{\pi}{2}$	$\alpha = 0$	$\alpha = \frac{\pi}{2}$	$\alpha = 0$	$\alpha = \frac{\pi}{2}$	$\alpha = 0$	$\alpha = \frac{\pi}{2}$	$\alpha = 0$	$\alpha = \frac{\pi}{2}$	$\alpha = 0$	$\alpha = \frac{\pi}{2}$
Horizontal	$1/2$	$-1/3$	0	0	$1/2$	$-1/5$	0	0	0	0	0	0	$-1/2$	$1/3$
Vertical	0	0	$-1/2$	0	0	0	$-1/2$	$1/5$	$-1/2$	$1/3$	$1/2$	$-1/3$	0	0

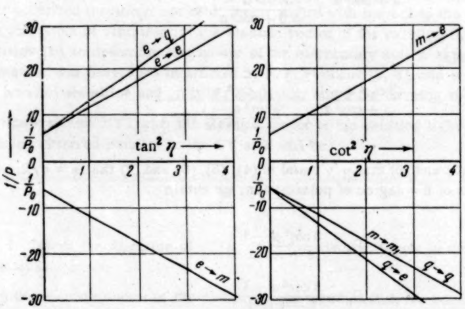

Fig. 1.

It is known that the multipolarity of a radiating system can be determined uniquely only when the polarization limit is greater than $^1/_3$. For absorbing oscillators there are no such limitation. Since in complex molecules the transition with emission always occurs between the same pair of electronic levels independently of the absorption band in which luminescence is excited, the character of the radiating system evidently remains unchanged whether luminescence is excited in a long-wave or short-wave absorption band. Therefore in our determination of the character of elementary oscillators in different regions of the absorption spectrum the absorbing system will change while the emitting system remains unchanged. Thus in all cases we can uniquely determine the character of the oscillators.

In practice the formulas can be used very conveniently in graphical form. Formulas (2) to (8) with the first factor designated by P_0 can be written as

$$e \to e: \qquad \frac{1}{P} = \frac{1}{P_0} + \left(\frac{1}{P_0} - 1\right) \tan^2 \eta; \qquad (2'')$$

$$e \to q: \qquad \frac{1}{P} = \frac{1}{P_0} + \left(\frac{1}{P_0} + 1\right) \tan^2 \eta; \qquad (3'')$$

$$q \to e: \qquad \frac{1}{P} = -\frac{1}{P_0} = \left(\frac{1}{P_0} + 1\right) \cot^2 \eta; \qquad (4'')$$

$$q \to q: \qquad \frac{1}{P} = -\frac{1}{P_0} - \left(\frac{1}{P_0} - 1\right) \cot^2 \eta; \qquad (5'')$$

$$m \to m: \qquad \frac{1}{P} = -\frac{1}{P_0} - \left(\frac{1}{P_0} - 1\right) \cot^2 \eta; \qquad (6'')$$

$$m \to e: \qquad \frac{1}{P} = \frac{1}{P_0} + \left(\frac{1}{P_0} - 1\right) \cot^2 \eta; \qquad (7'')$$

$$e \to m: \qquad \frac{1}{P} = -\frac{1}{P_0} - \left(\frac{1}{P_0} + 1\right) \tan^2 \eta. \qquad (8'')$$

With the values of $\tan^2\eta$ or $\cot^2\eta$ plotted horizontally and $1/P$ plotted vertically these formulas are represented by straight lines (Fig. 1) with very different slopes. These differences of direction are quite appreciable even when the maximum observed polarization is small (in the figures the value 15% is taken). When $P_0 = {}^1/_2$ these straight lines are mutually perpendicular.

LITERATURE CITED

[1] S. I. Vavilov, J. Exptl.-Theoret. Phys. (USSR) 10, 1363 (1940); Compl. Works vol. 2 (1952).

[2] P. P. Feofilov, Doklady Akad. Nauk SSSR 55, 407 (1947).

[3] P. P. Feofilov, Doklady Akad. Nauk SSSR 44, 159 (1944).

[4] V. L. Levshin, Photoluminescence of Liquids and Solids (Moscow-Leningrad, 1951) [in Russian].

[5] V. L. Levshin, Trudy FIAN (Phys. Inst. Acad. Sci.) 1, 19 (1955).

[6] F. Perrin, Ann. phys. 12, 169 (1929).

Received July 18, 1957

INVERSION OF THE TEMPERATURE DEPENDENCE OF MOLECULAR FRAGMENT LINE INTENSITIES IN A MASS SPECTRUM

G. D. Tantsyrev and V. L. Tal'roze

(Presented by Academician V. N. Kondrat'ev July 6, 1957)

It is known that the degree of dissociation of molecules which have been ionized by electrons increases with rising gas temperature (see, for examples, [1, 2]). This effect results, in particular, in the need for stabilizing the temperature of an ion source during mass spectrometric analysis of a mixture of polyatomic gases.

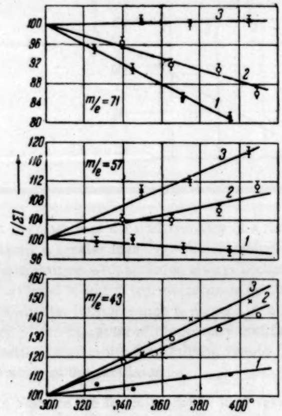

Fig. 1. Temperature dependence of the relative intensity of fragment lines in the mass spectrum of n-heptane for different electron energies.

At present only the first attempts have been made to establish a theory of dissociative molecular ionization, and no quantitative information is available concerning the temperature dependence of intensity distributions in molecular mass spectra despite the fact that qualitatively there are clear causes for such dependence. Specifically, from the statistical theory of the disintegration of an intermediate molecular ion [3] it is clear why the mass spectra of more highly polyatomic molecules should show greater temperature dependence; such molecules have a greater probability of energy concentration in any bond which is sufficient for the breaking of the bond.

All known measurements of the temperature dependence of intensity distributions in mass spectra have been obtained for electron energies from 50 to 90 ev, in which range the distribution depends very little on the electron energy. But for the establishment of a theory of dissociative ionization it is evidently most important to know the temperature dependence of mass spectra at low electron energies close to the potentials for the appearance of ion fragments.

The present authors have obtained such measurements for n-heptane, which was chosen because the greatest temperature dependence is observed in the mass spectra of heavy hydrocarbons.

The experiments were performed with a MS-1a mass spectrometer [4] equipped for temperature measurement and stabilization in an ion source [5]. It had previously been proved [6] that the temperature measured by a thermocouple in an ion source is the true temperature of the ionized gas.

The line intensity distribution in the mass spectrum was measured for different electron energies. Figure 1 shows the results for ion lines $C_5H_{11}^+$ (71 amu), $C_4H_9^+$ (57 amu) and $C_3H_7^+$ (43 amu).

The gas temperature in °C for the ionization region is plotted along the horizontal axis, while the vertical axis shows the ratio of a given line intensity I to the total intensity ΣI of the lines in the mass spectrum (as a percentage of the value at 300°). In these experiments the electrons were not monochromatic, and the energy range was about ±1 ev. Curves 1 correspond to 30-ev electrons, curves 2 to 17-ev and curves 3 to 13-ev.

In all cases the temperature dependence of $I/\Sigma I$ is approximately linear. A reduction of electron energy leads to a shift of the temperature coefficient of $I/\Sigma I$ for these lines towards higher positive values. For the lines of $C_4H_9^+$ and $C_5H_{11}^+$ there are electron energies at which the temperature coefficient passes through zero, so that an "inversion" is observed. These electron energies may be called the "potentials of temperature dependence inversion."

The observed effects can clearly be interpreted by assuming that an initial molecular ion (in our case $C_7H_{16}^+$) formed immediately after collision with an electron does not immediately disintegrate to form all possible ion fragments, but proceeds through stages. For example, disintegrations occur first at C—C bonds; the resulting ion fragments then disintegrate at C—C and C—H bonds. Accordingly, the observed variation of the temperature coefficient of the yield of $C_nH_{2n+1}^+$ ions as the electron energy is reduced can be attributed to reduced extent of disintegration of the initial molecular ion; $C_nH_{2n+1}^+$ ions at low electron energies simply have fewer possible ways of disintegrating further. A rise in temperature affects disintegration processes of the original molecular ion to a greater extent than it affects subsequent disintegration of $C_nH_{2n+1}^+$ ions. From a theoretical point of view there should be special interest in the "inversion potential" at which, according to the described scheme, there is equality of the temperature dependences of the processes of the formation and disintegration of $C_nH_{2n+1}^+$.

Quantitative utilization of the observed effect will require measurements of the temperature dependences and exact potentials for the appearances of all ions in the mass spectrum of a molecule (determined in the vicinity of such potentials); for this purpose the electrons could be quasi-monochromatized [7, 8].

LITERATURE CITED

[1] R. E. Fox and I. A. Hipple, J. Chem. Phys. 15, 208 (1947).

[2] V. H. Dibeler and F. Cordero, J. Research NBS 46, 1 (1951).

[3] H. M. Rosenstock, M. B. Wallenstein, A. L. Wahrhaftig, and H. Eyring, Proc. Nat. Acad. Sci. USA 38, 8, 667 (1952).

[4] V. L. Tal'roze, G. D. Tantsyrev and Ia. A. Iukhvidin, Zavodskaya Lab. 21, 10, 1175 (1955).

[5] G. D. Tantsyrev, L. L. Dekabrun, and V. L. Tal'roze, J. Tech. Phys. (USSR) 25, 11, 1983 (1955).

[6] V. L. Tal'roze and E. L. Frankevich, J. Tech. Phys. (USSR) 26, 3, 497 (1956).*

[7] R. E. Fox, W. M. Hicham, T. Kjeldaas, and D. J. Grove, Phys. Rev. 84, 859 (1951).

[8] E. L. Frankevich and V. L. Tal'roze, Pribory i Tekhnika Eksperimenta No. 2, 48 (1957).

Received June 29, 1957

Institute of Chemical Physics, Academy of Sciences, USSR

---

* Soviet Physics — Technical Physics, p. 479.

ON THE THEORY OF PHOTOELECTRETS

V. M. Fridkin, N. T. Kashukeev, and I. S. Zheludev

(Presented by Academician A. V. Shubnikov July 27, 1957)

In 1937 G. Nadzhakov [1-3] discovered and investigated photoelectrets in polycrystalline sulfur. During photoconduction in a layer of polycrystalline sulfur space charge accumulated and was maintained for a long time after removal of the polarizing field. A dielectric polarized through photoconduction resembles the electrets discovered by Eguchi in 1921, so that Nadzhakov named it a "photoelectret."

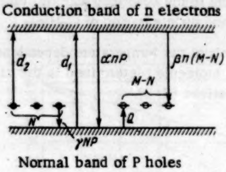

Fig. 1. Energy levels of electrons in sulfur.

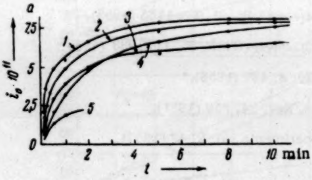

Fig. 2. Dependence of the initial depolarization current (proportional to the photoelectret charge) on the polarization time (for a sulfur single crystal). Polarizing field U = 1.5 kv/cm. Illumination during polarization: 1) $110 \cdot 10^{-6}$, 2) $55 \cdot 10^{-6}$, 3) $33 \cdot 10^{-6}$, 4) $17 \cdot 10^{-6}$, 5) $7 \cdot 10^{-6}$ watt/cm².

The scheme of electronic energy levels in monocrystalline sulfur which was proposed by P. S. Tartakovskii and G. Rekalova [4] and the investigation of space charge in photoconduction which was carried out by P. S. Tartakovskii and D. M. Kaminker [5] permit the following conclusions concerning the mechanism of photoelectret formation. Light induces transitions of electrons from their normal band into the conduction band, where they move in the direction of the field and can then drop into trapping levels below the conduction band (Fig. 1). In sulfur the traps can be associated with inhomogeneities of the crystal structure. As has been shown by Nadzhakov and Kashukeev [6], the dark depolarization of a photoelectret can be attributed to thermal transitions of electrons from the normal band to unoccupied traps, thus increasing the dark p-type conduction. The activation energy corresponding to an electronic transition from the normal band to a trap was 0.48 ev, which agrees with [4].

The present paper attempts to explain certain experimental results obtained during an investigation of photoelectrets [7].

Let d_1 be the number of electrons per unit space and time which under the influence of light pass from the normal band to the conduction band, and let d_2 be the number of electrons which are induced by light to jump from filled traps to the conduction band.

$$d_1 = s_1 E, \tag{1}$$

$$d_2 = s_2 N E = kN. \tag{2}$$

Here E is the intensity of the light (illumination), N is the concentration of traps filled with electrons, s_1 and s_2 are coefficients which depend on light absorption and the quantum yield. If we assume exciton absorption of light in sulfur and that the transitions of electrons to the conduction band from the normal band and from traps results from "exciton collisions of the second kind" [8], then for d_1 and d_2 we can obtain expressions similar to those in [8, 9].

The kinetic equations which describe the filling of traps with electrons, in accordance with the scheme depicted in Fig. 1, are as follows:

$$\frac{dn}{dt} = d_1 + kN - \beta n(M - N) - \alpha nP, \tag{3}$$

$$\frac{dN}{dt} = Q + \beta n(M - N) - kN - \gamma NP, \tag{4}$$

$$\frac{dP}{dt} = d_1 + Q - \alpha nP - \gamma NP, \tag{5}$$

$$P = N + n, \tag{6}$$

where M is the concentration of traps; N is the concentration of electrons in traps; n is the electron concentration in the conduction band; P is the hole concentration in the normal band; Q is the number of electrons per unit space and time which are induced by thermal motion to pass from the normal band to trapping levels; and α, β, and γ are recombination coefficients whose meaning is clear from the scheme in Fig. 1.

Our problem becomes the determination of the time dependence of N, because the electron concentration in traps will be considered proportional to the charge of the photoelectret. Here, of course, we are not considering the kinetics of electron motion in the conduction band and thus the influence of the field strength on the charge of the photoelectret.

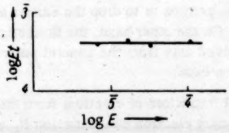

Fig. 3. Verification of the law of interchangeability for the formation of photoelectret charge (in a sulfur single crystal).

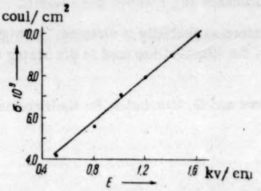

Fig. 4. Dependence of the photoelectret charge density σ (for a sulfur single crystal) on the polarizing field. Time of polarization t = 10 min; illumination during polarization $E = 100 \cdot 10^{-6}$ watt/cm².

Since at room temperature thermal transitions of electrons from the normal band to traps can be neglected [6] we set Q = 0. Regarding n/M and N/M as small parameters, we confine ourselves to linear terms in Eqs. (3) and (4). Remembering also that $d_2 \ll d_1$, we obtain with zero initial values the following solution of Eqs. (3) and (4):

$$N = N_c(1 - e^{-s_1 Et}), \tag{7}$$

where the electron concentration in the stationary state is

$$N_c = s_1 / s_2. \tag{8}$$

As previously noted, this solution applies to the case in which during polarization only a small fraction of empty levels are filled with electrons.

Expression (7) for the time dependence of the electron density in traps expresses the saturation effect discovered in [7] during an investigation of the relation between the photoelectret charge, the time of polarization and the illumination.

Figure 2 shows the experimental curves obtained in [7] for the dependence of the initial photoelectret depolarization current (proportional to the magnitude of photoelectret polarization) on the polarization time for varying illumination (in sulfur single crystals). It can be seen from the curves that (7) satisfactorily represents the exponential character of the relation between the photoelectret charge and illumination and polarization time.

It also follows from (7) and (8) that a law of interchangeability is satisfied for the formation of a photoelectret. This means that for any polarization time t and any illumination E the charge of a photoelectret is only a function of the product Et. The curves in Fig. 2 were used to provide an experimental check of the law of interchangeability for a sulfur single crystal. Figure 3 shows the dependence of the exposure Et required to produce a definite photoelectret charge on the illumination E. It is easily seen that the law of interchangeability is satisfied for all intensities of illumination used in polarizing a sulfur single crystal. The illumination varied from $110 \cdot 10^{-6}$ watt/cm^2 to $7 \cdot 10^{-6}$ watt/cm^2.

The theoretical deduction and experimental verification of the law of interchangeability for photoelectrets are of independent interest. This law can serve as the basis of electrophotography on photoelectrets [10, 11] by analogy with the corresponding law of interchangeability for photochemical processes in silver halides. Consideration of the kinetics of electron motion in the conduction band during polarization should lead to deviations from the law of interchangeability. This may explain certain violations of the law which have been observed during a brief polarization time for sulfur single crystals [7].

As suggested above, the saturation which has been observed during an investigation of the dependence of photoelectret charge on polarization time and on illumination may result from the filling of only a small fraction of empty levels with electrons. This hypothesis was supported by an experimental investigation of the dependence of photoelectret charge on the polarizing field strength. Figure 4 shows the field dependence of the photoelectret charge density (for a sulfur single crystal) as measured by integrating the depolarization current with respect to time. The results show that for sulfur there is direct proportionality between the photoelectret charge and the polarizing field, and that saturation is absent. Saturation was not observed even in fields of the order of 20 kv/cm. The polarizing conditions were such that the charge of the photoelectret did not change over a broad range of values for the illumination and polarization time; thus saturation occurred due to the mechanism previously mentioned. These results support the foregoing hypothesis that during the formation of a photoelectret there occurs partial filling of levels with electrons, which, in turn, permits us to drop the earlier assumption [7] that electrons fill the entire finite number of traps in the crystal. On the other hand, the theoretical dependence of the photoelectret charge on the polarizing field can be derived only from the general polarization mechanism including the kinetics of electron motion in the conduction band.

When in the kinetic equations [4, 5] account is taken of the thermal transitions of electrons from the normal band to traps [6], we arrive at a temperature dependence of the stationary electron concentration N_C and thus of the photoelectret charge. In this case the photoelectret charge, which is proportional to the stationary electron density in traps, is reduced with rising temperature. This results from the fact that thermal transitions of electrons from the normal band to trapping levels reduce the total polarization of the crystal produced by the external field and caused by a nonuniform charge distribution. Investigations of the temperature dependence of the photopolarizability of sulfur single crystals, by Nadzhakov and Kashukeev [6], confirm these results.

When the temperature effect is taken into account the law of interchangeability is violated. At high temperatures the departures from this law must increase with reduction of the illumination used in polarizing the crystal.

The authors are deeply grateful to Academicians A. V. Shubnikov and G. Nadzhakov for their continued interest in this work.

LITERATURE CITED

[1] G. Nadjakoff, Physik Z. 39, 6, 226 (1938).

[2] G. Nadzhakov, Compt. rend. 204, 1865 (1937).

[3] G. Nadzhakov, Yearbook of Sofia Univ., Phys.-Math. Fac. 33, 1 (Mathematics and Physics) (1936-1937).

[4] P. Tartakovskii and G. Rekalova, J. Exptl.-Theoret. Phys. (USSR) 10, 1025 (1940).

[5] P. S. Tartakovskii and D. M. Kaminker, J. Exptl.-Theoret. Phys. (USSR) 10, 2, 139 (1940).

[6] G. Nadzhakov and N. T. Kashukeev, Bull. of Bulgarian Acad. Sci.,Phys. Ser. 3, 103 (1952) [In Bulgarian].

[7] V. M. Fridkin, Crystallography (USSR) 1, 5, 557 (1956).

[8] V. P. Zhuze and S. M. Ryvkin, Doklady Akad. Nauk SSSR 77, 2, 241 (1951).

[9] M. Borisov and St. Kynev, Dokl. Bolgar. Akad. Nauk 7, 2, 25 (1954).

[10] I. S. Zheludev and V. M. Fridkin, Dokl. Bolgar. Akad. Nauk 10, 2, 109 (1957).

[11] V. M. Fridkin, Crystallography (USSR) 2, 1, 130 (1957).

Received July 27, 1957

THERMAL CONDUCTIVITY OF TELLURIUM

Academician Kh. I. Amirkhanov (Azerbaidzhan Academy of Sciences),
G. B. Bagduev and M. A. Kazhlaev

None of the numerous articles on tellurium is devoted to an investigation of its thermal conductivity. In the articles by Wold [1] and by one of the present authors [2] there are to be found only the value of the thermal conductivity at room temperature and its variation in a magnetic field.

The present article presents the results of investigations of the temperature dependence of thermal conductivity λ in pure tellurium from 10° to 500°. Fine-crystalline specimens were prepared in the form of bars by cold pressing under 4000 kg/cm^2 and by hot pressing at 400° under 360 kg/cm^2 for 6 hours. The tellurium was first purified by triple fractional distillation in a vacuum of 10^{-4} mm Hg in order to obtain spectrally pure specimens.

The thermal conductivity was determined by the plane compensating method [3] in a vacuum which protected the specimens from oxidation at the melting point.

The experimental errors did not exceed 1-2% near room temperature and 4-5% at the melting point. The results are shown in Fig. 1. The temperature curve of the thermal conductivity λ has a minimum at 250°, where λ reduced to $^2/_3$ of its value at room temperature. Upon passing through the melting point the thermal conductivity of a specimen rises from $5 \cdot 10^{-3}$ cal/cm · sec · deg before melting to $4.8 \cdot 10^{-2}$ cal/cm · sec · deg and drops rapidly upon further heating.

In addition, special measurements were made of the temperature dependence of the specific heat in an adiabatic microcalorimeter of the kind described in [9]. These studies showed the absence of any structural changes in tellurium up to the melting point, and specifically of the polymorphic transformation at 250° which is mentioned in some articles [1].

Interpretation of the results must be based, first, on the existence of a number of mechanisms for the thermal conductivity of semiconductors [4] and, secondly, on the fact that above room temperature tellurium is a semiconductor with mixed conduction and with a wide forbidden band $\Delta E = 0.38$ ev [7].

The presence of both positive and negative carriers in tellurium further complicates the already complex picture of the thermal conductivity, as is shown by our experimental data.

The curves in Fig. 2 show the temperature dependence of different components of thermal conduction in tellurium. Experimental curve 1 represents our data up to 400°. Curve 2 depicts the temperature dependence of the phonon part of the thermal conductivity as calculated from Eucken's law $\lambda T = c$. The constant $\underline{c}$ was determined from our data in the range 10-100°, where $\lambda \sim T^{-1}$; here $c = 1.1$. For higher temperatures $\underline{c}$ was extrapolated. A comparison of curves 1 and 2 gives curve 3.

The values of the electron-hole thermal conductivity calculated from the formula of Davydov and Shmushkevich [8],

$$\lambda_{\text{e-h}} = L(\sigma_+ + \sigma_-) + L\frac{2\sigma_+\sigma_-}{\sigma_+ + \sigma_-}\left(\frac{\Delta E}{2kT} + 2 + r\right)^2, \qquad (1)$$

which takes into account various conditions for the motion of charges in semiconductors with mixed conduction, as well as electron-hole recombinations in a thermal field, fit well on curve 3. The factor in front of the second bracket was given in [7] as 0.5 L over the entire investigated temperature range.

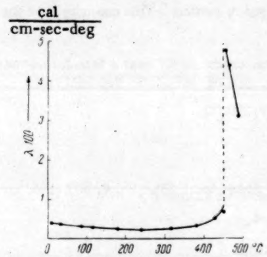

Fig. 1. Temperature dependence of the thermal conductivity of tellurium from 10° to 500°.

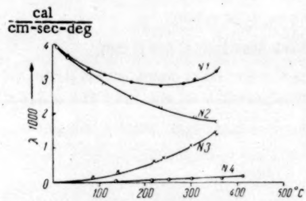

Fig. 2. Temperature dependence of various components of the thermal conductivity of solid tellurium.

Finally, curve 4 represents the Wiedemann-Franz law $\lambda_e = L\sigma$ together with our data for the electrical conductivity.

Our experimental results permit us to conclude that thermal conductivity in tellurium over the entire intrinsic conductivity range results not only from quasi-elastic lattice vibrations and the thermal diffusion of charge carriers, but also from the diffusion and recombinations of pairs of electrons and holes.

The sharp increase in thermal conductivity upon passing through the melting point is evidently due to higher carrier concentration. This explanation is favored by work on electrical conductivity and the Hall effect [5, 6].

The electrical conductivity of tellurium increases to $\sigma = 2.4 \cdot 10^3$ ohm^{-1} · cm^{-1} upon passing through the melting point. The Hall constant drops from 0.4 to 0.02.

The data given above show that at the passage through the melting point a huge number of tellurium atoms are dissociated, producing a sharp increase in the number of free charge carriers.

Thus the almost 10-fold increase in the thermal conductivity of tellurium as its temperature rises through the melting point supplements rather than conflicts with other experimental facts (the rise of electrical conductivity and the reduction of the Hall effect).

The increase of thermal conductivity associated with the change of state of aggregation of a semiconductor is a complex process in which not only electron-hole but also phonon thermal conductivity participates. However, the phonon part of the sharp rise of the total thermal conductivity of tellurium at the melting point can be regarded as small, because the volume of the tellurium increases smoothly without a jump, and according to A. F. Ioffe and A. R. Regel' [4, 5] in the liquid state very close to the melting point it retains to a considerable extent the chain structure which is completely destroyed around 550°.

The rapid decrease in thermal conductivity above the melting point can be explained by the fact that the change of structure of tellurium is accompanied by metallization of bonds in the melt, with the characteristic mixed conductivity of this semiconductor becoming conductivity of a single sign in the crystallization region. Here there disappears the part of the thermal conductivity which results from the diffusion and recombination of pairs of electrons and holes. Consequently, the thermal conductivity is due principally to the thermal diffusion of carriers. Thus our experiments with the melting of tellurium embrace the small temperature range (460-490°) between two extreme states of the melt which change into each other continuously: the semiconducting state immediately after melting (452°) and the metallic state (550°).

For a tellurium melt in the semiconducting state (452°) the thermal conductivity calculated from the formula in [1], taking account of heat transfer by the diffusion and recombination of electron-hole pairs, amounts to $1.38 \cdot 10^{-1}$ cal/cm · sec · deg. In the metallic state (550°) the thermal conductivity is calculated using the same formula without the second term. In this case $\lambda = 10^{-2}$ cal/cm · sec · deg. Both of these values fit well on our experimental curve when it is extended at both ends.

We studied Te–Se solid solutions in addition to pure tellurium. The thermal conductivity versus temperature curves of these solutions resemble that for pure tellurium, but differ in the minimum thermal conductivity, which is observed at a different temperature for each solution and in the character of the increase of λ upon melting and its diminution after melting.

The dependence of the thermal conductivity of a Te–Se solid solution on the selenium content enables us to compute the mean free path of phonons scattered by phonons and impurity centers. This quantity is of the order of magnitude of six interatomic distances.

At the present time we are continuing our investigations of thermal conductivity over a broader temperature range.

LITERATURE CITED

[1] P. Wold, Phys. Rev. 7, 169 (1916).

[2] Kh. I. Amirkhanov, A. Z. Daibov, and V. P. Zhuze, Doklady Akad. Nauk SSSR 98, 4, 557 (1954).

[3] Kh. I. Amirkhanov, Izvest. Akad. Nauk Azerb. SSR 1946, No. 4.

[4] A. V. Ioffe and A. F. Ioffe, Izvest. Akad. Nauk SSSR 22, 1 (1956).

[5] A. I. Blum and A. R. Regel', J. Tech. Phys. (USSR) 23, 5 (1953).

[6] A. Epstein and H. Fritzsche, Bull. Am. Phys. Soc. 29, 3, 28 (R-2) (1954).

[7] T. Fukuroi, S. Tanuma, and S. Tobisawa, Sci. Repts. Research Insts. Tohoku Univ. Ser. A6, 159 (1954).

[8] B. I. Davydov and I. M. Shmushkevich, Uspekhi Fiz. Nauk 24, 1, 24 (1940).

[9] Kh. I. Amirkhanov and A. M. Kerimov, Doklady Akad. Nauk SSSR 110, 4, 578 (1956).

Received July 16, 1957

CROSS SECTION FOR THE TRANSFER OF A MUON FROM A PROTON TO A DEUTERON

S. S. Gershtein

(Presented by Academician L. D. Landau August 13, 1957)

The experimentally observed fact that the catalysis of the nuclear reaction p + D = He^3 by muons in hydrogen depends on the deuterium concentration is based essentially on the transfer of muons from protons to deuterons [1]. In the present article the cross section of this process is calculated.

The Hamilton of the $pD\mu$ system in mesonic atom units (e = 1; h = 1; m_μ = 1) is

$$H = -\frac{1}{2M_1}\Delta_{\mathbf{R}_1} - \frac{1}{2M_2}\Delta_{\mathbf{R}_2} - \frac{1}{2}\Delta_{\mathbf{r}} - \frac{1}{r_1} - \frac{1}{r_2} + \frac{1}{R} \tag{1}$$

where M_1 and M_2 are the proton and deuteron masses, respectively; $R = |\mathbf{R}_1 - \mathbf{R}_2|$ is the internuclear separation; $r_1 = |\mathbf{r} - \mathbf{R}_1|$, $r_2 = |\mathbf{r} - \mathbf{R}_2|$ are the distances of the meson from the proton and the deuteron.

Assuming that a muon jumps across between K orbits, the wave function of the system can be written as

$$\Psi = A(\mathbf{R})\,\Sigma_g(\mathbf{r}, R) + B(\mathbf{R})\,\Sigma_u(\mathbf{r}, R); \tag{2}$$

Σ_g, Σ_u are the symmetric and antisymmetric wave functions of the muon in the field of two fixed nuclei (depending on R as a parameter):

$$\left(-\frac{1}{2}\Delta_{\mathbf{r}} - \frac{1}{r_1} - \frac{1}{r_2} + \frac{1}{R}\right)\Sigma_{g,u} = E_{g,u}(R)\,\Sigma_{g,u}. \tag{3}$$

Inserting (2) into (1) and considering (3), after multiplying by Σ_g and Σ_u, respectively, and integrating over the coordinates of the muon, we obtain the following equations for A(R) and B(R):

$$\begin{gathered}
-\frac{1}{2M}\Delta_{\mathbf{R}}A + \left(E_g - \frac{1}{2M}K_{gg} - E\right)A - \frac{1}{2M}K_{gu}B - \frac{1}{M}\mathbf{S}_{gu}\,\vec{\nabla}_{\mathbf{R}}B = 0,\\
-\frac{1}{2M}\Delta_{\mathbf{R}}B + \left(E_u - \frac{1}{2M}K_{uu} - E\right)B - \frac{1}{2M}K_{ug}A + \frac{1}{M}\mathbf{S}_{gu}\,\vec{\nabla}_{\mathbf{R}}A = 0,
\end{gathered} \tag{4}$$

where

$$\begin{gathered}
M = \frac{M_1 M_2}{M_1 + M_2};\\
\frac{1}{M}\mathbf{S}_{gu} = \int \Sigma_g \left(\frac{1}{M_1}\vec{\nabla}_{\mathbf{R}_1} + \frac{1}{M_2}\vec{\nabla}_{\mathbf{R}_2}\right)\Sigma_u\,(d\mathbf{r}),\\
\frac{1}{M}K_{gg} = \int \Sigma_g \left(\frac{1}{M_1}\Delta_{\mathbf{R}_1} + \frac{1}{M_2}\Delta_{\mathbf{R}_2}\right)\Sigma_g\,(d\mathbf{r})\,\text{etc.}
\end{gathered} \tag{5}$$

When R → ∞

$$\Sigma_{g,u} = \frac{1}{\sqrt{2}}\left(\psi(r_1) \pm \psi(r_2)\right); \tag{6}$$

here $\psi(r_1)$, $\psi(r_2)$ are the wave functions of the muon at the proton and deuteron, respectively.

For the functions $a(R) = (A + B)\frac{1}{\sqrt{2}}$; $b(R) = (A - B)\frac{1}{\sqrt{2}}$, which describe the motion of the deuteron with respect to μ-mesonic hydrogen and of the proton with respect to μ-mesonic deuterium, we have the equations

$$\begin{gathered}
-\frac{1}{2M}\Delta_{\mathbf{R}}a + \left[\frac{1}{2}(E_g + E_u) - \frac{1}{4M}(K_{gg} + K_{uu} + K_{gu} + K_{ug}) - E\right]a + \\
+\left[\frac{1}{2}(E_g - E_u) - \frac{1}{4M}(K_{gg} - K_{uu} + K_{ug} - K_{gu})\right]b + \frac{1}{M}S\frac{db}{dR} = 0, \\
-\frac{1}{2M}\Delta_{\mathbf{R}}b + \left[\frac{1}{2}(E_g + E_u) - \frac{1}{4M}(K_{gg} + K_{uu} - K_{gu} - K_{ug}) - E\right]b + \\
+\left[\frac{1}{2}(E_g - E_u) - \frac{1}{4M}(K_{gg} - K_{uu} - K_{ug} + K_{gu})\right]a + \frac{1}{M}S\frac{da}{dR} = 0, \\
S = (S_{gu})_{\mathbf{R}}.
\end{gathered} \tag{7}$$

It can be shown that, accurate to within exponentially small terms and terms $\sim\frac{1}{R^4}$ for $R \gg 1$,

$$\begin{gathered}
E_g + E_u \simeq -1, \\
K_{gg} + K_{uu} \simeq 2\int \psi(r_1)\,\Delta_{r_1}\psi(r_1)\,(d\mathbf{r}) = -1 \\
K_{gu} + K_{ug} \simeq 2\frac{M_2 - M_1}{M_2 + M_1}\int \psi(r_1)\,\Delta_{r_1}\psi(r_1)\,(d\mathbf{r}) = -\frac{M_2 - M_1}{M_2 + M_1}.
\end{gathered}$$

The quantities $K_{gg} - K_{uu}$, $K_{gu} - K_{ug}$, S are exponentially small, and the corresponding terms in (7) which contain $\frac{1}{M}$ at distances R that are important for our problem, can be neglected by comparison with $E_g - E_u$.

In the approximation of (6) $E_g - E_u \approx {}^4/_3\,Re^{-R}$. A more exact calculation, taking into account the distortion of the muon wave function around one nucleus through the influence of the other, gives

$$E_g - E_u \simeq \frac{4}{e}Re^{-R}.$$

Assuming that collisions occur at thermal velocities, it is sufficient to take into account only the S wave in the relative motion of the nuclei. The equations for the radial functions $u = Ra(R)$ and $v = Rb(R)$ become

$$\begin{gathered}
\frac{d^2u}{dR^2} + 2M\varepsilon u + M(E_u - E_g)v = 0, \\
\frac{d^2v}{dR^2} + 2M\left[\varepsilon + \frac{1}{2}\left(\frac{1}{M_1} - \frac{1}{M_2}\right)\right]v + M(E_u - E_g)u = 0.
\end{gathered} \tag{8}$$

(Zero energy is taken to be the energy of a μ-mesonic hydrogen atom.) The term $\frac{1}{2M_1} - \frac{1}{2M_2}$ takes into account the energy difference of the muon bond with a proton and a deuteron.

$M(E_u - E_g)$ at distances which are important for our problem can be approximated by $e^{-\alpha(R-R_1)}$ with $R_1 = 3.38$ and $\alpha = 1 - \frac{1}{R_1} \approx 0.704$. In this range the energy ϵ can be neglected.

Equations (8) then become ($x = R - R_1$):

$$\begin{gathered}
\frac{d^2u}{dx^2} + e^{-\alpha x}v = 0, \quad \frac{d^2v}{dx^2} + k_0^2v + e^{-\alpha x}u = 0; \\
k_0^2 = -\frac{M_2 - M_1}{M_2 + M_1} = \frac{1}{3}.
\end{gathered} \tag{9}$$

When $x \to -\infty$ ($k_0^2 \ll e^{-\alpha x}$) the solutions of (9) are given by

$$\begin{aligned} u + v &= C_1\left[J_0\left(\frac{2}{\alpha}\, e^{-\alpha x/2}\right) + \delta N_0\left(\frac{2}{\alpha} e^{-\alpha x/2}\right)\right], \\ u - v &= C_2 K_0\left(\frac{2}{\alpha}\, e^{-\alpha x/2}\right), \end{aligned} \tag{10}$$

where $J_0(z)$ and $N_0(z)$ are Bessel functions of the first and second kinds; $K_0(z)$ is a Bessel function with imaginary argument; and C_1, C_2, and δ are constants.

The $pD\mu$ system possesses an energy level very close to 0 [2]. As a result resonance occurs and the constant δ is negligibly small. C_1 and C_2 are determined from the condition that the asymptotic solution for $x \to +\infty$ is

$$u \simeq x + \beta; \quad v \simeq \gamma e^{ik_0 x}.$$

The values of γ and β are obtained by numerical integration of (9) with the initial conditions (10).*

For the solutions $u_1 = v_1 = J_0 \cdot \left(\frac{2}{\alpha} e^{-\alpha x/2}\right)$ and $u_2 = -v_2 = K_0 \cdot \left(\frac{2}{\alpha}\ e^{-\alpha x/2}\right)$, taken at $x = -2$, the asymptotic forms $x \to +\infty$ are

$$\begin{gathered} u_1 \cong a_1 x + b_1, \quad v_1 \cong c_1 \cos(k_0 x + \delta_1), \\ a_1 = -0.489, \quad b_1 = 1.257, \quad c_1 = 1.06, \quad \delta_1 = 258°; \\ u_2 \cong a_2 x + b_2, \quad v_2 \cong c_2 \cos(k_0 x + \delta_2), \\ a_2 = 0.202, \quad b_2 = -0.281, \quad c_2 = 0.254, \quad \delta_2 = 29°. \end{gathered}$$

The transfer cross section is

$$\sigma = 4\pi \frac{k_0}{k} |\gamma|^2 = 4\pi \frac{k_0}{k} \frac{\sin^2(\delta_1 - \delta_2)}{\left(\frac{a_1}{c_1}\right)^2 + \left(\frac{a_2}{c_2}\right)^2 - 2\frac{a_1}{c_1}\frac{a_2}{c_2}\cos(\delta_1 - \delta_2)} \approx 1.5\pi \frac{k_0}{k}.$$

(Among the numbers $a_1, a_2, b_1, b_2, \ldots$ we have the relation $a_1 b_2 - b_1 a_2 = k_0 c_1 c_2 \sin(\delta_1 - \delta_2)$, as a result of which $\operatorname{Im} \beta = k_0 |\gamma|^2$).

The result agrees with $\sigma = \pi \frac{k_0}{k}$, which was used in [1] to explain experimental data; the best agreement is obtained at $\sigma = 0.5\pi \frac{k_0}{k}$.

The cross section given in [3], which was calculated in a Born approximation [4] (representing essentially the opposite limiting case) differs from ours by a factor of $1.5 \cdot 10^2$. It must also be noted that in Jackson's article [3], due to the use of nonorthogonal wave functions in the calculations (Appendix D), the probability of the formation of a μ-mesonic molecule is three orders of magnitude greater than was calculated in [2]. In [3] it is concluded incorrectly that the dependence of the pD reaction on the D concentration is determined by the competition between muon jumps from protons to deuterons with the formation of $pp\mu$ mesonic molecules. As was shown in [1], this dependence is determined by the probability of a muon "jump" to a deuteron during the muon lifetime with respect to the decay $\mu \to e + \nu + \tilde{\nu}$.

In conclusion I wish to thank L. D. Landau and Ia. B. Zel'dovich for their interest and valuable comments.

LITERATURE CITED

[1] Ia. B. Zel'dovich and A. D. Sakharov, J. Exptl. Theoret. Phys. (USSR) 32, 947 (1957).**

---

* I take this opportunity to thank M. G. Neigauz and S. M. Lomnev for the numerical integration.

** [See Soviet Physics – JETP, p. 775].

[2] Ia. B. Zel'dovich, Doklady Akad. Nauk SSSR 95, 493 (1954).

[3] J. D. Jackson, Phys. Rev. 106, 330 (1957).

[4] J. D. Jackson and H. Schiff, Phys. Rev. 89, 359 (1953).

Received August 1, 1957

THE THEORY OF THE MOTION OF SMALL AEROSOL PARTICLES IN A DIFFUSION FIELD

B. V. Deriagin, Corresponding Member of the Academy of Sciences USSR, and S. P. Bakanov

§1. We have previously [1-3] considered the forces acting in a diffusion field on an aerosol particle of radius r much larger than the mean free molecular paths λ_1, λ_2. We first considered the influence of the Stefanov flow, taking account of the boundary conditions on the surface of a particle. One of these conditions is the absence of slipping of the gaseous mixture on particle surfaces under isothermal conditions. This condition is violated in the presence of the temperature gradient which results from thermophoresis. A question arises as to whether there are slipping and "phoresis" resulting from a concentration gradient which must be taken into account in a complete theory of the behavior of aerosol particles in diffusion fields. However, a rigorous gas-kinetic calculation of such "diffusion phoresis" is complicated by the fact that the velocity distribution of gas molecules in a layer of thickness λ depends on distance from a particle surface. The problem is simplified when $r \ll \lambda_1, \lambda_2$, in which case the velocity distribution of molecules striking the surface of a particle is not disturbed by the pressence of the latter.

§2. Let us consider a mixture of gases with molecular masses m_1 and $m_2 > m_1$ in the presence of small gradients of the partial densities concentrations n_1 and n_2 which satisfy the conditions grad $(n_1 + n_2)$ = grad $p/kT = 0$, where p is the total pressure.

Let the velocities of two molecules of the first component of the mixture be $\mathbf{c}_1$ and $\mathbf{c}$ before their collision and $\mathbf{c}_1'$ and $\mathbf{c}'$ afterwards; for the second component we have, correspondingly, $\mathbf{c}_2$, $\mathbf{c}$ and $\mathbf{c}_2'$, $\mathbf{c}'$. We denote accordingly $\Phi(\mathbf{c}) = \Phi$, $\Phi(\mathbf{c}') = \Phi'$, etc. Specifically, if $f(\mathbf{c}, \mathbf{r})$ and $F(\mathbf{c}, \mathbf{r})$ are the molecular velocity distributions of the first and second components, then $f(\mathbf{c}_1, \mathbf{r}) = f_1$, etc. and $F(\mathbf{c}_2, \mathbf{r}) = F_2$, etc. If b_1 is the impact parameter* between molecules of the first kind, g_1 is their relative velocity before collision, and ϵ_1 is the azimuth of the collision plane, the probability of a collision is $g_1 b_1 db_1 d\epsilon_1 \equiv k_1 d\mathbf{k}$. Similarly, we introduce $k_2 d\mathbf{k}$ for molecules of the second kind and $k_{12} d\mathbf{k}$ for molecules of different kinds. The kinetic equations are

$$\begin{aligned} \mathbf{c}_1 \frac{\partial f_1}{\partial \mathbf{r}} &= \iint (f'f_1' - ff_1)\, k_1 \, d\mathbf{k}\, d\mathbf{c} + \iint (f_1'F_2' - f_1F_2)\, k_{12}\, d\mathbf{k}\, d\mathbf{c}_2, \\ \mathbf{c}_2 \frac{\partial F_2}{\partial \mathbf{r}} &= \iint (F'F_2' - FF_2)\, k_2 \, d\mathbf{k}\, d\mathbf{c} + \iint (f_1'F_2' - f_1F_2)\, k_{12}\, d\mathbf{k}\, d\mathbf{c}_1. \end{aligned} \tag{1}$$

Following Chapman and Cowling [4], we shall seek a solution of (1) in the form

$$f_1 = f_1^{(0)} [1 - \mathbf{D}_1 \operatorname{grad} n_1], \qquad F_2 = F_2^{(0)} [1 - \mathbf{D}_2 \operatorname{grad} n_1], \tag{2}$$

where $f_1^{(0)}$ and $F_2^{(0)}$ are equilibrium distribution functions of each component in the system of coordinates which is rigidly attached to the center of mass of the mixture, $\mathbf{D}_1 = \mathbf{c}_1 D(c_1)$, $\mathbf{D}_2 = \mathbf{c}_2 D(c_2)$, where $D(c_1)$ and $D(c_2)$ are scalar functions.

We shall seek the unknown functions $\mathbf{D}_1$ and $\mathbf{D}_2$ as the expansions

---

* The impact parameter is the perpendicular distance from the scattering center to the molecular trajectory before collision.

$$\mathbf{D}_1 = \sum_{-\infty}^{\infty} d_p \mathbf{a}_1^{(p)}, \qquad \mathbf{D}_2 = \sum_{-\infty}^{\infty} d_p \mathbf{a}_2^{(p)}, \tag{3}$$

where

$$\begin{aligned} \mathbf{a}_1^{(0)} &= \frac{\rho_1\rho_2}{\rho n_1 m_1^{1/2}}\mathbf{C}_1, \quad \mathbf{a}_1^{(p)} = \mathbf{C}_1 S_{3/2}^{(p)}(\mathbf{C}_1^2) \quad \text{for} \quad p > 0; \\ \mathbf{a}_2^{(0)} &= -\frac{\rho_1\rho_2}{\rho n_2 m_2^{1/2}}\mathbf{C}_2, \quad \mathbf{a}_2^{(p)} = \mathbf{C}_2 S_{3/2}^{(p)}(\mathbf{C}_2^2) \quad \text{for} \quad p < 0; \end{aligned} \tag{4}$$

ρ_1 and ρ_2 are the densities of the first and second components; $\rho = \rho_1 + \rho_2$; $S_{3/2}^{(p)}(\mathbf{C}_1^2)$ are Sonine polynomials; $\mathbf{C}_1 = (m_1/2kT)^{1/2}\mathbf{c}_1$; $\mathbf{C}_2 = (m_2/2kT)^{1/2}\mathbf{c}_2$.

When in Eq. (1) we substitute for f_1 and F_2 their values from (2) and take into account that $\frac{\partial f_1^{(0)}}{\partial \mathbf{r}} = \frac{f_1^{(0)}}{n_1} \operatorname{grad} n_1$, $\frac{\partial F_2^{(0)\prime}}{\partial \mathbf{r}} = -\frac{F_{(2)}^{0}}{n_2} \operatorname{grad} n_1$, $f^{(0)}f_1^{(0)} = f^{(0)\prime}f_1^{(0)\prime}$,

$$f_1^{(0)}F^{(0)} = f_1^{(0)\prime}F_2^{(0)\prime}, \quad F^{(0)}F_2^{(0)} = F^{(0)\prime}F_2^{(0)\prime}$$

after dividing by grad n_1 we obtain

$$\begin{aligned} -\mathbf{c}_1\frac{f_1^{(0)}}{n_1} &= \iint f^{(0)}f_1^{(0)}(\mathbf{D}_1' + \mathbf{D}' - \mathbf{D}_1 - \mathbf{D})\,k_1 d\mathbf{k}\, d\mathbf{c} + \\ &+ \iint f_1^{(0)}F_2^{(0)}(\mathbf{D}_1' + \mathbf{D}_2' - \mathbf{D}_1 - \mathbf{D}_2)\,k_{12}\, d\mathbf{k}\, d\mathbf{c}_2, \\ \mathbf{c}_2\frac{F_2^{(0)}}{n_2} &= \iint F^{(0)}F_2^{(0)}(\mathbf{D}' + \mathbf{D}_2' - \mathbf{D} - \mathbf{D}_2)\,k_2\, d\mathbf{k}\, d\mathbf{c} + \\ &+ \iint f_1^{(0)}F_2^{(0)}(\mathbf{D}_1' + \mathbf{D}_2' - \mathbf{D}_1 - \mathbf{D}_2)\,k_{12}\, d\mathbf{k}\, d\mathbf{c}_1. \end{aligned} \tag{5}$$

After scalar multiplication of the first and second equations of (5) by $\mathbf{a}_1^{(p)}d\mathbf{c}_1$ and $\mathbf{a}_2^{(p)}d\mathbf{c}_2$, respectively, integration over all possible values of $\mathbf{c}_1$ and $\mathbf{c}_2$ and addition we have

$$\begin{aligned} &\frac{1}{n_2}\int F_2^{(0)}\mathbf{c}_2\cdot\mathbf{a}_2^{(p)}\, d\mathbf{c}_2 - \frac{1}{n_1}\int f_1^{(0)}\mathbf{c}_1\cdot\mathbf{a}_1^{(p)}d\mathbf{c}_1 = \\ &= \iiint f^{(0)}f_1^{(0)}(\mathbf{D}' + \mathbf{D}_1' - \mathbf{D} - \mathbf{D}_1)\,\mathbf{a}_1^{(p)}k_1\, d\mathbf{k}\, d\mathbf{c}_1\, d\mathbf{c} + \\ &+ \iiint f_1^{(0)}F_2^{(0)}(\mathbf{D}_1' + \mathbf{D}_2' - \mathbf{D}_1 - \mathbf{D}_2)(\mathbf{a}_1^{(p)} + \mathbf{a}_2^{(p)})\,k_{12}\, d\mathbf{k}\, d\mathbf{c}_1\, d\mathbf{c}_2 + \\ &+ \iiint F^{(0)}F_2^{(0)}(\mathbf{D}' + \mathbf{D}_2' - \mathbf{D} - \mathbf{D}_2)\,\mathbf{a}_2^{(p)}\,k_2\, d\mathbf{k}\, d\mathbf{c}\, d\mathbf{c}_2. \end{aligned} \tag{6}$$

The expression which has been obtained will be denoted by $n_1n_2\delta_p$. From the orthogonality of Sonine polynomials it follows that

$$\delta_p = 3(2kT)^{1/2}/2n_1n_2 \quad \text{for} \quad p = 0; \qquad \delta_p = 0 \quad \text{for} \quad p \neq 0. \tag{7}$$

When the expressions in (3) for $\mathbf{D}_1$ and $\mathbf{D}_2$ are inserted in (6) we obtain the equations

$$\delta_p = \sum_{-\infty}^{\infty} d_q a_{pq}, \tag{8}$$

in which the d_q are unknowns and the a_{pq} are the expressions

$$a_{pq}=\frac{1}{n_1n_2}\Big\{\iiint f^{(0)}f_1^{(0)}\left(\mathbf{a}^{(q)\prime}+\mathbf{a}_1^{(q)\prime}-\mathbf{a}^{(q)}-\mathbf{a}_1^{(q)}\right)\mathbf{a}_1^{(p)}k_1\,\mathbf{dk}\,\mathbf{dc}\,\mathbf{dc}_1+$$
$$+\iiint f_1^{(0)}F_2^{(0)}\left(\mathbf{a}_1^{(q)\prime}+\mathbf{a}_2^{(q)\prime}-\mathbf{a}_1^{(q)}-\mathbf{a}_2^{(q)}\right)\left(\mathbf{a}_1^{(p)}+\mathbf{a}_2^{(p)}\right)k_{12}\,\mathbf{dc}\,\mathbf{dc}_1\,\mathbf{dc}_2+$$
$$+\iiint F^{(0)}F_2^{(0)}\left(\mathbf{a}^{(q)\prime}+\mathbf{a}_2^{(q)\prime}-\mathbf{a}^{(q)}-\mathbf{a}_2^{(q)}\right)\mathbf{a}_2^{(p)}k_2\,\mathbf{dk}\,\mathbf{dc}\,\mathbf{dc}_2\Big\}. \tag{9}$$

Equations (8) are solved by successive approximations. In the zeroth approximation we set q = 0 and are left with the single equation $\delta_0 = d_0a_{00}$. Hence

$$\mathbf{D}_1^{(0)}=\frac{\delta_0\mathbf{a}_1^{(0)}}{a_{00}},\quad \mathbf{D}_2^{(0)}=\frac{\delta_0\mathbf{a}_2^{(0)}}{a_{00}}.$$

In the first approximation (q = −1, 0, 1)

$$\begin{aligned}&d_{-1}a_{-1-1}+d_0a_{0-1}+d_1a_{1-1}=0,\\&d_{-1}a_{-10}+d_0a_{00}+d_1a_{10}=\delta_0,\\&d_{-1}a_{-11}+d_0a_{01}+d_1a_{11}=0.\end{aligned} \tag{10}$$

Denoting the determinant of (10) by A, we obtain

$$d_{-1}=-\frac{\delta_0}{A}\begin{vmatrix}a_{0-1} & a_{1-1}\\ a_{01} & a_{11}\end{vmatrix},\ d_0=\frac{\delta_0}{A}\begin{vmatrix}a_{-1-1} & a_{1-1}\\ a_{1-1} & a_{11}\end{vmatrix},\ d_1=-\frac{\delta_0}{A}\begin{vmatrix}a_{-1-1} & a_{0-1}\\ a_{-11} & a_{01}\end{vmatrix}, \tag{11}$$

$$\mathbf{D}_1^{(1)}=d_0\mathbf{a}_1^{(0)}+d_1\mathbf{a}_1^{(1)};\quad \mathbf{D}_2^{(1)}=d_0\mathbf{a}_2^{(0)}+d_{-1}\mathbf{a}_2^{(1)}. \tag{12}$$

Thus the problem of obtaining the distribution functions in any approximation is reduced to the calculation of the corresponding integrals a_{pq} (see [4]).

The relations in (11) become

$$d_{-1}=-\frac{3}{2n_1n_2}\left(\frac{m_0M_1M_2}{\pi}\right)^{1/2}\frac{B'_{-1}}{A'm_0^{1/2}\sigma_{12}^2},\quad d_0=\frac{3}{2n_1n_2}\left(\frac{m_0M_1M_2}{\pi}\right)^{1/2}\frac{B'_0}{A'm_0\sigma_{12}^2},$$
$$d_1=-\frac{3}{2n_1n_2}\left(\frac{m_0M_1M_2}{\pi}\right)^{1/2}\frac{B'_1}{A'm_0^{1/2}\sigma_{12}^2}, \tag{13}$$

where B'_0, B'_1, B'_{-1} and A' are dimensionless quantities which correspond to the determinants in (11); $m_0 = m_1 + m_2$; $M_1 = m_1/m_0$; $M_2 = m_2/m_0$; σ_1 and σ_2 are the diameters of molecules of the first and second components; $\sigma_{12} = (\sigma_1 + \sigma_2)/2$.

The distribution functions which have been obtained describe in first approximation the mutual diffusion field of two gases:

$$f_1^{(1)}=n_1\left(\frac{m_1}{2\pi kT}\right)^{3/2}e^{-C_1^2}\left\{1+\left[d_0\frac{\rho_1\rho_2}{\rho n_1m_1^{1/2}}+d_1S_{3/2}^{(1)}(C_1^2)\right]C_1\operatorname{grad}n_1\cos\vartheta_1\right\}, \tag{14}$$

$$F_2^{(1)}=n_2\left(\frac{m_2}{2\pi kT}\right)^{3/2}e^{-C_2^2}\left\{1+\left[-d_0\frac{\rho_1\rho_2}{\rho n_2m_2^{1/2}}+d_{-1}S_{3/2}^{(1)}(C_2^2)\right]C_2\operatorname{grad}n_2\cos\vartheta_2\right\}, \tag{15}$$

where ϑ_1 and ϑ_2 are the angles between $\mathbf{C}_1$ and $\mathbf{C}_2$ and the direction opposite to grad n_1.

§3. An aerosol particle in a diffusion field possesses, in addition to Brownian movement, an orderly velocity **u** such that the average momentum transferred to the particle by collisions with molecules will vanish. We consider such small values of grad n_1 that **u** ~ grad n_1 ≪ $\mathbf{c}_2$. Hereinafter we shall drop terms that are proportional to u^2 and $u \cdot \text{grad } n_1$.

The momentum dp_1 transferred per unit time through collisions with molecules of the first kind to an element dS of the surface of a spherical particle in the direction **u** is

$$dp_1 = \int m_1 (c_1 + u)_u (c_1 + u)_n f_1 \, d\mathbf{c}_1 \, dS, \tag{16}$$

where $(c_1 + u)_u$ and $(c_1 + u)_n$ are projections of the vector $\mathbf{c}_1 + \mathbf{u}$ on the **u** direction and the normal **n** to dS, respectively. When we denote the angle between $\mathbf{c}_1$ and **n** by ψ_1, the angle between **u** and **n** by θ, the azimuth of $\mathbf{c}_1$ in the system associated with **n** by φ, we have $\cos \vartheta_1 = \cos \psi_1 \cos \theta + \sin \psi_1 \sin \theta \cos \varphi$. The expansion of (16) gives

$$dp_1 = m_1 \int (c_1 \cos \vartheta_1 + u)(c_1 \cos \psi_1 + u \cos \theta)\, n_1 \left(\frac{m_1}{2\pi kT}\right)^{3/2} e^{-C_1^2} \times$$
$$\times \left\{1 + \left[d_0 \frac{\rho_1 \rho_2}{\rho n_1 m_1^{1/2}} + d_1 S_{1/2}^{(1)}(C_1^2)\right] C_1 \,\text{grad}\, n_1 \cos \vartheta_1 \right\} c_1^2 dc_1 \sin \psi_1 d\psi_1 d\varphi.$$

Integrating under the conditions given above, we obtain

$$p_1 = -m_1 n_1 \bar{c}_1 \frac{\cos^2 \theta + 1}{2} \left\{\left(\frac{kT}{8m_1}\right)^{1/2} \left[d_0 \frac{\rho_1 \rho_2}{\rho n_1 m_1^{1/2}} - \frac{1}{2} d_1\right] \text{grad}\, n_1 + \frac{u}{2}\right\}. \tag{17}$$

Similarly, for the momentum transferred by molecules of the second component, we obtain

$$p_2 = -m_2 n_2 \bar{c}_2 \frac{\cos^2 \theta + 1}{2} \left\{\left(\frac{kT}{8m_2}\right)^{1/2} \left[-d_0 \frac{\rho_1 \rho_2}{\rho n_2 m_2^{1/2}} - \frac{1}{2} d_{-1}\right] \text{grad}\, n_1 + \frac{u}{2}\right\}. \tag{18}$$

In the case of specular reflection the recoil momentum vanishes for molecules evaporated from the surface of a particle. For any other law of reflection the additional momentum is easily calculated but does not change the order of magnitude of u. Setting the sum $p_1 + p_2$ equal to zero, we obtain

$$u = \left(\frac{kT}{8}\right)^{1/2} \frac{\text{grad}\, n_1}{n_1 m_1^{1/2} + n_2 m_2^{1/2}} \left[2d_0 \frac{\rho_1 \rho_2}{\rho} \left(\frac{1}{m_2^{1/2}} - \frac{1}{m_1^{1/2}}\right) + n_1 d_1 + n_2 d_{-1}\right]. \tag{19}$$

In order to transform to the system of reference associated with the walls of the vessel that contains the diffusing mixture we consider that the total flow of molecules through a small area fixed with respect to the walls is zero. From this condition in the given system we immediately obtain the velocity of the center of gravity of the system, which when combined with (19) gives the velocity u' with respect to the walls:

$$u' = -\frac{3}{2}\left(\frac{m_0 M_1 M_2 kT}{2\pi}\right)^{1/2} \frac{\text{grad}\, n_1}{A' \sigma_{12}^2 \rho_2} \left\{\frac{B_0' M_2}{1 + n_{12} m_{12}} \left[\frac{1 - \sqrt{m_{12}}}{1 + n_{21}\sqrt{m_{21}}} - \frac{m_{12} - 1}{1 + n_{21}}\right] + \right.$$
$$\left. + \frac{(B_1' + n_{21} B_{-1}')\, M_2^{1/2}}{2(n_{21} + \sqrt{m_{12}})}\right\}, \tag{20}$$

where $m_{12} = m_1/m_2$, $m_{21} = m_2/m_1$, $n_{12} = n_1/n_2$, $n_{21} = n_2/n_1$.

A numerical calculation for a mixture of air and water vapor (p = 1 atmos, T_0 = 293°K) gives $u' = 1.47 \cdot 10^{-2}/l$ cm/sec, where l is the distance in centimeters at which the relative humidity drops from 100% to zero.

We note that the first term in the curly brackets of (20) is related to the diffusion coefficient of the mixture.*

We now point out, in conclusion, that for a highly porous body in which pseudomolecular flow can occur the following effect must be present. Let a porous diaphragm separate two vessels with different concentrations of the gaseous mixture. A quasi-stationary state in such a system will correspond to a discontinuity of the total pressure. This will induce flow of the mixture with the linear velocity u' compensating its motion through the pores of the diaphragm. This pressure discontinuity must be directly proportional to the difference of concentrations on both sides of the porous diaphragm and inversely proportional to the average pore diameter and can be measured with a manometer, as was discovered by G. A. Batova.

LITERATURE CITED

[1] B. V. Deriagin and S. S. Dukhin, Doklady Akad. Nauk SSSR 106, 851 (1956).

[2] B. V. Deriagin and S. S. Dukhin, Doklady Akad. Nauk SSSR 111, 613 (1956).

[3] S. S. Dukhin and B. V. Deriagin, Doklady Akad. Nauk SSSR 112, 407 (1957).**

[4] S. Chapman and J. G. Cowling, The Mathematical Theory of Nonuniform Gases (Cambridge, 1939).

Received October 9, 1957

Institute of Physical Chemistry, Academy of Sciences,
USSR

---

* We are indebted to O. M. Todes for calling our attention to this.

** [See Soviet Physics – Doklady, p. 41].

NUCLEAR QUADRUPOLE MOMENTS

A. N. Kushnirenko

(Presented by Academician N. N. Bogoliubov, June 20, 1957)

The electric quadrupole moments of nuclei have been discussed in many papers [1-8]. Since the final word has not been said on this subject for the shell model the present author has considered it again. The wave function of the nucleus is given as a linear combination of Slater functions consisting of one-nucleon wave functions. For strong spin-orbit coupling these are [9]

$$\psi_{\alpha_i}(\bar{r}_i, s_i, t_i) = R_{\beta_i}(r_i) \begin{vmatrix} a_i Y_{l_i, m_i}(\theta_i, \varphi_i) \\ b_i Y_{l_i, m_i+1}(\theta_i, \varphi_i) \end{vmatrix} T_{\tau_i}(t_i), \tag{1}$$

where $\bar{r}_i$, s_i, t_i are, respectively, the space, spin, and isotopic spin coordinates of the ith nucleon, $\alpha_i = (n_i, j_i, j_{zi}, \tau_{\zeta i})$, $\beta_i = (n_i, l_i, j_i)$ are sets of quantum numbers which characterize the state of a nucleon; n_i is the principal quantum number; l_i is the orbital quantum number; j_{zi} is the quantum number of the projection of the total angular momentum on an arbitrary z axis; m_i is the magnetic quantum number; $\tau_{\zeta i}$ is the quantum number of the isotopic spin of the ith nucleon; $R_{\beta_i}(r_i)$ is the radial wave function; $Y_{l,m}(\theta, \varphi)$ is the spherical wave function; $T_{\tau_i}(t_i)$ is the wave function of the isotopic spin; and a_i and b_i are known coefficients [9].

The coefficients of the expansion of the nuclear wave function in Slater functions are obtained from conservation of the projection of angular momentum on the z axis, of the square of the angular momentum and of the square of the isotopic spin of the nucleus. Using the given wave function and the general formula for the quadrupole moment [10], we obtain a formula for the nuclear quadrupole moment:

$$\begin{aligned} Q_{zz} = \sum_{i,k} |c_k|^2 \frac{A_i^{(k)}}{2j_i^{(k)}(j_i^{(k)}+1)} \left[j_i^{(k)}(j_i^{(k)}+1) - 3j_{zi}^{(k)}\right] + \\ + \sum_{\substack{i,k,j \\ (k \neq j)}} c_k^* c_j \delta_{\tau_j^k, \tau_k^j} \prod_{\substack{n \\ (n \neq i)}} \delta_{\alpha_n^k, \alpha_n^j} A_i^{(k,j)} B_i^{(k,j)}, \end{aligned} \tag{2}$$

where i is the proton index; k and j are Slater function indices; c_k is the amplitude of the kth Slater function; n has all values from 1 to A except n = i; A is the number of particles in the nucleus;

$$A_i^{(k)} = \int R^2_{\beta_i^{(k)}}(r) r^4 \, dr; \quad A_i^{(k,j)} = \int R_{\beta_i^{(k)}}(r) R_{\beta_i^{(j)}}(r) r^4 \, dr; \tag{3}$$

$$\begin{aligned} B_i^{(k,j)} = \int (3\cos^2\theta - 1) \{ a_i^{(k)} a_i^{(j)} Y^*_{l_i^{(k)}, m_i^{(k)}} Y_{l_i^{(j)}, m_i^{(j)}} + \\ + b_i^{(k)} b_i^{(j)} Y^*_{l_i^{(k)}, m_i^{(k)}+1} Y_{l_i^{(j)}, m_i^{(j)}+1} \} \, d\Omega_i. \end{aligned} \tag{4}$$

TABLE 1

Nucleus	$3\mathrm{Li}^{7}$	$4\mathrm{Be}^{7}$	$5\mathrm{B}^{9}$	$4\mathrm{Be}^{9}$	$5\mathrm{B}^{11}$	$3\mathrm{Al}^{27}$
Q_{zz} theor. Q_{zz} exp.	−0.013 <0	−0.012 $Q_{zz}(\mathrm{Li}^7) \sim$ $\sim Q_{zz}(\mathrm{Be}^7)$	0.016 —	0.025 $\simeq$ (0.02)	0.0250 0.0355±2	0.07 0.149±2
Nucleus	$29\mathrm{Cu}^{63}$	$29\mathrm{Cu}^{65}$	$17\mathrm{Cl}^{35}$	$31\mathrm{Ga}^{69}$	$31\mathrm{Ga}^{71}$	$83\mathrm{Bi}^{209}$
Q_{zz} theor. Q_{zz} exp.	−0.085 −0.157±31	−0.086 −0.145±29	−0.059 −0.06635±2	0.09 0.243	0.092 0.152	−0.35 −0.4

It can be shown that the value of the coefficient $A_i^{(k)}$ is in the range $(R^2/3, R^2)$ and that its average value is approximately $0.6\ R^2$, where R is the nuclear radius.

Table 1 gives the electric quadrupole moments of some light nuclei which were calculated from Eq. (2) assuming $A_i^{(k)} \approx 0.6\ R^2$. The calculation did not take mixing of configurations into account.

The last (triple) sum in Eq. (2) shows that in the presence of mixed shell configurations an additional electric quadrupole moment arises. Thus, for example, an analysis of shell structures shows the closeness of proton levels $4d_{5/2}$, $6g_{7/2}$ and $6h_{11/2}$. These levels begin to fill up with protons almost simultaneously. Therefore the protons on these levels are in complex states which are linear combinations of the states $4d_{5/2}$, $5g_{7/2}$, and $6h_{11/2}$. It can be assumed that such complex configurations are responsible for at least a part of the anomalously large positive electric quadrupole moment of certain nuclei with $Z > 50$.

In conclusion I wish to thank D. D. Ivanenko, S. I. Larin and Ia. A. Smorodinskii for valuable comments and discussions.

LITERATURE CITED

[1] B. H. Flowers, Phil. Mag. 43, 1330 (1952).

[2] A. Bohr and B. R. Mottelson, Kgl. Danske Videnskab. Selskab. Mat.-fys. Medd. 27, 16 (1953).

[3] M. A. Perks, Proc. Phys. Soc. A68, 1083 (1955).

[4] H. Horie and A. Arima, Phys. Rev. 99, 778 (1955).

[5] J. Rainwater, Phys. Rev. 79, 432 (1950).

[6] R. Van Wageningen and J. de Boer, Physica 18, 369 (1952).

[7] S. A. Moskowski and C. H. Townes, Phys. Rev. 93, 306 (1953).

[8] F. I. Kligman, J. Exptl.-Theoret. Phys. (USSR) 18, 4, 346 (1948).

[9] D. I. Blokhintsev, Elements of Quantum Mechanics (1949) [in Russian].

[10] J. Blatt and V. Weisskopf, Theoretical Nuclear Physics (John Wiley and Sons, New York, 1952); (Moscow, 1954) [Russian translation].

Received May 30, 1957

T. G. Shevchenko Kiev State University

ON THE THEORY OF THE ANISOTROPY OF CUBIC CRYSTALS

N. A. Potapkov

(Presented by Academician N. N. Bogoliubov August 22, 1957)

Magnetic anisotropy is characterized by the so-called anisotropy constants [1]. The temperature dependence of these constants for cubic crystals is considered in [2] by the method of approximate second quantization neglecting spin-wave interactions.

In the present paper we consider spin-wave interactions for anisotropic ferromagnets with cubic symmetry. Dyson's method [3] was used for the spin-wave interactions.

The Hamiltonian of the system is

$$\mathscr{H} = \mu \sum_{j} (HS_j) - \frac{1}{2} I \sum_{j\delta} (S_j S_{j+\delta}) + \frac{1}{4!} \delta I \sum_{\substack{j,\ \delta_1,\ \delta_2,\ \delta_3,\ \alpha' \\ \delta_1 \neq \delta_2 \neq \delta_3}} S_j^{\alpha'} S_{j+\delta_1}^{\alpha'} S_{j+\delta_2}^{\alpha'} S_{j+\delta_3}^{\alpha'}, \tag{1}$$

where $\alpha' = (x', y', z')$; H is the external magnetic field; μ is the Bohr magneton; δI characterizes the magnetic interaction; I is the ordinary exchange integral; S_j is the spin operator of the electron at crystal site (atom) $\underline{j}$; δ is the vector line which joins an atom to one of its nearest neighbors.

For an arbitrarily oriented external magnetic field the direction of magnetization does not coincide with the direction of a crystallographic axis. The Hamiltonian of the system is conveniently written in the (x, y, z) coordinate system with the $\underline{z}$ axis in the direction of magnetization. The operators $S^{x'}$, $S^{y'}$, $S^{z'}$ are expressed in terms of S^x, S^y, S^z as follows:

$$\begin{gathered} S^{x'} = S^x \cos\theta \cos\varphi - S^y \sin\varphi + S^z \sin\theta \sin\varphi, \\ S^{y'} = S^x \cos\theta \sin\varphi + S^y \cos\varphi + S^z \sin\theta \sin\varphi, \\ S^{z'} = -S^x \sin\theta + S^z \cos\theta. \end{gathered} \tag{2}$$

We also define the operators

$$S_\lambda = N^{-1/2} \sum_j \exp(i\lambda j) S_j, \quad S_\lambda^{\pm} = S_\lambda^x \pm i S_\lambda^y, \tag{3}$$

where λ is the reciprocal lattice vector. The operators satisfy the relations

$$\begin{gathered} [S_\lambda^z S_\mu^+] = N^{-1/2} S_{\lambda+\mu}^+, \quad [S_\lambda^z S_\mu^-] = -N^{-1/2} S_{\lambda+\mu}^-, \\ [S_\lambda^+ S_\mu^-] = +2N^{-1/2} S_{\lambda+\mu}^z. \end{gathered} \tag{4}$$

The ground state of the system is defined as

$$S_j |0\rangle = 0, \quad S_j^z |0\rangle = -S |0\rangle \tag{5}$$

for all $\underline{j}$, or equivalently,

$$S_\lambda^-|0\rangle = 0, \quad S_\lambda^z|0\rangle = -N^{1/2}S\delta_{\lambda 0}|0\rangle \tag{6}$$

for all λ. Following Dyson, excited states are defined thus:

$$|a\rangle = \prod_\lambda [(2S)^{-1/2 a_\lambda}(a_\lambda!)^{-1/2}(S_\lambda^+)^{a_\lambda}]|0\rangle, \tag{7}$$

where a_λ is the number of spin waves with wave vector λ. The states with $\sum a_\lambda > 1$ are unnormalized and nonorthogonal. The nonorthogonality of states $|a\rangle$ results in an interaction between spin waves which is called the kinematical interaction.

The operation of the Hamiltonian $\mathscr{H}$ on the state $|a\rangle$ gives

$$\mathscr{H}|a\rangle = \left[E_0 + \sum_\lambda a_\lambda(L + \varepsilon_\lambda)\right]|a\rangle + \sum_b Q_{ba}|b\rangle. \tag{8}$$

Here

$$E_0 = -\mu NH^z - \frac{1}{2}I\gamma_0 NS^2 + \frac{1}{4!}\delta I\gamma_{000}\omega NS^4; \tag{9}$$

$$\varepsilon_\lambda = \left[IS - \frac{6}{4!}\delta IS^3\frac{\gamma_{000}}{\gamma_0}(1-\omega)\right](\gamma_0 - \gamma_\lambda); \tag{10}$$

$$L = \mu H^z + \frac{1}{4!}\delta IS^3\gamma_{000}(6-10\omega); \tag{11}$$

$$\gamma_\lambda = \sum_\delta e^{i\lambda\delta}, \quad \gamma_{\lambda_1\lambda_2\lambda_3} = \sum_{\delta_1,\,\delta_2,\,\delta_3} e^{i(\delta_1\lambda_1 + \delta_2\lambda_2 + \delta_3\lambda_3)}; \tag{12}$$

$$\omega = \cos^4\alpha_1 + \cos^4\alpha_2 + \cos^4\alpha_3, \tag{13}$$

where $\cos\alpha_i$ are direction cosines of the magnetization direction with respect to the crystallographic axes; Q_{ba} is determined from the expressions for the commutators of $\mathscr{H}$ and S_λ^+.

We now write the energy operator $\mathscr{H}$ in the ideal spin-wave model [3]:

$$\mathscr{H} = E_0 + \sum_\lambda(L + \varepsilon_\lambda)\dot{\alpha}_\lambda\alpha_\lambda + \sum_{\lambda\rho\sigma}\Gamma_{\rho\sigma}^\lambda\dot{\alpha}_{\sigma+\lambda}\dot{\alpha}_{\rho-\lambda}\alpha_\rho\alpha_\sigma + \dots, \tag{14}$$

where $\Gamma_{\rho\sigma}^\lambda$ is determined from the expressions for the double commutators $[[\mathscr{H}, S_\rho^+], S_\sigma^+]$.

The third term represents the scattering of two spin waves. The energy operator contains additional terms which describe the scattering of three and four spin waves, although these will be dropped in calculating the free energy.

For the free energy of a single atom we obtain

$$F = F_0 + F_A, \tag{15}$$

where F_A is the free energy of crystal anisotropy;

$$F_A = K_1^0\omega\left\{1 - \frac{1}{S}10Z_{5/2}(\beta L')\theta^{5/2} - \frac{3}{2S}\pi\nu Z_{3/2}(\beta L')\theta^{3/2} + \right.$$
$$\left. + \frac{1}{S^2}45[Z_{3/2}(\beta L')]^2\theta^3\right\},$$

$$K_1^0 = \frac{1}{4!}\delta I\gamma_{000}S^4, \quad L' = \mu H^z, \quad \theta = \frac{T}{2\pi T_c}, \quad Z_n(x) = \sum_{j=1}^\infty j^{-n}e^{-jx}, \quad \nu = \frac{a^2}{v^{2/3}}. \tag{16}$$

The term containing θ^3 in the expression for F_A represents a spin-wave interaction (the scattering of two spin-waves). The terms in (14) for $\mathscr{H}$ which describe the scattering of three and four spin waves give a contribution to the free energy which is proportional to $\theta^{9/2}$ and θ^6, respectively. In the temperature range up to $T = {}^1/_4 T_c$ the term which describes the spin-wave interaction does not exceed 10% (for $s = 1$) and 20% (for $s = {}^1/_2$) of the corresponding term in the Bloch approximation.

In conclusion I wish to thank S. V. Tiablikov for valuable discussions.

LITERATURE CITED

[1] S. V. Vonsovskii and Ia. S. Shur, Ferromagnetism (Moscow, 1948) [in Russian].

[2] S. V. Tiablikov and A. A. Gusev, Fiz. Metal. i Metalloved. 2, 3, 385 (1956).

[3] F. J. Dyson, Phys. Rev. 102, 1217 (1956).

Received August 19, 1957

V. A. Steklov Mathematics Institute, Academy of Sciences USSR

ON THE SEMICLASSICAL INTERPRETATION OF QUANTUM EFFECTS IN THE THEORY OF THE RADIATING ELECTRON

A. A. Sokolov and I. M. Ternov

(Presented by Academician N. N. Bogoliubov October 18, 1957)

1. In the present article we wish to present a semiclassical interpretation of quantum effects associated with the motion of an extreme relativistic electron in a magnetic field [1, 2].

We know that the classical equations which describe the motion of an extreme relativistic electron in a synchrotron and take account of the radiation are

$$\frac{E\ddot{z}}{c^2} + \frac{\dot{E}\dot{z}}{c^2} - \frac{er\dot{\varphi}H_r}{c} = -\frac{\dot{z}W^{\mathrm{cl}}}{c^2}, \tag{1}$$

$$\frac{E\ddot{r}}{c^2} + \frac{\dot{E}\dot{r}}{c^2} - \frac{Er\dot{\varphi}^2}{c^2} + \frac{er\dot{\varphi}H_z}{c} = -\frac{\dot{r}W^{\mathrm{cl}}}{c^2}, \tag{2}$$

$$\dot{E} = \dot{E}^{\mathrm{o}} - W^{\mathrm{cl}}, \tag{3}$$

where r, z, φ are cylindrical coordinates; $H_z = Br^{-q}$, $H_r = -qzBr^{-(q+1)}$ are the components of the magnetic field; $\underline{q}$ is the decay exponent of the magnetic field ($0 < q < 1$). The classical expression for the radiated energy is

$$W^{\mathrm{cl}} = \frac{R^2}{\rho^2}\,\overline{W^{\mathrm{cl}}}, \quad \overline{W^{\mathrm{cl}}} = \frac{2}{3}\,\frac{e^2c}{R^2}\left(\frac{E}{m_0c^2}\right)^4, \tag{4}$$

where $\overline{W^{\mathrm{cl}}}$ is the average radiated energy, which is independent of the coordinate $x = r - R$ of betatron oscillations, and the radius of the instantaneous equilibrium orbit R and the radius of curvature ρ can be obtained from

$$E = eBR^{1-q} = eBr^{-q}\rho. \tag{5}$$

Hence in a linear approximation we have

$$\rho \simeq R + qx. \tag{6}$$

The expression for the energy acquired by an electron from the accelerating mechanism (the fundamental harmonic) can be represented as follows in the linear approximation of the phase oscillations:

$$\dot{E}^{\mathrm{o}} = \frac{cV_0}{2\pi r}\sin(\varphi - \omega_0 t) = \frac{cV_0}{2\pi r}(\sin\varphi_0 + \psi\cos\varphi_0), \tag{7}$$

where V_0/e is the amplitude of the potential across the accelerating gap; ω_0 is the angular frequency of the high-frequency field, which is related to the radius of the synchrotron equilibrium orbit through $R_0 = c/\omega_0$. Here $\omega_0 t + \varphi_0$ characterizes the uniform revolutions of the electron and $\psi = \varphi - \omega_0 t - \varphi_0$ contains only the oscillating part.

Taking these last relations into account, instead of (1)-(3) we have in linear approximation

$$\ddot{z}+\gamma\dot{z}+\omega_z^2 z=-\frac{\overline{W}^{\mathrm{cl}}}{E}\,\dot{z}; \tag{8}$$

$$\ddot{x}+\gamma\dot{x}+\omega_r^2 x=-\frac{\overline{W}^{\mathrm{cl}}}{E}\,\dot{x}-\ddot{R}-\frac{x\ddot{R}}{R}, \tag{9}$$

$$r\dot{E}=(1-q)\,E\left(\ddot{R}+\frac{x\ddot{R}}{R}\right)=\frac{V_0 c}{2\pi}\left(\sin\varphi_0+\psi\cos\varphi_0\right)-rW^{\mathrm{cl}}, \tag{10}$$

where $\omega_z=\sqrt{q}\,\frac{c}{R}$, $\omega_r=\sqrt{1-q}\,\frac{c}{R}$. Eliminating from the right-hand side of (9) the quantity $\ddot{R}+x\ddot{R}/R$, we obtain the following equation to describe radial betatron oscillations:

$$\ddot{x}+\gamma\dot{x}+\omega_r^2 x=-\frac{q}{1-q}\,\frac{\overline{W}^{\mathrm{cl}}}{E}\,\dot{x}, \tag{11}$$

which means that when a continuous "frictional force" is introduced into the theory of betatron oscillations, in addition to the "small" damping constant $\gamma=\dot{E}/E$ we must also take into account the large damping constants [3-5]

$$\Gamma_z=\frac{\overline{W}^{\mathrm{cl}}}{E}\ll\gamma,\quad \Gamma_r=\frac{q}{1-q}\,\Gamma_z. \tag{12}$$

Introducing the coordinate $X=R-R_0$, which is associated with the phase ψ through the relation $X=-\frac{R_0^2}{c}\dot{\psi}$, and considering that $\overline{W}^{\mathrm{cl}}=\left(\frac{R}{R_0}\right)^{2-4q}W_0$ (W_0 corresponds to $R=R_0$), we obtain the following equation for determination of the phase oscillations:

$$\ddot{\psi}+\Gamma\dot{\psi}+\Omega^2\psi=-\frac{c}{(1-q)\,R_0^2E_0}\left(\frac{cV_0\sin\varphi_0}{2\pi}-R_0W_0\right)=0, \tag{13}$$

where the equilibrium point of the phase will be obtained from

$$\frac{cV_0}{2\pi R_0}\sin\varphi_0=W_0; \tag{14}$$

the angular velocity of slow synchrotron oscillations is

$$\Omega=\sqrt{\frac{c^2V_0\cos\varphi_0}{2\pi(1-q)\,R_0^2E_0}}=\sqrt{\frac{cW_0\cot\varphi_0}{(1-q)\,R_0E_0}}\ll\omega_r; \tag{15}$$

$\Gamma=\frac{3-4q}{1-q}\,\frac{W_0}{E}\sim\Gamma_r$ is the "large" damping constant of the synchrotron oscillations.

2. As we know, in studying the radiation from an accelerated electron we must evaluate the influence of the discreteness of the radiation, because by quantum theory during one revolution the relatively small number of quanta $N\sim\alpha\frac{E}{m_0c^2}$ [2] is emitted, especially when $E<E_{1/5}$.

In order to describe the discrete character of the radiation we introduce the fluctuation force

$$\mathbf{F}^{\mathrm{fluct.}}=-\frac{\mathbf{v}}{c^2}\sum_i\left\{\frac{R}{\rho}\,\bar{\varepsilon}\delta\,(t-t_i)-\frac{R^2}{\rho^2}\,\overline{W}^{\mathrm{cl}}\right\}. \tag{16}$$

The introduction of the fluctuation force is formally equivalent in Eqs. (8), (9) and (10) to the substitutions (with the radiated harmonic number ν):

$$\overline{W}^{\text{cl}} \to \sum_i \bar{\varepsilon}\delta(t-t_i) = \sum_i \hbar \frac{c}{R} \nu\hat{\delta}(t-t_i),$$
$$W^{\text{cl}} \to \frac{R}{\rho} \sum_i \bar{\varepsilon}\delta(t-t_i) = \sum_i \left(1 - q\frac{x}{R}\right) \hbar \frac{c}{R} \nu\hat{\delta}(t-t_i). \tag{17}$$

Then these equations become

$$\ddot{z} + \gamma\dot{z} + \omega_z^2 z = -\sum_i \frac{\dot{z}}{E} \bar{\varepsilon}\delta(t-t_i) = -\sum_i \frac{c\cos\theta}{E} \bar{\varepsilon}\delta(t-t_i); \tag{18}$$

$$\ddot{x} + \gamma\dot{x} + \omega_r^2 x = -\sum_i \frac{\dot{x}}{E} \bar{\varepsilon}\delta(t-t_i) - \ddot{R} - \frac{\dot{x}\dot{R}}{R}, \tag{19}$$

$$r\dot{E} = (1-q)\, E\left(\dot{R} + \frac{x\dot{R}}{R}\right) = \frac{cV_0}{2\pi}(\sin\varphi_0 + \psi\cos\varphi_0) -$$
$$- \sum_i R\bar{\varepsilon}c\left[1 + (1-q)\frac{x}{R}\right]\hat{\delta}(t-t_i). \tag{20}$$

Equation (18) characterizes the axial oscillations with account of quantum fluctuations.

In order to obtain the final equations for the radial oscillations we must in the right-hand side of (19) replace $\ddot{R} + \dot{x}\dot{R}/R$ by its value given in (20), dropping the terms which are proportional to ψ. Thus

$$\ddot{x} + \gamma\dot{x} + \omega_r^2 x = \frac{R}{E(1-q)} \frac{d}{dt} \sum_i \bar{\varepsilon}\delta(t-t_i). \tag{21}$$

We note that the energy of the fluctuation radiation is inversely proportional to ρ [6] rather than to ρ^2 as in the classical case. But it must be remembered that the probability of a transition is also inversely proportional to ρ:

$$w(\nu, t_i) = \frac{R}{\rho} \bar{w}(\nu, t_i), \tag{22}$$

where

$$\bar{w}(\nu, t_i) = \frac{e^2}{\pi\sqrt{3}\, c\hbar} \frac{c}{R} \left(\frac{m_0c^2}{E}\right)^2 \int\limits_{\frac{2}{3}\nu (m_0c^2/E)^3}^{\infty} K_{5/3}(\xi)\, d\xi. \tag{23}$$

Therefore in the transition to continuous radiation we again obtain the classical formula

$$\lim_{\Delta t_i \to 0} \sum_i \bar{\varepsilon}\delta(t-t_i) = \int\limits_0^\infty d\nu \int\limits_0^\infty \frac{R}{\rho}\bar{\varepsilon}\frac{R}{\rho}\bar{w}(\nu, t_i)\,\hat{\delta}(t-t_i)\, dt_i = \left(\frac{R}{\rho}\right)^2 \overline{W}^{\text{cl}}. \tag{24}$$

In exactly the same way the "large" damping constants can be derived by passing to the limit from quantum fluctuation forces to continuous radiation:

$$\lim_{\Delta t_i \to 0} \frac{R}{E(1-q)} \frac{d}{dt} \sum_i \bar{\varepsilon}\delta(t-t_i) =$$
$$= \frac{R}{E(1-q)} \frac{d}{dt} \int\limits_0^\infty d\nu \int\limits_0^\infty \bar{\varepsilon}\left(1 - \frac{qx}{R}\right) \bar{w}\delta(t-t_i)\, dt_i = -\Gamma_r \dot{x} \tag{25}$$

etc.

The square of the amplitude of the radial oscillations with account of the fluctuation force from (21) is given by

$$a^2 = a_0^2 \exp\left[-\int_0^t \gamma(t')\,dt'\right] + \\ + \frac{55}{24\sqrt{3}(1-q)^2}\frac{e^2}{m_0c}\frac{\hbar}{m_0cR_0}\int_0^t \exp\left[-\int_{t'}^t \gamma(t'')\,dt''\right]\left(\frac{E(t')}{m_0c^2}\right)^5 dt'. \qquad (26)$$

In order to obtain the formula given in [2, 6] it must be remembered that

$$\exp\left[-\int_{t'}^t \gamma(t'')\,dt''\right] = \frac{E(t')}{E(t)}.$$

The corresponding formula for the axial oscillations will be smaller by about the factor $(E/m_0c^2)^2$. In [3-5] it is assumed that besides the effect of the fluctuation force on betatron oscillations there remains in addition the "large" classical value of the damping constants Γ_z, Γ_r.

For synchrotron oscillations in the presence of quantum fluctuations, substituting $x = 0$ and $X = -\frac{R_0^2}{c}\psi$ into (20) we obtain

$$R\dot{E} = -\frac{E_0R_0^2(1-q)}{c}\ddot{\psi} = \frac{E_0R_0^2(1-q)\,\Omega^2}{c}\psi + \frac{V_0c\sin\varphi_0}{2\pi} - \sum_i \hbar\nu c\delta(t-t_i). \qquad (27)$$

Considering that the period $T = 2\pi/\Omega \gg 2\pi/\omega_r$ of synchrotron oscillations is much greater than the mean time $\Delta t_i = t_{i+1} - t_i$ between two successive acts of emission, we can average (27) over the time Δt, satisfying the condition $\Delta t_i \ll \Delta t \ll T$. Then for the phase oscillations we obtain the classical equation in which the quantum fluctuation force goes over into the "frictional force" with a "large" damping constant Γ.* This is evidently related to the fact that the phase oscillations result from the change of the total energy, which is influenced by quantum effects only for very large values $E \sim E_{1/2}$ [1], whereas the fluctuation force will affect radial betatron oscillations at relatively low energies $E \sim E_{1/5}$ [2].

LITERATURE CITED

[1] A. A. Sokolov, N. P. Klepikov, and I. M. Ternov, J. Exptl.-Theoret. Phys. (USSR) 24, 249 (1953).

[2] A. A. Sokolov and I. M. Ternov, J. Exptl.-Theoret. Phys. (USSR) 25, 698 (1953); Doklady Akad. Nauk SSSR 97, 823 (1954).

[3] A. A. Kolomenskii and A. N. Lebedev, CERN, Symposium, 1 (Geneva, 1956), p. 447.

[4] M. S. Livingston, CERN, Symposium 1 (Geneva, 1956), p. 439.

[5] I. Henry, Phys. Rev. 106, 1057 (1957).

[6] A. N. Matveev, Doklady Akad. Nauk SSSR 107, 671 (1956).**

[7] M. Sands, Phys. Rev. 97, 470 (1955).

[8] A. N. Matveev, Nuovo cimento 5, 1782 (1957).

Received October 14, 1957

M. V. Lomonosov Moscow State University

---

* In [3, 7, 8], on phase oscillations, both the fluctuation force and the "large" damping constant are taken into account.

** [See Soviet Physics – "Doklady," p. 271].

SOVIET PHYSICS—DOKLADY VOL. 2, NO. 6 NOV.-DEC., 1957

(Translation of all papers in the Physics Sections of the Proceedings of the Academy of Sciences of the USSR, Vol. 117, Nos. 1-6, published by the American Institute of Physics, July, 1958)

CONTENTS

		Russian	
	Page	Issue No.	Page
1. The Conversion Spectrum of Ho^{160}. E. P. Grigor'ev, B. S. Dzhelepov, A. V. Zolotavin, B. Kratsik, B. K. Preobrazhenskii, and I. S. Ianchevskaia	479	1	53
2. On the Question of a Barrier-Layer Photoelectromotive Force in Photocells Containing Dyes. I. A. Karpovich and A. T. Vartanian	484	1	57
3. A Radiochemical Investigation of the Reaction Si^{30} (p, π^+) Si^{31}. S. Sekerskii and A. K. Lavrukhina	487	1	61
4. On the Theory of Nonstationary Discontinuities in Relaxing Fluids. E. V. Stupochenko and I. P. Stakhanov	490	1	65
5. On the Fluctuations of the Parameters of Certain Linear Systems. V. I. Bespalov	494	2	209
6. The Thermodynamics of Almost Perfectly Ordered Solid Solutions. M. A. Krivoglaz	498	2	213
7. On the Relationship Between Fluorescence Frequencies and the Effectiveness of Certain Quenchers. V. V. Zelinskii, V. P. Kolobkov, and N. I. Kondaraki	501	3	391
8. Calculation of the Electrical Conductivity of Semiconductors with High Impurity Content. R. Zigenlaub	505	3	395
9. On the Mobility of Electrons and Holes in a Liquid Semiconductor. I. Z. Fisher	510	3	399
10. Inelastic Proton-Proton Cross Section Above 7 Bev. K. I. Alekseeva and N. L. Grigorov	514	4	593
11. Some Characteristics of the K Emission Spectrum of Titanium in Titanates. E. E. Vainshtein, M. N. Bril', and I. B. Staryi	518	4	597
12. On the Theory of Diffusion Oscillations in a Gas Discharge Plasma. O. V. Prudkovskaia	521	4	601
13. Duration of the Excited State and Quantum Yield of Fluorescence from Chlorophyll in vitro and in vivo. L. A. Tumerman	525	4	605
14. The Influence of "Entrainment" on Thermomagnetic Effects in Bismuth Selenide. Kh. I. Amirkhanov, R. I. Bashirov, A. Z. Daibov, and I. M. Tsidil'kovskii	528	5	781
15. Approximate Dispersion Relations for Nucleon-Nucleon Scattering. V. Z. Blank and P. S. Isaev	532	5	785
16. On the Theory of Phase Transitions. N. N. Bogoliubov, D. N. Zubarev and Iu. A. Tserkovnikov	535	5	788

(continued)

CONTENTS (Continued)

17. Dispersion Relations for Virtual Processes. A. A. Logunov 540 5 792

18. X-rays from a Strong Pulsed Discharge in Xenon. I. M. Podgornyi and S. A. Chuvatin 543 5 795

19. Determination of the Character of an Elementary Radiator for Nonparallel Absorbing and Emitting Oscillators. A. N. Sevchenko and G. P. Gurinovich 546 5 798

20. Inversion of the Temperature Dependence of Molecular Fragment Line Intensities in a Mass Spectrum. G. D. Tantsyrev and V. L. Tal'roze . . . 550 5 802

21. On the Theory of Photoelectrets. V. M. Fridkin, N. T. Kashukeev, and I. S. Zheludev 552 5 804

22. Thermal Conductivity of Tellurium. Kh. I. Amirkhanov, G. B. Bagduev, and M. A. Kazhlaev 556 6 953

23. Cross Section for the Transfer of a Muon from a Proton to a Deuteron. S. S. Gershtein 559 6 956

24. The Theory of the Motion of Small Aerosol Particles in a Diffusion Field. B. V. Deriagin and S. P. Bakanov 563 6 959

25. Nuclear Quadrupole Moments. A. N. Kushnirenko 568 6 963

26. On the Theory of the Anisotropy of Cubic Crystals. N. A. Potapkov 570 6 965

27. On the Semiclassical Interpretation of Quantum Effects in the Theory of the Radiating Electron. A. A. Sokolov and I. M. Ternov 573 6 967

SIGNIFICANCE OF ABBREVIATIONS MOST FREQUENTLY ENCOUNTERED IN SOVIET PHYSICS PERIODICALS

AN SSSR	*Academy of Sciences, USSR*
FIAN	*Physics Institute, Academy of Sciences USSR*
GITI	*State Scientific and Technical Press*
GITTL	*State Press for Technical and Theoretical Literature*
GOI	*State Optical Institute*
GONTI	*State United Scientific and Technical Press*
Gosenergoizdat	*State Power Press*
Gosfizkhimizdat	*State Physical Chemistry Press*
Gozkhimizdat	*State Chemistry Press*
GOST	*All-Union State Standard*
Goztekhizdat	*State Technical Press*
GTTI	*State Technical and Theoretical Press*
GUPIAE	*State Office for Utilization of Atomic Energy*
IF KhI	*Institute of Physical Chemistry Research*
IFP	*Institute of Physical Problems*
IL	*Foreign Literature Press*
IPF	*Institute of Applied Physics*
IPM	*Institute of Applied Mathematics*
IREA	*Institute of Chemical Reagents*
ISN (Izd. Sov. Nauk)	*Soviet Science Press*
IIaP	*Institute of Nuclear Studies*
Izd	*Press (publishing house)*
KISO	*Solar Research Commission*
LETI	*Leningrad Electrotechnical Institute*
LFTI	*Leningrad Institute of Physics and Technology*
LIM	*Leningrad Institute of Metals*
LITMiO	*Leningrad Institute of Precision Instruments and Optics*
Mashgiz	*State Scientific-Technical Press for Machine Construction Literature*
MATI	*Moscow Aviation Technology Institute*
MGU	*Moscow State University*
Metallurgizdat	*Metallurgy Press*
MOPI	*Moscow Regional Institute of Physics*
NIAFIZ	*Scientific Research Association for Physics*
NIFI	*Scientific Research Institute of Physics*
NIIMM	*Scientific Research Institute of Mathematics and Mechanics*
NII ZVUKSZAPIOI	*Scientific Research Institute of Sound Recording*
NIKFI	*Scientific Institute of Motion Picture Photography*
OIIaI	*Joint Institute of Nuclear Studies*
ONTI	*United Scientific and Technical Press*
OTI	*Division of Technical Information*
OTN	*Division of Technical Science*
RIAN	*Radium Institute, Academy of Sciences of the USSR*
SPB	*All-Union Special Planning Office*
Stroiizdat	*Construction Press*
URALFTI	*Ural Institute of Physics and Technology*

NOTE: Abbreviations not on this list and not explained in the translation have been transliterated, no further information about their significance being available to us.—*Publisher.*

The expanded program of the American Institute of Physics comprises translation of four leading Soviet physics journals, as listed below. These translations, by competent, qualified scientists, provide all research laboratories and libraries with accurate and up-to-date information of the results of research in the U.S.S.R.

Soviet Physics — Technical Physics

A translation of the "Journal of Technical Physics" of the Academy of Sciences of the U.S.S.R. The translation began with the 1956 issues, and is being continued. Twelve issues per year, approximately 3,000 Russian pages. Annually $90.00 domestic, $95.00 foreign.

Soviet Physics — Acoustics

A translation of the "Journal of Acoustics" of the Academy of Sciences of the U.S.S.R. The translation began with the 1955 issues. Four issues per year, approximately 400 Russian pages. Annual price, beginning with the 1957 issues, $12.00 domestic, $14.00 foreign. Prices for each volume prior to 1957, $20.00 domestic, $22.00 foreign.

Soviet Physics — "Doklady"

A translation of the "Physics Section" of the Proceedings of the Academy of Sciences of the U.S.S.R. The translation began with the 1956 issues. Six issues per year, approximately 900 Russian pages. Annually $25.00 domestic, $27.50 foreign.

Soviet Physics — JETP

A translation of the "Journal of Experimental and Theoretical Physics" of the Academy of Sciences of the U.S.S.R. Translation began with the 1955 issues. Twelve issues per year, approximately 4,000 Russian pages. Annual price, beginning with the 1957 issues, $75.00 domestic, $79.00 foreign. Prices for back volumes may be obtained from the American Institute of Physics upon request.

Subscriptions should be addressed to the American Institute of Physics, 335 East 45th Street, New York 17, N. Y.